

TESI DI DOTTORATO

UNIVERSITÀ DEGLI STUDI DI NAPOLI “FEDERICO II”



DIPARTIMENTO DI INGEGNERIA BIOMEDICA, ELETTRONICA E
DELLE TELECOMUNICAZIONI

DOTTORATO DI RICERCA IN INGEGNERIA ELETTRONICA E DELLE
TELECOMUNICAZIONI

**GNSS MULTISYSTEM INTEGRITY FOR
PRECISION APPROACHES IN CIVIL AVIATION**

MASSIMO CIOLLARO

Il coordinatore del corso di dottorato
Ch.mo Prof. Giovanni POGGI

I tutori
Ch.mo Prof. Giorgio FRANCESCHETTI,
Ch.mo Prof. Mario CALAMIA

Anno Accademico 2007-2008

Long is the way and hard, that out of Hell leads up to Light
(J. Milton, Paradise Lost)

Table of Contents

| | |
|---|------------|
| Introduction | VII |
| Chapter 1 | 11 |
| Definitions and Assumptions for a GNSS System | 11 |
| 1.1 GNSS systems..... | 11 |
| 1.2 The Integrity concept..... | 18 |
| 1.3 General assumptions for a GPS system | 26 |
| Chapter 2 | 35 |
| The Integrity Concept..... | 35 |
| 2.1 GPS/SBAS Integrity Concept..... | 35 |
| 2.2 RAIM..... | 39 |
| 2.3 Galileo Integrity Concept..... | 45 |
| Chapter 3 | 53 |
| GPS integrity applications: GPS with RAIM algorithms..... | 53 |
| 3.1 Overview of the analysis..... | 53 |
| 3.2 Worst Case Bias..... | 58 |
| 3.3 Nominal conditions: no failures..... | 59 |
| 3.4 Single failure..... | 60 |
| 3.5 Dual failure | 62 |
| Chapter 4 | 67 |
| GPS Integrity applications: GPS with EGNOS..... | 67 |
| 4.1 Overview of the analysis..... | 67 |
| 4.2 Effects of satellite clock anomalies at the Signal In Space level | 71 |
| 4.3 Effects of satellite clock anomalies at the user level..... | 72 |
| 4.4 EGNOS reaction to GPS clock anomalies | 74 |
| 4.5 Integrity assessment with the Stanford-ESA Integrity Diagrams | 79 |
| 4.6 Summary of the results and conclusions | 80 |
| Chapter 5 | 83 |
| Multisystem Integrity | 83 |
| 5.1 A combined system..... | 83 |
| 5.2 GPS and Galileo with RAIM algorithms | 88 |
| 5.3 GPS and Galileo with the Galileo Integrity algorithm | 99 |
| 5.4 Other multisystem integrity techniques | 120 |
| Conclusions..... | 123 |
| Appendix A..... | 127 |
| Error sources | 127 |

| | | |
|--------------------------|--|------------|
| A.1. | Control Segment errors: satellite clock and ephemeris..... | 127 |
| A.2. | Propagation errors..... | 130 |
| A.3. | User level errors..... | 137 |
| A.4. | Error distributions..... | 138 |
| Appendix B..... | | 141 |
| | Overbounding techniques | 141 |
| Bibliography..... | | 145 |

Introduction

The introduction of the new European satellite navigation system Galileo will dramatically change the current scenario dominated by the US Navstar GPS system. Indeed, Galileo will bring new concepts and breakthrough ideas to guarantee not only a very accurate position, but also a high margin of safety through its built-in integrity algorithm. Integrity is the assurance, for the user, that the total system is able to provide an accurate position and that, in case of any failure, the system is able to timely warn the user and eventually correct the problem. Current GPS needs augmentation systems to provide integrity, while Galileo will be able to satisfy the very demanding safety requirements in civil aviation precision approaches without any further augmentations. However, it is very important to point out that the two systems will not be in competition, because Galileo is designed to be interoperable with GPS. Therefore, once Galileo will be finally deployed, users will be able to rely on two constellations: this means a high improvement in the accuracy of the position and a higher margin of safety due to the combined system. Thus, it is necessary to assess performances of a combined system, defining its parameters and its concepts and finally deriving a new multisystem integrity concept, which is able to take the best from both GPS and Galileo. The aim of this thesis is then to propose new multisystem integrity algorithms able to get all the benefits coming out from a combined system. To do this, a deep analysis of the integrity concept and its applications in civil aviation for each single system is mandatory. This represents the basis for the derivation of a standard multisystem scenario, where integrity is the added value.

The thesis is divided in five chapters, starting from the current state of the art and going further to the new concepts and ideas that will be presented throughout the documents.

In the first chapter, general definitions and basic mathematical and statistical models that characterise modern satellite navigation systems are described. Then, the integrity concept is introduced, starting from the operational parameters that describe it and the minimum requirements a navigation system should satisfy for civil aviation applications.

In the second chapter, the way the integrity service is provided by different systems is deeply explained: GPS in combination with a proper augmentation system (SBAS), GPS in combination with specific receiver algorithms (RAIM) and Galileo stand-alone. In particular, the specific equations and algorithms used to provide integrity in the different systems are analysed: Protection Levels computation for GPS/SBAS and RAIM algorithms, Probability of Hazardously Misleading Information (HMI) computation for Galileo.

Therefore, in the next two chapters some applications of the integrity concept for GPS for civil aviation are shown. Indeed, in the third chapter, RAIM algorithms for GPS are thoroughly analysed and tested in the single failure and dual failure cases. These tests are performed for specific geometry and specific receiver conditions. The purpose of this analysis is to show that RAIM algorithms, designed to detect only one failure, aren't able to protect user in case of two failures when using a single system (e.g., only GPS). This analysis provides the basis for one of the multisystem integrity techniques described in the last chapter.

On the other hand, the fourth chapter analyses the augmented version of current GPS that is GPS in combination with the SBAS system. The European version of SBAS is EGNOS, which started to transmit his signal in 2006. This analysis deals with real signal processing in order to evaluate EGNOS reactions in presence of clock anomalies on GPS satellites. This analysis represents a first original contribution to the thesis, because an innovative and original technique is used. Indeed, the study that has been performed has considered a set of 2 years of data (2006 and 2007) and combines a Signal in Space approach with a user level approach.

In the last chapter, the multisystem integrity is introduced. First, there's the need to define a combined system GPS+Galileo. Therefore, statistical and mathematical models defined for a single system in the previous chapters are here modified and extended. This study represents a second original contribution to the thesis, because, at the present, there aren't common accepted values for the different parameters that characterize a combined system. Then, a few multisystem integrity techniques are proposed and relative results are shown: this represents the third original contribution to the thesis. A first method considers the combination of GPS and Galileo orbital data together with the estimation of their range errors as the input for an extended RAIM algorithm. Thus, several RAIM algorithms have been

modified and extended in order to include data coming from a dual constellation, even in a multiple failures scenario. A second technique is based on the new Galileo Integrity algorithm, which is then modified in order to include also GPS data. This technique proposes an approach to combine the two systems that is different from the approach followed with the previous method. Indeed, the Galileo Integrity equation is based on a different concept with respect to the RAIM algorithms. Other possible techniques are then briefly introduced and described.

Finally, the most interesting results are discussed and possible future research topics are introduced: indeed, the current scenario is continuously evolving, since the Galileo system is still under development and the GPS system is being upgraded to a modernised version.

Chapter 1

Definitions and Assumptions for a GNSS

System

Global Navigation Satellite System (GNSS) is the standard generic term for satellite navigation systems that provide autonomous geo-spatial positioning with global coverage. A GNSS allows small electronic receivers to determine their location (longitude, latitude, and altitude) to within a few metres using time signals transmitted along a line of sight by radio from satellites. Receivers on the ground with a fixed position can also be used to calculate the precise time as a reference for scientific experiments.

As of 2008, the United States NAVSTAR Global Positioning System (GPS) is the only fully operational GNSS. The Russian GLONASS is a GNSS in the process of being restored to full operation. The European Union's Galileo positioning system is a GNSS in initial deployment phase, scheduled to be operational in 2013. China has indicated it may expand its regional Beidou navigation system into a global system (COMPASS). India's IRNSS, a regional system, is intended to be completed and operational by 2012.

1.1 GNSS systems

GNSSs that provide enhanced accuracy and integrity monitoring usable for civil navigation are classified as follows:

- *GNSS-I* is the first generation system and is the combination of existing satellite navigation systems (GPS and GLONASS) with Satellite Based Augmentation Systems (SBAS) or Ground Based Augmentation Systems (GBAS). In the United States, the satellite based component is the Wide Area Augmentation System (WAAS), in Europe it is the European Geostationary Navigation Overlay Service (EGNOS), and in Japan it is the Multi-Functional Satellite

Augmentation System (MSAS). Ground based augmentation is provided by systems like the Local Area Augmentation System (LAAS).

- *GNSS-2* is the second generation of systems that independently provides a full civilian satellite navigation system, exemplified by the European Galileo positioning system. These systems will provide the accuracy and integrity monitoring necessary for civil navigation. This system consists of two frequencies for civil use and a third frequency dedicated to system integrity. Development is also in progress to provide a modernized version of GPS for civil use with two frequencies, making it a GNSS-2 system.

The original motivation for satellite navigation was for military applications. Satellite navigation allows for hitherto impossible precision in the delivery of weapons to targets, greatly increasing their lethality whilst reducing inadvertent casualties from misdirected weapons. Satellite navigation also allows forces to be directed and to locate themselves more easily, reducing the “fog of war”.

However, GNSS systems have a wide variety of civil uses:

- Navigation, ranging from personal hand-held devices for trekking, to devices fitted to cars, trucks, ships and aircraft
- Time transfer and synchronization
- Location-based services
- Surveying
- Entering data into a geographic information system
- Search and rescue
- Geophysical Sciences
- Tracking devices used in wildlife management
- Asset Tracking, as in trucking fleet management
- Road Pricing
- Location-based media

Note that the ability to supply satellite navigation signals is also the ability to deny their availability. The operator of a satellite navigation system potentially has the ability to degrade or eliminate satellite navigation services over any territory it desires.

1.1.1 Current global navigation systems

The United States' Global Positioning System (GPS) as of 2008 is the only fully functional, fully available global navigation satellite system. It consists of up to 32 medium Earth orbit satellites in six different orbital planes, with the exact number of satellites varying as older satellites are retired and replaced. Operational since 1978 and globally available since 1994, GPS is currently the world's most utilized satellite navigation system.

The formerly Soviet, and now Russian, *Global'naya Navigatsionnaya Sputnikovaya Sistema*, or GLONASS, was a fully functional navigation constellation but since the collapse of the Soviet Union has fallen into disrepair, leading to gaps in coverage and only partial availability. The Russian Federation has pledged to restore it to full global availability by 2010 with the help of India, who is participating in the restoration project.

1.1.2 Upcoming Global Navigation Systems

The European Union and European Space Agency agreed on March 2002 to introduce their own alternative to GPS, called the Galileo positioning system. The system is scheduled to be working from 2013. The first experimental satellite, GIOVE-A, was launched on 28 December 2005. A second experimental satellite, GIOVE-B, was launched in April 2008. Galileo is expected to be compatible with the modernized GPS system. Hybrid receivers will then be able to combine signals from both Galileo and GPS satellites to greatly increase coverage and position accuracy.

The Indian Regional Navigational Satellite System (IRNSS) is an autonomous regional satellite navigation system being developed by Indian Space Research Organization, which would be under the total control of Indian government. The government approved the project in May 2006, with the intention of the system to be completed and implemented by 2012. It will consist of a constellation of 7 navigational satellites by 2012. All the 7 satellites will be placed in the Geostationary orbit (GEO) to have a larger signal footprint and lower number of satellites to map the region. It is intended to provide an absolute position accuracy of better than 20 meters throughout India and within a region extending approximately 2,000 km around it. A goal of complete Indian control has been stated, with the space segment, ground segment and user receivers all being built in India.

China has indicated they intend to expand their regional navigation system, called *Beidou* or *Big Dipper*, into a global navigation system; a program that has been called *Compass* in China's official news agency Xinhua. The Compass system is proposed to utilize 30 medium Earth orbit satellites and five geostationary satellites. Having announced they are willing to cooperate with other countries in Compass's creation, it is unclear how this proposed program impacts China's commitment to the international *Galileo* position system.

The Quasi-Zenith Satellite System (QZSS) is a proposed three-satellite regional time transfer system and enhancement for GPS covering Japan. The first satellite is scheduled to be launched in 2008.

1.1.3 GPS frequency plan

Current GPS signals consist of two radio frequency (RF) links: L1 and L2 [5]. L1 carrier frequency is at 1575.42 MHz, while the carrier frequency for L2 is at 1227.6 MHz. Utilizing these links, the space vehicles (SVs) of the Satellite System shall provide continuous earth coverage for signals which provide to the US the ranging codes and the system data needed to accomplish the GPS navigation (NAV) mission. These signals shall be available to a suitably equipped user with RF visibility to an SV.

Single frequency receivers (Standard Positioning Service – SPS) use only the L1 signal, while dual frequency receivers (Precise Positioning Service – PPS) combine it with the L2 signal. Obviously, a dual frequency receiver provides more accurate results, since it can get rid of the ionospheric error. Modern GPS will provide a third signal, the L5 signal, with carrier frequency at 1176.450 MHz. This will add further benefits to the final users.

1.1.4 Galileo frequency plan

The Galileo navigation signals will be transmitted in the four frequency bands indicated in the next figure [1]. These four frequency bands are the E5a, E5b, E6 and E1 bands. They will provide a wide bandwidth for the transmission of the Galileo Signals. Note that E5a and E5b signals are part of the E5 signal in its full bandwidth.

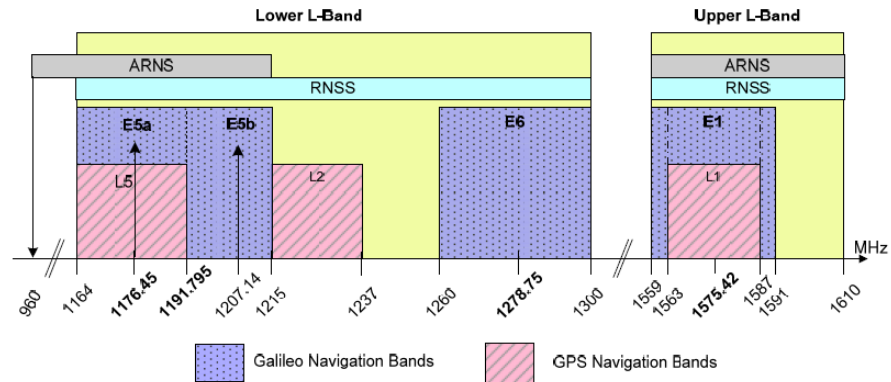


Figure 1-1: Galileo Frequency Plan

The Galileo frequency bands have been selected in the allocated spectrum for Radio Navigation Satellite Services (RNSS) and in addition to that, E5a, E5b and E1 bands are included in the allocated spectrum for Aeronautical Radio Navigation Services (ARNS), employed by Civil-Aviation users, and allowing dedicated safety-critical applications.

The next table summarizes signal specifications for current and modern GPS and for Galileo, including also the type of modulation that is used.

| | Frequency Band | Carrier Frequency (MHz) | Bandwidth (MHz) | Modulation | PRN codes (Mchip/s) | Services |
|----------------|----------------|-------------------------|-----------------|-------------|--|----------------------|
| Current GPS | L1 | 1575.42 | 24 | BPSK | C/A=1.023 and P(Y)=10.23 | SPS PPS (with L2) |
| | L2 | 1227.6 | 22 | BPSK | P(Y)=10.23 or C/A=1.023 | PPS (with L1) |
| Modernized GPS | L1 | 1575.42 | 24 | BPSK | C/A=1.023 P(Y)=10.23 | SPS PPS |
| | | | | BOC | C _D =1.023 | |
| | | | | TMBOC | C _P =1.023 | |
| | L2 | 1227.6 | 22 | BPSK | P(Y)=10.23 C/A=1.023 CM=10.23 CL=767.25 | SPS PPS |
| L5 | 1176.450 | 24 | QPSK | 10.23 | SPS/SOL | |
| Galileo | E1 | 1575.420 | 32 | CBOC | B=1.023 | OS/CS/SOL |
| | | | | | C=1.023 | - |
| | E6 | 1278.750 | 40 | M-BOC (TBC) | B=5.115 | CS |
| | | | | | C=5.115 | - |
| | E5 | 1191.795 | 51 | AltBOC | | |
| | E5a | 1176.450 | 27.795 | QPSK | I=10.230 | OS |
| | | | | | Q=10.230 | - |
| E5b | 1207.140 | 23.205 | QPSK | I=10.230 | OS/CS/SOL | |
| | | | | Q=10.230 | - | |

Table 1-1: GPS and Galileo signal specifications

1.1.5 Navigation solution base-line

In general, the basic linearized GPS measurement equation is:

$$\mathbf{y} = \mathbf{G} \cdot \mathbf{x} + \epsilon$$

Eq. 1-1

where \mathbf{x} is the four dimensional position vector about which the linearization has been made, containing the receiver coordinates in a selected reference system and the receiver clock bias:

$$\mathbf{x} = \begin{pmatrix} x \\ y \\ z \\ b \end{pmatrix}$$

Eq. 1-2

\mathbf{y} is an N dimensional vector containing the raw pseudorange measurements minus the expected ranging values based on the location of the satellites and the expected location of the user:

$$\mathbf{y} = \boldsymbol{\rho} - \boldsymbol{\rho}_0$$

Eq. 1-3

where $\boldsymbol{\rho}_0$ contains the initial guess of the receiver position \mathbf{x}_0 and of the receiver clock bias b_0 . N is the number of available measurements, which is given by the number of satellites in view. Clearly, $N=4$ is the minimum number of measurements needed to solve Eq. 1-1.

\mathbf{G} is the design matrix in the same coordinate system of \mathbf{x} and $\boldsymbol{\epsilon}$ is an N dimensional vector containing the errors in \mathbf{y} .

The weighted least squares solution for \mathbf{x} can be found by

$$\mathbf{x}_{wls} = (\mathbf{G}^T \cdot \mathbf{W} \cdot \mathbf{G})^{-1} \cdot \mathbf{G}^T \cdot \mathbf{W} \cdot \mathbf{y} = \mathbf{K} \cdot \mathbf{y}$$

Eq. 1-4

where \mathbf{K} is the weighted pseudo-inverse of \mathbf{G} and where \mathbf{W} is the inverse of the covariance matrix. Assuming that the error sources for each satellite are uncorrelated with the error sources for any other satellite, all off-diagonal elements of \mathbf{W} are set to zero. The diagonal elements are the inverses of the variances corresponding to each satellite:

$$\mathbf{W} = \begin{pmatrix} \frac{1}{\sigma_1^2} & \dots & 0 \\ \vdots & \ddots & \vdots \\ 0 & \dots & \frac{1}{\sigma_N^2} \end{pmatrix}$$

Eq. 1-5

These variances are defined in the range domain and are different for each satellite, because they depend on the elevation angle. They correspond to the

User Equivalent Range Error (UERE), because they include contributions for several sources of error, as described in Appendix A.

The four elements vector \mathbf{x}_{wls} represents the weighted least square solution containing the correction to be applied to the initial guess of the receiver position (\mathbf{x}_0) and of the user clock bias (b_0). The weighted least square loop usually converges in 3-4 iterations, even if the initial guess of the user position and the user clock are set to zero.

The 1-sigma vertical accuracy in the position domain is given by:

$$\sigma_V = \sqrt{[(\mathbf{G}^T \cdot \mathbf{W} \cdot \mathbf{G})^{-1}]_{3,3}}$$

Eq. 1-6

while in the horizontal plane the 1-sigma accuracy is given by:

$$\sigma_H = \sqrt{[(\mathbf{G}^T \cdot \mathbf{W} \cdot \mathbf{G})^{-1}]_{1,1} + [(\mathbf{G}^T \cdot \mathbf{W} \cdot \mathbf{G})^{-1}]_{2,2}}$$

Eq. 1-7

These measures give the 1-sigma expected accuracy in the vertical dimension and the 2-dimensional RMS expected accuracy in the horizontal dimensions respectively. The 1-sigma accuracy means that for the 68% of the time the position error lays inside a circle whose radius is equal to the accuracy requirement. The accuracies of these measures depend on the accuracies of the satellite covariances in the \mathbf{W} matrix. On the other hand, the 95% accuracy corresponds to the 2-sigma value. Therefore, the 95% position accuracy is given by $1.96 \cdot \sigma_V$ and $1.96 \cdot \sigma_H$ for the vertical and horizontal cases respectively. This means that for the 95% of the time the position error lays inside a circle whose radius is equal to the accuracy requirement.

The position error is given by $\mathbf{x}_{wls} - \mathbf{x}$ and it is usually computed in a local coordinate system (i.e., North, East, Up). Therefore, the vertical position error is the difference between the true Up component of the receiver position and the computed Up component of the receiver position.

1.2 The Integrity concept

Integrity is foremost a guarantee for the user that the information provided by the total system is correct and a critical operation can be safely

accomplished. Integrity strongly depends on the specific application and on the specific environment. All modern satellite navigation systems should provide the integrity service, because it is crucial in critical operations, such as airplane landing or safe approach to harbour. However, integrity is strictly related to other operational parameters, which will be here exposed. In order to accomplish a critical application, these parameters should assume a specific value, which is different for each application. These values are defined by international organisations in order to achieve the desired level of safety in the different environments, such as civil aviation, maritime and rail. Thus, the system (or the set of systems) used to calculate the position should be designed properly in order to fulfil these requirements, which are defined at the user level. In particular, GPS and Galileo have their own integrity concepts: the former uses an augmentation of the pre-existing system and it is now standardised and implemented in many receivers; the latter is still under development and it will provide its own integrity service as a stand-alone system.

1.2.1 Operational parameters

The Operational Parameters give a measure of the quality of a navigation system.

Accuracy

Accuracy is the degree of conformance between the estimated position and the actual position. For any estimated position at a specific location, the probability that the position error is within the accuracy requirement should be at least 95 percent. Therefore, the accuracy requirement is defined as a 2-sigma value. Different accuracy requirements are provided for the horizontal and vertical errors.

Integrity

Integrity is a measure of the trust which can be placed in the correctness of the information supplied by the total system. Integrity includes the ability of a system to provide timely and valid warnings to the user (alerts) when the system must not be used for the intended operation. The integrity performance is specified by means of three parameters:

- *Alert limit (AL)*: this is the maximum allowable error in the user position solution before an alarm is to be raised within the specific time to alarm. This alarm limit is dependent on the considered

operation and each user is responsible for determining its own integrity in regard of this limit for a given operation following the information provided by the GNSS signal. There is a *Vertical Alert Limit (VAL)* and a *Horizontal Alert Limit (HAL)*.

- *Time To Alert (TTL)*: the time to alert is defined as the time starting when an alarm condition occurs to the time that the alarm is displayed at the user interface. Time to detect the alarm condition is included as a component of this requirement.
- *Integrity Risk (IR)*: this is the probability during the period of operation that an error, whatever is the source, might result in a computed position error exceeding a maximum allowed value, called Alert Limit, and the user is not informed within the specific time to alarm.

Continuity

Continuity is the ability of a navigation system to provide required service over a specified period of time without interruption. Continuity relates to the capability of the navigation system to provide a navigation output with the specified accuracy and integrity throughout the intended operation, assuming that it was available at the start of the operation. The continuity risk is the probability that the system will be unintentionally interrupted and will not provide guidance information for the intended operation.

Availability

The availability of a navigation system is the ability of the system to provide the required function and performance at the initiation of the intended operation. Availability is an indication of the ability of the system to provide usable service within the specified coverage area. Signal availability is the percentage of time that navigational signals transmitted from external sources are available for use. Availability is a function of both the physical characteristics of the environment and the technical capabilities of the transmitter facilities.

1.2.2 Integrity requirements for civil aviation

The integrity requirements are proposed by the user community, in order to reach a certain level of trust in the position information. They represent the

desired values of the operational parameters for a specific operation and they are different for each application. These requirements don't depend on the system used to provide the position solution: indeed, it is the system (or the set of systems) used to provide the position that has to satisfy the requirements for a specific critical operation.

The integrity requirements for the civil aviation have been standardised by the International Civil Aviation Organisation (ICAO) and they assume different values for each specific phase of flight.

1.2.2.1 Phases of flight

The performance requirements are defined for the following operations identified by the ICAO:

Oceanic En Route: this phase covers operations over ocean areas generally characterized by low traffic density and no independent surveillance coverage.

Domestic En Route: operations in this phase are typically characterized by moderate to high traffic densities. This necessitates narrower route widths than in the oceanic en route phase. Independent surveillance is generally available to assist in ground monitoring of aircraft position.

Terminal Area: operation in the terminal area is typically characterized by moderate to high traffic densities, converging routes, and transitions in flight altitudes. Narrow route widths are required. Independent surveillance is generally available to assist in ground monitoring of aircraft position.

Non Precision Approach (NPA): non precision approach aids provide a landing aircraft with horizontal position information (2-dimensional approaches). Also called LNAV (Lateral Navigation).

Approach and landing operations with vertical guidance – APV. Different types of APV approaches may be identified. They may be separated into two broad classes depending on the method retained for the provision of the vertical guidance during the approach: the first class which corresponds to APV approaches operationally approved today in some states rely on GNSS lateral guidance and on barometric vertical guidance generated through a Flight Management System (FMS). However barometric vertical guidance suffers from limitations in term of accuracy and a number of potential

integrity failures due to the necessity of manual input of local atmospheric pressure and of temperature compensation. Therefore the ICAO GNSS panel identified two performance levels identified as *APV-I* and *APV-II* which rely on GNSS vertical guidance rather than pure barometric vertical guidance. The lateral performance of these service levels is similar to ILS (Instrument Landing System) Cat I, while the vertical accuracy is slightly reduced. However the lateral and vertical integrity requirement is similar to ILS CAT I, making this performance level very attractive for the aviation community.

Precision Approach (PA): during precision approach aids provide landing aircraft with vertical and horizontal guidance and positioning information (3-dimensional approaches). *CAT-I*, *CAT-II* and *CAT-III* categories of aircraft approaches are defined by ICAO according to the level of confidence that an adequately trained pilot in a suitably equipped aircraft can place into the system he is using to help him landing the aircraft safely. The precision approach is divided in two main segments: the aircraft first follows the indication provided by the landing system, then the pilot takes over in the final part and visually checks whether the aircraft is in a position to land. CAT-I conditions exist when the Decision Height (DH) is at 200 feet (about 60 m) or above and the Runway Visible Range (RVR) is 2400 feet (about 730 m) or greater; CAT-II conditions exist when the decision height is between 100 and 200 feet (between 30 – 60 m) and the RVR is 1200 feet (about 365 m) or greater; CAT-III conditions exist when the visibility is poorer and include conditions with zero visibility. Category III is subdivided in the following categories:

- *CAT-IIIa*: path descends to touchdown zone. Requires a RVR greater than 200m
- *CAT-IIIb*: automatic landing includes rollout to a safe taxi speed. Requires a RVR greater than 50m
- *CAT-IIIc*: fully automatic landing, including taxiing. No RVR requirement

In addition to the previously described phases of flight, a new procedure has been recently added, called *LPV-200*, which will provide vertical guided approach capability to an altitude as low as 200 feet (61 meters).

The following figure shows the evolution of the different phases of flight during an aircraft operation.

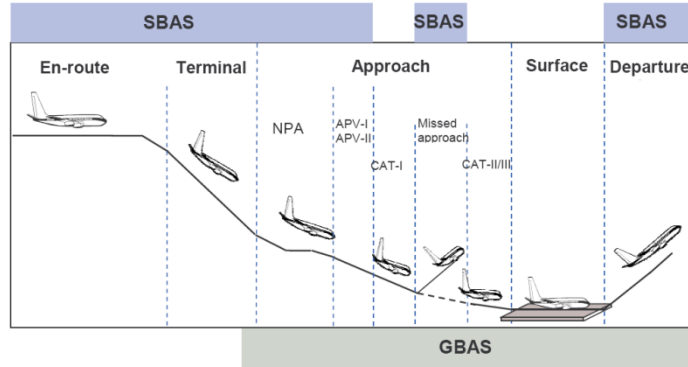


Figure 1-2: Evolution of aeronautic phases of flight

1.2.2.2 Performance requirements for navigation and approach in aeronautical applications

Accuracy, integrity, continuity and availability include overall system performances (ground sensors and infrastructures, airborne sensors, pilot or auto-pilot); in particular accuracy performance includes aircraft navigation sensor accuracy and pilot capacity to flow on a specified desired path. The measure of lateral/vertical position deviation from the desired path is named *TSE (Total System Error)* as shown in the next picture.

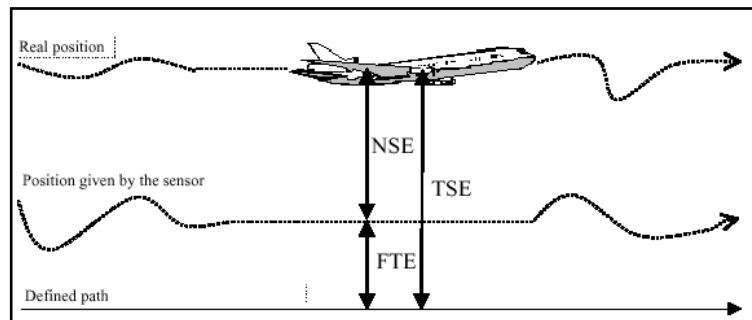


Figure 1-3: Total System Error is constituted by Navigation Sensor Error and Flight Technical Error

The TSE is composed by *Flight Technical Error (FTE)* and *Navigation Sensor Error (NSE)*; the first one is linked to the ability of the pilot or auto-pilot to conduct and control the aircraft flight path over the defined flight path while the NSE refers to aircraft sensor errors together with the input signal errors to the navigation sensors, such as GNSS SIS errors. Thus,

assuming these error components are random and independent, the mean square value of the TSE can be expressed as:

$$\sigma_{TSE}^2 = \sigma_{FTE}^2 + \sigma_{NSE}^2$$

Eq. 1-8

The performance requirements in avionic applications are defined by ICAO and described in the GNSS Standards and Recommended Practices (SARPs) [7]. ICAO has created a special panel, widely known as GNSSP (GNSS Panel), in charge of deriving the GNSS-SARPS. These SARPS provide specific performance requirements for GNSS, so that the fulfilment thereof results in the suitability of the system for one or more RNP levels. They also constitute a basic technical standard for GNSS systems, including ground and space based augmentations (GBAS and SBAS respectively).

In the process of SARPS derivation, the FTE component is removed in order to obtain requirements for the GNSS navigation system, isolated and uncoupled from the pilot or auto-pilot system.

In the next table, the navigation performance requirements for civil aviation are shown. Requirements for the new LPV-200 procedure are provided by [8]. Requirements for CAT-II and CAT-III have not been published yet.

| Typical Operation | Accuracy (95%) | Alert Limits | Integrity | Time To Alert | Continuity | Availability |
|----------------------|------------------------|------------------------|---------------------------------------|---------------|---|--------------------|
| En-route oceanic | 3.7 km (H) N/A (V) | 7.4 km (H) N/A (V) | 1-1x10 ⁻⁷ / h | 300 s | 1-1x10 ⁻⁴ / h to 1-1x10 ⁻⁸ / h | 0.99 to 0.99999 |
| En-route continental | 0.74 km (H) N/A (V) | 3.7 km (H) N/A (V) | 1-1x10 ⁻⁷ / h | 15 s | 1-1x10 ⁻⁴ / h to 1-1x10 ⁻⁸ / h | 0.99 to 0.99999 |
| En-route, Terminal | 0.74 km (H) N/A (V) | 1.85 km (H) N/A (V) | 1-1x10 ⁻⁷ / h | 15 s | 1-1x10 ⁻⁴ / h to 1-1x10 ⁻⁸ / h | 0.99 to 0.99999 |
| NPA, departure | 220 m (H) N/A (V) | 556 m (H) N/A (V) | 1-1x10 ⁻⁷ / h | 10 s | 1-1x10 ⁻⁴ / h to 1-1x10 ⁻⁸ / h | 0.99 to 0.99999 |
| APV I | 16 m (H) 20 m (V) | 40 m (H) 50 m (V) | 1-2x10 ⁻⁷ / app (150 s) | 10 s | 1-8x10 ⁻⁶ / 15 s | 0.99 to 0.99999 |
| APV II | 16 m (H) 8 m (V) | 40 m (H) 20 m (V) | 1-2x10 ⁻⁷ / app (150 s) | 6 s | 1-8x10 ⁻⁶ / 15 s | 0.99 to 0.99999 |
| LPV-200 | 16 m (H) 4 m (V) | 40 m (H) 35 m (V) | 1-2x10 ⁻⁷ / app (150 s) | 6 s | 1-8x10 ⁻⁶ / 15 s | 0.99 to 0.99999 |
| CAT I | 16 m (H) 4 m (V) | 40 m (H) 10 m (V) | 1-2x10 ⁻⁷ / app (150 s) | 6 s | 1-8x10 ⁻⁶ / 15 s | 0.99 to 0.99999 |

Table 1-2: Operational Performance Requirements for Civil Aviation Operations

It can be observed that requirements provided by the Panel are presented as SIS (Signal-In-Space) requirements. However, some of the parameters cannot actually be applied as SIS requirements without defining the user requirements. As a result, the Panel has developed the concept of a “*fault-free receiver*” with a defined (nominal) performance to be used to measure the SIS. The fault-free receiver is defined to be a receiver with a nominal accuracy performance and because it is assumed to have no failures it does not contribute to the integrity and continuity performance. Besides, a range of values is given for the SIS continuity and availability requirements for certain phases of flight. This is due because the requirements are dependent on several factors relating to the air traffic environment in which the GNSS system is being used. These factors include the traffic density, the complexity of the airspace, the availability of alternative navigation aids, the availability of dependent surveillance (e.g. radar) and the possibility of ATC (Air Traffic Control) intervention. It is therefore not possible to give a single, globally applicable, continuity and availability requirements. For example the lower values given above are the minimum requirements for which a system is considered to be practical.

In general these values are determined by airspace needs to support sole means navigation where GNSS has either replaced the existing navigation and infrastructure, or where no infrastructure previously existed.

Navigation systems meeting all or parts of the Required Navigation Performance (RNP) parameters can support different operating procedures:

Supplementary procedure: navigation system meeting only RNP accuracy and integrity performance. Then there is a need for a back up navigation system certified as “sole means”. However, during its operation the navigation system can compute navigation solutions irrespective of the sole mean system.

Primary procedure: navigation system meeting RNP accuracy and integrity performances. In this case the navigation system can be used as primary mean of navigation due to the correctness of the position information computed by the navigation sensor. A primary procedure shall be complemented by a back up related procedure to be used in case of loss of continuity of service or unavailability, in order to start an alternative procedure to conduct the aircraft. A sole mean system as back up is not required.

Sole means procedure: navigation system meeting all RNP parameter performances. In this case the navigation system can be used as unique system in charge of assuring the security levels in terms of performances and continuity of the performances.

1.3 General assumptions for a GPS system

1.3.1 Probability of Failure

When defining the satellite failure probability, some basic assumptions are commonly used:

- All satellites are identical, and operate identically and independently
- The GPS constellation is in a steady state, i.e. the satellites in orbit have randomly distributed ages (i.e., certain ones are at the start of their operational lives and others at the end)
- All failure probability density functions have exponential models of the form [2]:

$$f(t) = e^{-\lambda t}$$

Eq. 1-9

where $\lambda = \frac{1}{MTBF}$ and MTBF is the Mean Time Between Failures and it is given by:

$$MTBF = \frac{\text{Total Hours of Operation}}{\text{Number of Failures}}$$

The corresponding life distribution is:

$$F(t) = \int_0^t \lambda e^{-\lambda x} dx = [-e^{-\lambda x}]_0^t = 1 - e^{-\lambda t}$$

Eq. 1-10

The corresponding reliability function is therefore given by the expression:

$$R(t) = 1 - F(t) = e^{-\lambda t}$$

Eq. 1-11

It should be noted that different probability density functions could be considered rather than the exponential model, in order to keep track, for example, of the age of the satellites or the type of failure which affects the most the satellite. Therefore, instead of a constant failure rate, a variable failure rate should be considered. However, this analysis is beyond this study and it is left for future works.

From the above expressions, the probability p that at time t_0 a satellite is working well and that during the period t_0+T (where T is the period of operation) a failure occurs is given by the following expression:

$$p = \frac{F(t_0 + T) - F(t_0)}{R(t_0)} = \frac{e^{-\lambda t_0} - e^{-\lambda(t_0+T)}}{e^{-\lambda t_0}} = 1 - e^{-\lambda T}$$

Eq. 1-12

It can be seen that the probability of failure only depends on the parameter T , i.e. the period of operation. It does not depend on t_0 (corresponding to lack of memory).

Thus, the probability $P_{fail,n,k}$ of having k unscheduled simultaneous failures on n satellites is:

$$P_{fail,n,k} = \binom{n}{k} p^k q^{n-k}$$

Eq. 1-13

where p is the individual satellite failure probability and $q=1-p$. Usually, for $k=1$, it is assumed:

$$P_{fail,n,1} \approx n \cdot p$$

Eq. 1-14

The GPS SPS signal specification [3] allows 3 major failures per year per constellation, where a major service failure is defined as a pseudorange error in excess of 150m. This value has been recently revised to 30m [4]. More precisely, GPS SPS Performance Standard (2001) has defined a major service failure as a departure from nominal system ranging accuracy that causes the SPS instantaneous ranging error of a healthy satellite to exceed 30 meters while the User Range Accuracy (URA) multiplied out to 4.42 standard deviations indicates less than 30 meters. URA is the expected GPS SIS range accuracy and it is a parameter broadcast in the navigation message.

3 major failures per year per constellation (24 satellites in the case of nominal GPS constellation) lead to a probability of failure per satellite of $\sim 10^{-5}/h/SV$. Aviation community, based on simulations and collected data, has assumed an average of 8 GPS satellites in view when calculating the satellite failure probability. Thus, the common used value for the probability of failure among all the satellites in view is:

$$P_{fail} = 1 \times 10^{-4}/h$$

Eq. 1-15

This is the value recommended in RTCA-MOPS from En-route to NPA [9].

1.3.1.1 Precision approach for GPS satellites

For precision approach (e.g., LPV-200 category) the satellite failure probability is computed considering the time the Control Segment needs to detect and inform the user of an integrity failure from the onset of such failure. This time is assumed to be 1 hour for GPS, even if it is expected to be shorter. Therefore, during the approach, which lasts 150 seconds, there is one independent integrity sample and therefore the probability of having 1 failure is given by:

$$P_{fail,app} = 1 \times 10^{-4}/approach$$

Eq. 1-16

In this way, the probability of having one failure during the approach is bounded by the capability of the system to detect that failure, because the user doesn't know when, during the detection time interval, the approach is going to be performed (or, vice versa, the user doesn't know when the failure occurred when the approach operation started). In this method it is assumed that the independent sample is in the 150 seconds that are considered for the approach.

It should be noted that modernized GPS is expected to detect failures and inform user in a shorter time, therefore the value of the probability of failure is expected to be smaller.

Moreover, considering the equations described in the previous section, it is possible to derive also in this case the failure probability per satellite and the probability of multiple independent simultaneous failures. Furthermore, also common mode failures should be introduced now: a common mode failure is defined as a fault condition in which multiple satellite range

measurements simultaneously experience errors which could be consistent in the sense that they could be undetectable by RAIM, but also by the system. The rate of common mode faults causing multiple satellite integrity failures is usually assumed to be 1.3×10^{-8} per approach [17].

The next table summarizes these results.

| Parameters | Recommended values |
|--|---------------------------------------|
| GPS Satellite Failure Probability per satellite En-route to NPA | $1 \times 10^{-5}/h/SV$ |
| GPS Satellite Failure Probability (8 satellites in view) En-route to NPA | $1 \times 10^{-4}/h$ |
| GPS Satellite Failure Probability per satellite Precision Approach | $1 \times 10^{-5}/\text{approach}/SV$ |
| GPS Satellite Failure Probability (8 satellites in view) Precision Approach | $1 \times 10^{-4}/\text{approach}$ |
| GPS Common Mode Failures Probability Precision Approach | $1.3 \times 10^{-8}/\text{approach}$ |

Table 1-3: GPS Satellite failure probability

1.3.2 Probability of Missed Detection

A Missed Detection is defined to occur when a positioning failure is not detected. A positioning failure is defined as a position error exceeding the specified Alert Limit for a particular phase of flight. In the case of designing a RAIM algorithm, a positioning failure is defined as a position error exceeding a specific maximum value, called Protection Level, which guarantees the required Probability of Missed Detection (Figure 1-4). A RAIM algorithm is an algorithm directly implemented in the user receiver that checks the consistency of the measurements using their redundancy.

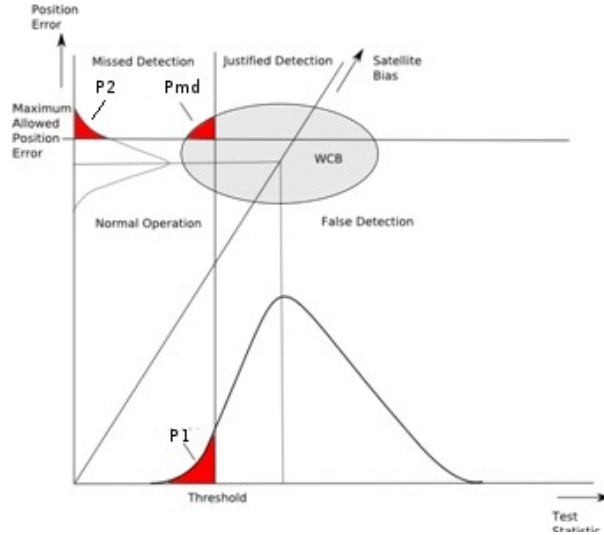


Figure 1-4: An estimation of the probability of missed detection can be made as the product of the cumulative test statistic ($P1$) and navigation system error distributions ($P2$)

For a RAIM algorithm, an estimation of the probability of missed detection can be made as the product of a cumulative test statistic and navigation system error distributions:

$$P_{md} = \Pr(VPL < VPE) \cdot \Pr(\text{TestStat} < \text{Threshold}) \quad \text{Eq. 1-17}$$

In Eq. 1-17 the first term represents the probability that the actual position error is greater than the computed protection level: this probability is normally distributed with mean equal to the magnitude of the bias affecting the failed satellite and with standard deviation given by Eq. 1-6 and Eq. 1-7 for the vertical and horizontal case respectively.

The second term of Eq. 1-17 represents the probability that the test statistic is below a certain threshold: this probability is characterized by a central chi-square distribution with $n-m$ degrees of freedom, where n is the number of available measurements and m the number of unknowns (i.e., 4 for a single constellation, 5 for a dual constellation).

A Missed Detection can lead to a Missed Alert if the positioning failure is not announced within the Time To Alert. The Probability of having a Missed Alert is called Integrity Risk. From the point of view of the user, the Missed Alert corresponds to a Misleading Information if the position error is

larger than the Protection Level, but lower than the Alert Limit and to a Hazardously Misleading Information if the position error is larger than both the Protection Level and the Alert Limit, being $PL < AL$. In the last case, the Integrity Risk is also known as Probability of Hazardously Misleading Information (Figure 1-5).

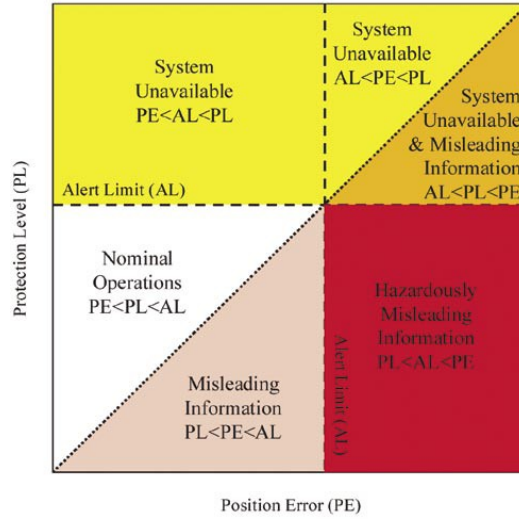


Figure 1-5: Protection Level vs. Position Error

In general, the allocated Integrity Risk is given by:

$$IR = \sum_{n=1}^N p_n P_{md,n}$$

Eq. 1-18

where p_n is the individual failure probability for each satellite, $P_{md,n}$ is the allocated probability of missed detection for each satellite integrity failure and N is the number of used satellites. An integrity failure is a failure in the system other than the nominal ones, which are known to the system and to the user. In other words, an integrity failure is a failure that leads to an HMI event.

It is usually assumed that the probability of individual satellite failure and the probability of missed detection are constant for each satellite. Moreover, in a conventional scheme it is usually assumed that only one satellite can fail.

Therefore,

$$P_{md} = \frac{IR}{N \cdot p} = \frac{IR}{P_{fail}}$$

Eq. 1-19

This means that the Integrity Risk is equally allocated among different satellites. It is now possible to derive the values of probability of missed detection using the value of the probability of failure and the integrity risk requirement described in the previous sections for non precision approach. Therefore, the maximum allowable probability of missed detection for NPA is:

$$P_{md} = \frac{1 \times 10^{-7}/h}{1 \times 10^{-4}/h} = 1 \times 10^{-3}/sample$$

Eq. 1-20

This value applies also to precision approach, where the probability of failure and the integrity risk are defined per approach (i.e., 150 seconds), because during an approach there is only one independent sample.

It should be noted that, even if the probability of having two independent simultaneous failures is very small, the case of multiple failures affecting the system should be taken into account when computing the probability of missed detection. However, in this study, even in presence of multiple failures, the same value for the probability of missed detection considered in the case of single failure will be conservatively used.

| Parameter | Recommended value |
|--|-------------------|
| Maximum Allowable Probability of Missed Detection GPS satellites | $10^{-3}/sample$ |

Table 1-4: Maximum Allowable Probability of Missed Detection for GPS

1.3.3 Probability of False Alarms

A false alarm is defined as the indication of a positioning failure when a positioning failure has not occurred. On the other hand, a true alarm is defined as the indication of a positioning failure when a positioning failure has occurred.

An alarm, true or false, has always an impact on the continuity of the system. Thus, the continuity budget should be partitioned between false alarms and true alarms.

However, for En-route to NPA, the continuity requirement is usually entirely allocated to the false alarm rate occurring in absence of failures [18].

Following this approach, the required Probability of False Alarm is defined by means of Continuity Risk and Correlation Time:

$$P_{fa} = CR \cdot CT$$

Eq. 1-21

or equivalently:

$$P_{fa} = \frac{CR}{\text{Independent samples}}$$

Eq. 1-22

The Continuity Risk for En-route to NPA ranges between $1 \times 10^{-4}/h$ and $1 \times 10^{-8}/h$. The lower value is the minimum requirement for areas with low traffic density and airspace complexity. The higher value given is appropriate for areas with high traffic density and airspace complexity.

The correlation time of the errors is assumed to be 2 minutes, which is the smoothing time constant of the receiver noise [23].

The common used value for the probability of false alarm for En-route to NPA is 3.33×10^{-7} per sample, as recommended also in MOPS.

For precision approach, it is recommended to allocate half of the continuity risk budget to false alarms. Moreover, in this case the continuity risk requirement is defined over an exposure time of 15 seconds and there is only one independent sample during an approach. Therefore the value to be considered is now $4 \times 10^{-6}/sample$ [17].

| Parameter | Recommended value |
|--|------------------------------|
| Probability of False Alarm GPS satellites En-route to NPA | $3.33 \times 10^{-7}/sample$ |
| Probability of False Alarm GPS satellites Precision Approach | $4 \times 10^{-6}/sample$ |

Table 1-5: Recommended value for Probability of False Alarm for GPS satellites

Chapter 2

The Integrity Concept

In the previous chapter, the integrity concept from the user point of view was introduced. In particular, integrity requirements for specific civil aviation applications were described. Now, in this chapter, the integrity concept from the point of view of a navigation system will be introduced.

Therefore, it will be described how a navigation system is able to satisfy the integrity requirements for a specific application.

Three different concepts will be discussed: the integrity provided to the user by an augmented GPS system, such as SBAS, that includes a ground network together with geostationary satellites; the integrity autonomously provided by the user receiver through specific algorithms (RAIM); the integrity that the new Galileo system will be able to provide to the user.

The three concepts will be here described together with their respective mathematical models.

2.1 GPS/SBAS Integrity Concept

2.1.1 Overview

The current GPS system is neither accurate nor reliable enough to be accepted as a sole means of navigation. One of the reasons is that there is no reliable and quick (within seconds) information to the user if problems with the system occur. As a consequence, for landing approaches, GPS can't be used. Airplanes still have to use ILS-systems (Instrument Landing Systems) if visibility is poor. But the installation and maintenance of ILS-systems on every airport is expensive. With the SBAS (Satellite Based Augmentation Systems) systems, CAT I approaches (limited visibility) will be possible without additional ILS systems. For CAT III approaches (zero visibility) even the SBAS will not suffice and ILS are still required.

2.1.2 SBAS Architecture

SBAS is the ICAO term for what is also commonly known as the Wide Area Augmentation System or WAAS. With this system the correction information is collected from a network of GPS reference stations which are located throughout the country. Since their positions are exactly known, the reference stations correct any measurement errors from the satellites for their area. Correction information from each reference station is gathered and linked to a master station where it is analysed together with local tropospheric as well as ionospheric information. This is then sent via a geostationary satellite communications link, currently provided by Inmarsat satellites, to an SBAS receiver on board the aircraft. This correction information is then used to amend the position derived from the signals received directly from the GNSS constellation resulting in increased positional accuracy of the aircraft up to better than 10 metres or up to Cat I precision. The Inmarsat communications satellites also act as additional navigation satellites for the aircraft.

Other wide area augmentation systems similar to the U.S. WAAS have been developed by Europe and Japan: the European Global Navigation Overlay System (EGNOS) and the Multi-function Transport Satellite System (MSAS) for wide area navigation in the Asia and Pacific region.

WAAS, EGNOS and MSAS have been developed to increase the safety for aviation.

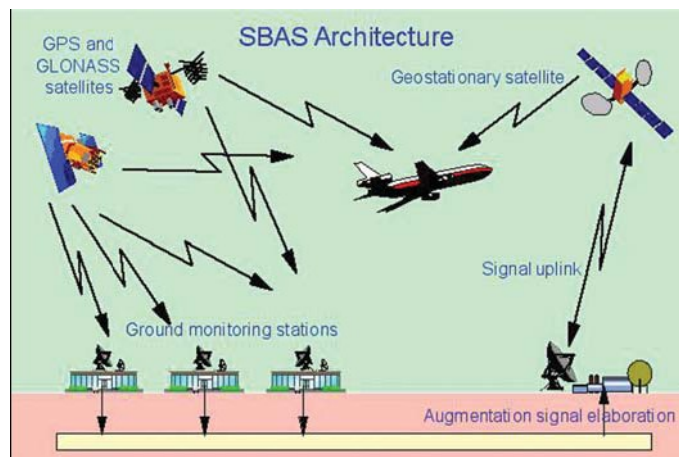


Figure 2-1: SBAS Architecture

2.1.3 SBAS Protection Levels

The protection level is an estimation of the maximum position error that the user is allowed to have within a given probability of not detecting a position error greater than the protection level itself. It is computed by the user receiver, it is defined in the vertical and horizontal planes and it is compared with the corresponding alert limit. When the protection level is greater than the alert limit, an alarm should be raised by the system, which is then declared unavailable to perform the intended critical operation.

The protection level concept is based on a fixed allocation of vertical and horizontal alert limits. Since user receiver geometries, which lead to high Horizontal Protection Level, are different from those that lead to high Vertical Protection Level values, an optimized fixed splitting cannot be selected for each user receiver and each location. Therefore, in the case of SBAS, considering that the vertical alert limit is the dominant requirement, a fixed allocation of the Integrity Risk has been specified accordingly, with 98% to the vertical case and 2% to the horizontal case. On the other hand, RAIM allocates the entire Integrity Risk to the horizontal or the vertical plane, according to the specific application. For example, RAIM allocates the entire IR to the horizontal plane for NPA, while the entire IR to the vertical plane for LPV-200.

According to RTCA-MOPS [9], the equipment shall use the following equations to calculate protection levels:

$$HPL_{SBAS} = \begin{cases} k_{H,NPA} \cdot d_{major} & \text{(en-route to LNAV)} \\ k_{H,PA} \cdot d_{major} & \text{(LNAV/VNAV, LP, LPV approach)} \end{cases} \quad \text{Eq. 2-1}$$

$$VPL_{SBAS} = k_V \cdot d_U \quad \text{Eq. 2-2}$$

where:

$$d_{major} = \sqrt{\frac{d_{east}^2 + d_{nort\ h}^2}{2}} + \sqrt{\frac{d_{east}^2 - d_{nort\ h}^2}{2} + d_{EN}^2} : \text{ is the error uncertainty along the semi-major axis of the error ellipse}$$

$d_{east}^2 = \sum_{i=1}^N s_{east,i}^2 \sigma_i^2$: is the variance of model distribution that overbounds the true error distribution in the east axis

$d_{north}^2 = \sum_{i=1}^N s_{north,i}^2 \sigma_i^2$: is the variance of model distribution that overbounds the true error distribution in the north axis

$d_{EN} = \sum_{i=1}^N s_{(east,i)} s_{north,i} \sigma_i^2$: is the covariance of model distribution in the east and north axis

$d_U^2 = \sum_{i=1}^N s_{U,i}^2 \sigma_i^2$: is the variance of model distribution that overbounds the true error distribution in the vertical axis

$s_{east,i}$ is the partial derivative of position error in the east direction

$s_{north,i}$ is the partial derivative of position error in the north direction

$s_{U,i}$ is the partial derivative of position error in the vertical direction

$$\sigma_i^2 = \sigma_{i,flt}^2 + \sigma_{i,UIRE}^2 + \sigma_{i,air}^2 + \sigma_{i,tropo}^2$$

Eq. 2-3

For a general least squares position solution, the projection matrix \mathbf{S} is defined as:

$$\begin{bmatrix} s_{east,1} & s_{east,2} & \cdots & s_{east,N} \\ s_{north,1} & s_{north,2} & \cdots & s_{north,N} \\ s_{U,1} & s_{U,2} & \cdots & s_{U,N} \\ s_{t,1} & s_{t,2} & \cdots & s_{t,N} \end{bmatrix} = (\mathbf{G}^T \cdot \mathbf{W} \cdot \mathbf{G})^{-1} \cdot \mathbf{G}^T \cdot \mathbf{W}$$

with:

$G_i = [-\cos El_i \sin Az_i \quad -\cos El_i \cos Az_i \quad -\sin El_i \quad 1]$ (where the positive azimuth is defined clockwise from North)

$$w_i = 1/\sigma_i^2$$

$k_{H,NPA}=6.18$ (en-route to LNAV)

$k_{H,PA}=6.0$ (LNAV/VNAV, LP, LPV)

$k_V=5.33$

The choice of k value is somewhat arbitrary: the fundamental underlying requirement is that SBAS service providers must send UDREs and GIVEs such that the values of HPL_{SBAS} and VPL_{SBAS} bound their respective errors

with target probabilities. However, [10] suggests a rationale to calculate k values: k is determined from a Rayleigh distribution for En route to NPA applications since the protection has to be bi-dimensional. For APV-I, II and CAT-I applications, two uni-dimensional k factors are determined from a Normal distribution corresponding to the lateral (cross-track) and vertical protections. K may be directly calculated from the knowledge of the cumulative distribution function (cdf) of the relevant statistical law. Therefore, the previous k values are calculated using a decorrelation time of 360 seconds and using the integrity risk requirements for NPA and for APV-I, II and CAT-I.

For en-route to LNAV approach, HPL_{SBAS} must bound horizontal radial error with a probability of $1-10^{-7}$ per hour, i.e., the probability that horizontal radial position error exceeds HPL_{SBAS} must not exceed 10^{-7} in any hour, except possibly for brief periods less than the time to alert. For LNAV/VNAV, LP and LPV approaches, the probability that horizontal cross-track error or vertical error or both exceed their respective protection levels must not exceed 2×10^{-7} per approach. Only one dimension is used for HPL_{SBAS} in LNAV/VNAV, LP and LPV approaches, since the along-track tolerance is so much larger than the cross-track. The worst case dimension is used. For vertical approach, RTCA has allocated 98% of the Integrity Risk and used the inverse cdf of a Gaussian distribution to find k_V .

2.2 RAIM

2.2.1 Overview

The integrity of a navigation system can be checked by using external systems such as SBAS to monitor the correctness of the signals used for position calculation. One major drawback of this approach is the inherent delay that is introduced in the detection of an error, due to the time it takes to uplink information on errors. This section will focus on internal monitoring, and in particular on RAIM. RAIM stands for Receiver Autonomous Integrity Monitoring and it is used to denote monitoring algorithm that uses nothing but the measurements of one particular navigation subsystem, usually a GPS receiver. Conventional RAIM algorithms are designed to protect user from a single satellite failure at a time. However, recent developments have shown RAIM potentiality to

provide integrity even in case of multiple failures for demanding flight categories as LPV-200 and APV-II.

Measurement information is used to compute a position. Some test statistic is derived from this position computation and is fed to an error detector that will warn the user when something is wrong. The error detection performance will have to obey the navigation requirements and it is important to determine the detection power (or ‘error detectability’) that depends on the measurement quality and configuration. It is in fact this detection power computation that monitors the system integrity, as it determines whether the system has the ability to provide timely warnings when the system is in error. If this is not the case, it will inform the user that using the system might be unsafe. It should be noted that position computation algorithms always assume that noise on the measurements has a zero mean. An error or bias - as it is commonly called - is therefore defined as the non-zero mean of measurement noise.

2.2.2 *Satellite Slope*

The slope, which relates the induced position error to the test statistic, can be calculated directly from geometry and it is different for each satellite. The satellite with the largest slope is the one that is the most difficult to detect and it produces the largest position error for a given test statistic (Figure 2-2).

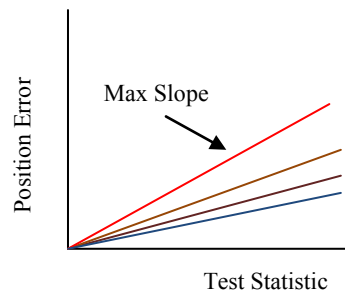


Figure 2-2: *Satellite Slope*

Slope is a geometry parameter and it can be directly computed from the specific satellite-user geometry, according to the following equations in the horizontal and vertical planes respectively:

$$Hslope_i = \frac{\sqrt{K_{1i}^2 + K_{2i}^2} \sigma_i}{\sqrt{1 - P_{ii}}}$$

Eq. 2-4

$$Vslope_i = \frac{|K_{3i}| \sigma_i}{\sqrt{1 - P_{ii}}}$$

Eq. 2-5

where $\mathbf{K} = (\mathbf{G}^T \cdot \mathbf{W} \cdot \mathbf{G})^{-1} \cdot \mathbf{G}^T \cdot \mathbf{W}$ is the weighted pseudo-inverse of the design matrix, being \mathbf{W} the inverse of the covariance matrix, while $\mathbf{P} = \mathbf{G} \cdot \mathbf{K}$. The geometry contribution to the slope is given by the \mathbf{K} and \mathbf{P} matrices.

A different slope concept has to be introduced when dealing with dual failure. The least detectable pair of satellites is given by the pair of satellite whose combination leads to the largest position error for a given test statistic. It has to be noted that the worst pair of satellites is not necessarily given by the two satellites which have the highest individual slopes, because the combined slope could have a different value.

Three methods to calculate dual failure slope have been considered: the relevant equations are not reported here for brevity, but they can be found in ([14], [15] and [16]). All methods lead to quite similar results: as expected, the highest slope in the dual failure case is larger than the highest slope in the single failure case. Therefore, the protection level in the dual failure case has to be inflated in order to protect the user and still satisfy the required probability of missed detection. However, it should be noted that in case of dual constellation and dual failure, the slope equations have to be slightly modified in order to include also data from the other constellation.

2.2.3 The least detectable satellite

The satellite with the highest slope is the least detectable satellite, as it is this satellite that (in the noiseless case) has the worst ratio of position error to test statistic size. There is no reason why it should always be the least detectable satellite that fails, and it should be clear that assuming this leads to an overestimation of P_{HMI} and an underestimation of RAIM availability. Still, the assumption is widely used and applied, since it is a conservative assumption.

2.2.4 RAIM Protection Levels

There are two main methods to calculate protection levels for a RAIM algorithm. These two methods lead to slightly different results. Therefore it is important to find out which one is the best choice for the specific application. Both methods consider the slope of the least detectable satellite, which is assumed to be one that has a failure.

One way to calculate Protection Levels in the vertical and horizontal planes is described in [25] and it uses the following equations for the vertical and horizontal cases respectively:

$$VPL_{FD} = \max\{V_{slope}\} T(N, P_{fa}) + k(P_{md})\sigma_V \quad \text{Eq. 2-6}$$

$$HPL_{FD} = \max\{H_{slope}\} T(N, P_{fa}) + k(P_{md})\sigma_H \quad \text{Eq. 2-7}$$

where:

- V_{slope} and H_{slope} are the satellite error slope in the vertical and horizontal planes
- $T(N, P_{fa})$ is the test statistic threshold and it is a function of the number of satellites (N) and the desired probability of false alarm (P_{fa}). Given the probability of false alarms, the threshold is found by inverting the incomplete gamma function:

$$1 - P_{fa} = \frac{1}{\Gamma(a)} \int_0^{T^2} e^{-s} s^{a-1} ds$$

where a is the number of degrees of freedom divided by two, or in terms of the number of measurements N and unknowns M :

$$a = \frac{N - M}{2}$$

- $k(P_{MD})$ is the number of standard deviations corresponding to the specified Probability of Missed Detection. The smaller the P_{MD} value, the higher the number of standard deviations should be considered, since longer tails for the Gaussian distribution should be taken into account.

- σ_V and σ_H are the standard deviations of the error in the position domain in the vertical and horizontal plane

It should be noted that when using RAIM it is common to allocate the whole Integrity Risk and so the whole P_{md} to only one plane (vertical or horizontal) according to the specific operation. For example, for LPV-200, the whole Integrity Risk is allocated to the vertical domain, being this one the most demanding requirement.

Another method to calculate protection level is described in [11] and it still considers the slope concept, but using different equations:

$$VPL = Vslope_{max} \cdot pbias_B \quad Eq. 2-8$$

$$HPL = Hslope_{max} \cdot pbias_B \quad Eq. 2-9$$

where $Vslope_{max}$ and $Hslope_{max}$ are again the maximum slopes in the vertical and horizontal plane, while $pbias_B$ denotes the particular $pbias$ required to force the data cloud to be such that the no-detection probability is equal to the required value in the test statistic domain. $Pbias$ is a general term for the bias component of satellite range error referred to parity space: more specifically, it will always mean the magnitude of the deterministic bias component. Therefore, the parity vector can be written as $\mathbf{p} = \mathbf{p}_{deterministic} + \mathbf{p}_{noise}$ and so $pbias = |\mathbf{p}_{deterministic}|$. $Pbias_B$ can be computed as the square root of the non-centrality parameter λ of the chi-square distribution of the test statistic.

This second method usually provides a larger protection level than the first method. This can be worse in terms of accuracy, but better in terms of required probability of missed detection. However, for very good geometries, the $pbias$ concept can underestimate the true position error, leading to less conservative values of the protection level, which could eventually not satisfy the required probability of missed detection. Therefore, the choice of the best method to use strongly depends on the specific application.

It should be noted that $pbias_B$ is normalized to the σ value, because the slope is computed by multiplying the geometry factor by σ .

For both methods, in case of dual failure single failure slopes should be substituted by dual failure slopes, as described in the previous section. In this case, a larger value for protection level will be found.

2.2.5 RAIM Test Statistic

It is not possible to obtain a direct measurement of the position error. Therefore, the overall consistency of the solution has to be investigated. Provided there are more than four measurements, the system is overdetermined and cannot be solved exactly. This is why a least squares solution is performed in the first place. Since all of the conditions realistically cannot be met exactly, there is a remaining error residual to the fit. Therefore, an estimate of the goodness of the fit is required, with the assumption that if the fit was good, the error in position is most likely small. An estimate of the ranging errors from the least squares fit and the basic measurement equation is given by [25]:

$$\epsilon_{wls} = \mathbf{y} - \mathbf{G} \cdot \mathbf{x}_{wls} = (\mathbf{I} - \mathbf{G} \cdot \mathbf{K}) \cdot \mathbf{y} = (\mathbf{I} - \mathbf{P}) \cdot \mathbf{y} \quad \text{Eq. 2-10}$$

where:

$$\mathbf{P} = \mathbf{G} \cdot \mathbf{K} = \mathbf{G} \cdot (\mathbf{G}^T \cdot \mathbf{W} \cdot \mathbf{G})^{-1} \cdot \mathbf{G}^T \cdot \mathbf{W} \quad \text{Eq. 2-11}$$

From these error estimates it is possible to define a scalar measure defined as the Weighted Sum of the Squared Errors (WSSE):

$$WSSE = \epsilon_{wls}^T \cdot \mathbf{W} \cdot \epsilon_{wls} = [(\mathbf{I} - \mathbf{P}) \cdot \mathbf{y}]^T \cdot \mathbf{W} \cdot [(\mathbf{I} - \mathbf{P}) \cdot \mathbf{y}] \quad \text{Eq. 2-12}$$

which is equivalent to:

$$WSSE = \mathbf{y}^T \cdot \mathbf{W} \cdot (\mathbf{I} - \mathbf{P}) \cdot \mathbf{y} \quad \text{Eq. 2-13}$$

The square root of WSSE plays the role of the basic observable, because this yields a linear relationship between a satellite bias error and the associated induced test statistic. The test statistic can be defined in both the horizontal and vertical planes. An alternative test statistic can be calculated

also in the parity space. However, it has been showed that the magnitude of the test statistic in the parity space is equivalent to the SSE test statistic [33]. Therefore, only the weighted form of the SEE test statistic (i.e., WSSE) will be hereafter considered as test statistic.

Typically, a certain threshold, which depends on the required probability of false alarm, is selected. If the statistic exceeds that threshold, then the position fix is assumed to be unsafe. On the other hand, if the statistic is below the threshold, then the position fix is assumed to be valid.

Thus, the statistic-vertical error plane is broken up into four regions consisting of: normal operation points, missed detections, successful detections and false alarms. Ideally, there would never be any missed detections or false alarms. In reality, a certain number of missed detections and false alarms are allowed, according to the P_{md} and P_{fa} requirements respectively.

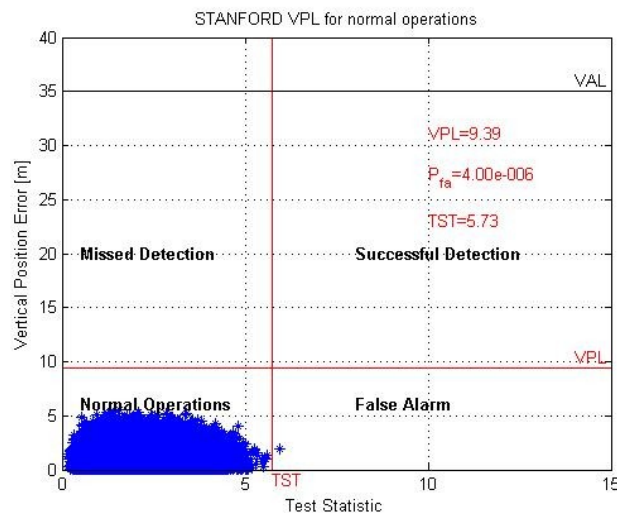


Figure 2-3: RAIM in nominal conditions

2.3 Galileo Integrity Concept

2.3.1 Overview

The integrity concept introduced by Galileo is innovative and has the aim to provide the user with a more powerful mean to check the integrity of the

system. Integrity concepts have been established and optimized for present SBAS like WAAS or EGNOS according to their required performances in terms of availability, integrity, and continuity. The performance requirements for Galileo are one order of magnitude more demanding compared to these present systems and therefore a new integrity concept, based on the established approaches, has been developed.

For Galileo a variety of user applications needs to be satisfied and neither the vertical nor the horizontal case is dominating. A combined integrity risk value is specified in the Galileo system requirements accordingly. For Galileo a ten times more stringent availability requirement compared to WAAS is specified (0.5% vs. 5% unavailability) and that the impact of a fixed split on the availability cannot be neglected. Thus, for Galileo the integrity risk is directly calculated at the Alert Limit and the result has to be below the specified Integrity Risk, which depends on the specific application. In this way, a not fixed allocation of the Integrity Risk is considered for Galileo. It has been shown in [12] that a fixed splitting is possible for availability requirements equal or below 95% but not for higher performance specifications up to 99.5% as it is required for Galileo.

The Galileo Integrity Risk computation algorithm will be part of the Galileo Safety-of-Life (SoL) service, which will add Integrity to the Galileo Open Service (OS). It is not clear yet if SoL service will be freely available to every user and when will be finally deployed, since OS has now the priority.

2.3.2 Galileo Ground Segment

Beside the global satellite network consisting of 27 satellites (plus three inactive spares) Galileo has the capability to monitor the satellite behaviour through its complex global distributed ground network consisting of more than 30 sensor stations. Taking these measurements into account satellite failures (orbit or clock) can be detected and alerts can be disseminated to the user.

The system takes care of always monitoring the constellation and to transmit in broadcast to the user information about the health status of each satellite through a three states flag (Integrity Flag) related to each satellite. The monitoring process is realised by a stations network (GSS stations) located all around the globe. This network carries out pseudorange measurements from every satellite and, through an inverse navigation algorithm, estimates the pseudorange error relevant to each satellite (*SISE: Signal In Space Error*). The estimation (*estimated-SISE*) carried out represents the range error contribution due to the satellite contribution, which impact on the user

solution. This estimation process unfortunately introduces another error that in the Galileo Integrity Concept has been assumed, according to an overbounding process, Gaussian with zero mean value.

2.3.3 Galileo Integrity equation

2.3.3.1 Definitions

The system supplies to the user three parameters related to each satellite of the Galileo constellation:

- *SISA (Signal In Space Accuracy)*, defined as the minimum standard deviation of the unbiased Gaussian distribution which overbounds the distribution of the SISE
- *SISMA (Signal In Space Monitoring Accuracy)*, defined as the minimum standard deviation of the unbiased Gaussian distribution which overbounds the error distribution of the estimation of SISE as determined by the integrity monitoring system
- *IF (Integrity Flag)*, a three states flag (“Use”/“Don’t Use”/“Not Monitored”) which describes the satellite health status.

Through this information the user receiver is able to run the *HPCA (HMI Probability Computation Algorithm)* and to carry out the integrity and continuity performances. So, to finally decide if a critical operation can be started, the user has to calculate its local Integrity Risk through the HPCA.

Both SISA and SISMA are conservatively defined at the worst user location (WUL), which is the location where the Signal in Space error (SISE) is maximum.

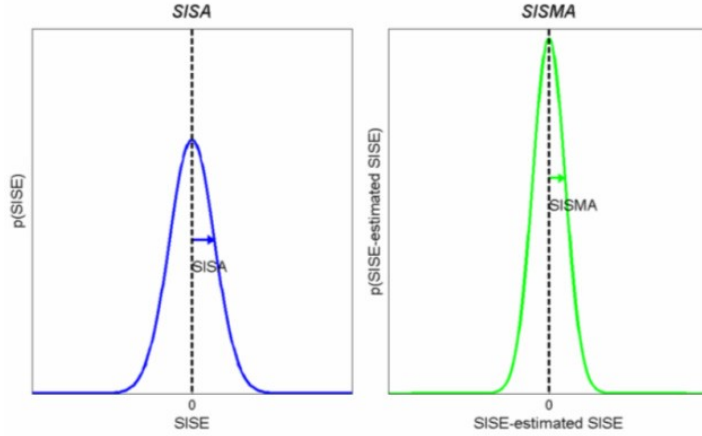


Figure 2-4: Graphical illustration of SISA and SISMA

The SISE is assumed to be a Gaussian distribution. In particular the distribution of the SISE is, in case of fault-free and single failure, respectively:

$$P_x(x) = \frac{1}{\sqrt{2\pi} \cdot SISA} e^{-\frac{1}{2} \left(\frac{x}{SISA}\right)^2} \quad \text{Eq. 2-14}$$

$$P_x(x) = \frac{1}{\sqrt{2\pi} \cdot SISMA} e^{-\frac{1}{2} \left(\frac{x-TH}{SISMA}\right)^2} \quad \text{Eq. 2-15}$$

Therefore:

$$\begin{aligned} SISE &\sim N(0, SISA) && \text{fault-free} \\ SISE &\sim N(TH, SISMA) && \text{faulty-mode (single failure)} \end{aligned}$$

where TH represents a conservative estimation of the bias magnitude in the faulty-mode.

Nominal values for SISA and SISMA have been assessed to be 0.85 meters and 0.70 meters respectively [30]. However, these values could be increased in case of degradations in the Ground Segment or in the signal.

2.3.3.2 Integrity at the User level

The integrity at user level is carried out by the receiver in terms of HMI probability, which depends on the user constellation geometry (after excluding all the satellites with flag “Don’t Use”), on the SISA value (used to model the SISE in fault-free conditions), on the SISMA value (for modelling the error in case of single failure), and of course it is a function of the receiver error too.

The HMI probability is composed of two parts. The first one takes into account the scenario in which all the satellites of the constellation with flag “Use” are transmitting correct signals (Fault-Free). The second one considers the possibility that one satellite with flag “Use” is failed (Faulty-Mode). Both these two terms are divided in a horizontal and in a vertical component.

The probability that more than one satellite at each instance in time is faulty but not detected is negligible for the user equation. Multiple and common failures are allocated in another branch of the integrity tree including not detected SISA and SISMA failures. Therefore these events are not allocated to the user integrity equation. The combined user integrity risk is then computed using the following equation [13]:

$$\begin{aligned}
 P_{HMI}(VAL, HAL) &= P_{HMI,V,FF} + P_{HMI,H,FF} + P_{HMI,V,FM} + P_{HMI,H,FM} \\
 &= 1 - \operatorname{erf}\left(\frac{VAL}{\sqrt{2} \cdot \sigma_{u,V,FF}}\right) + e^{-\frac{HAL^2}{2\sigma_{u,H,FF}^2}} \\
 &\quad + \sum_{j=1}^N P_{fail,sat_j} \left[\frac{1}{2} \left(1 - \operatorname{erf}\left(\frac{VAL + \mu_{u,V}(j)}{\sqrt{2} \cdot \sigma_{u,V,FM}(j)}\right) \right) + \frac{1}{2} \left(1 - \operatorname{erf}\left(\frac{VAL - \mu_{u,V}(j)}{\sqrt{2} \cdot \sigma_{u,V,FM}(j)}\right) \right) \right] \\
 &\quad + \sum_{j=1}^N P_{fail,sat_j} \left(1 - \chi_{2,\delta_{u,H}}^2 \operatorname{cdf}\left(\frac{HAL^2}{\sigma_{u,H,FM}^2(j)}\right) \right)
 \end{aligned}$$

Eq. 2-16

where:

for the vertical case with the error function:

$$\text{erf}(u) = \frac{2}{\sqrt{\pi}} \int_0^u e^{-x^2} dx$$

and for the horizontal case with the cumulative distribution function of the non-central Chi-Squared distribution with two degrees of freedom (with non-centrality parameter δ)

$$\chi_{2,\delta}^2 \text{cdf}(x) = \int_0^x \chi_{2,\delta}^2 \text{pdf}(t) dt$$

$$\chi_{2,\delta}^2 \text{pdf}(x) = \frac{1}{2} e^{-\frac{1}{2}(x+\delta)} \sum_{j=0}^{\infty} \frac{x^j \delta^j}{2^{2j} (j!)^2}$$

The further needed fault-free and faulty vertical standard deviations can be computed by (M_{topo} is the typical topocentric weighted design matrix used for least squares position estimation):

$$\sigma_{u,V,FF}^2 = \sum_{i=1}^N M_{topo}[3,i]^2 (SISA_i^2 + \sigma_{loc,i}^2)$$

$$\sigma_{u,V,FM}^2(j) = \sum_{i=1}^N M_{topo}[3,i]^2 (SISA_i^2 + \sigma_{loc,i}^2) + M_{topo}[3,j]^2 (SISMA_j^2 - SISA_j^2)$$

respectively for the horizontal case by

$$\sigma_{u,H,FF}^2 = \frac{\sigma_{u,FF,nn}^2 + \sigma_{u,FF,ee}^2}{2} + \sqrt{\left(\frac{\sigma_{u,FF,nn}^2 - \sigma_{u,FF,ee}^2}{2} \right)^2 + \sigma_{u,FF,ne}^2}$$

$$\sigma_{u,FF,nn}^2 = \sum_{i=1}^N M_{topo}[1,i]^2 (SISA_i^2 + \sigma_{loc,i}^2)$$

$$\sigma_{u,FF,ne}^2 = \sum_{i=1}^N M_{topo}[1,i] \cdot M_{topo}[2,i] (SISA_i^2 + \sigma_{loc,i}^2)$$

$$\sigma_{u,FF,ee}^2 = \sum_{i=1}^N M_{topo}[2,i]^2 (SISA_i^2 + \sigma_{loc,i}^2)$$

$$\sigma_{u,H,FM}^2(j) = \frac{\sigma_{u,FM,nn}^2(j) + \sigma_{u,FM,ee}^2(j)}{2} + \sqrt{\left(\frac{\sigma_{u,FM,nn}^2(j) - \sigma_{u,FM,ee}^2(j)}{2}\right)^2 + \sigma_{u,FM,ne}^2(j)}$$

$$\sigma_{u,FM,nn}^2(j) = \sum_{i=1}^N M_{topo}[1,i]^2 (SISA_i^2 + \sigma_{loc,i}^2) + M_{topo}[1,j]^2 (SISMA_j^2 - SISA_j^2)$$

$$\sigma_{u,FM,ne}^2(j) = \sum_{i=1}^N M_{topo}[1,i] \cdot M_{topo}[2,i] (SISA_i^2 + \sigma_{loc,i}^2) + M_{topo}[1,j] \cdot M_{topo}[2,j] (SISMA_j^2 - SISA_j^2)$$

$$\sigma_{u,FM,ee}^2(j) = \sum_{i=1}^N M_{topo}[2,i]^2 (SISA_i^2 + \sigma_{loc,i}^2) + M_{topo}[2,j]^2 (SISMA_j^2 - SISA_j^2)$$

where the index j indicates the faulty satellite.

The biases b_j at the thresholds TH_j ($b_j = TH_j$) are taken into account by

$$\begin{pmatrix} \infty_{u,n} \\ \infty_{u,e} \\ \infty_{u,v} \end{pmatrix} = \begin{pmatrix} M_{topo}[1,j] \cdot b_j \\ M_{topo}[2,j] \cdot b_j \\ M_{topo}[3,j] \cdot b_j \end{pmatrix}$$

and with it the non-centrality parameter δ

$$\delta_{u,H} = \begin{pmatrix} \infty_{u,n} & \infty_{u,e} \end{pmatrix} \cdot \begin{pmatrix} \xi_{FM}^2 & 0 \\ 0 & \xi_{FM}^2 \end{pmatrix} \cdot \begin{pmatrix} \infty_{u,n} \\ \infty_{u,e} \end{pmatrix}$$

The threshold TH_j for satellite j can be easily computed by the disseminated integrity information $SISA_j$ and $SISMA_j$ for that satellite and the allowed false alert probability k_{Pfa} (typical $k_{Pfa} = 5.212$):

$$TH_j = k_{Pfa} \cdot \sqrt{SISA_j^2 + SISMA_j^2}$$

Eq. 2-17

Considering the nominal values for SISA and SISMA, the previous equation gives a value of 5 meters. Therefore, the faulty-case foresees an undetected bias, whose typical magnitude is 5 meters, that affects the SISE estimation process. This means that, if the HMI Probability is below the Integrity Risk requirement, the user is protected even in case of an undetected failure on one satellite with a maximum magnitude of 5 meters. On the other hand, biases with greater magnitude are more likely to be detected by the Ground Segment, but they could be undetected in case of larger, degraded values of SISA and SISMA.

If the HMI probability exceeds the Integrity Risk allocated at user level, the receiver generates an alert in order to stop immediately the current critical operation.

The continuity performances are carried out by counting the number of critical satellites present in the current user geometry. This means that the receiver has to run N times (where N is the number of satellite in visibility with Integrity Flag "Use") the HPCA algorithm and takes care to number how many geometries lead to a HMI probability exceeding the specified threshold. When the number of critical satellites is over a certain threshold specified at system level, it is equivalent to say that the Discontinuity Risk exceeds the specified value and the requirements are not met. In this case the receiver has to timely warn the user. A critical satellite is defined as a satellite in the current user geometry whose loss or exclusion will unconditionally lead to exceed the tolerated HMI probability threshold in any integrity critical operation period.

Chapter 3

GPS integrity applications: GPS with RAIM algorithms

Galileo will be able to provide the integrity service in a stand-alone configuration, while current GPS needs augmentation systems such as SBAS or performing autonomous monitoring of the integrity through RAIM algorithms.

Two analyses have been carried out in this work in order to verify the performance of the current integrity implementations for GPS in combination with the European SBAS system, EGNOS, and with RAIM algorithms. In this way, the current integrity concept has been exploited and this study represents a good starting point for possible future developments in the new Galileo integrity concept.

The analysis that will be described in this chapter aims to explore RAIM potentiality to provide integrity at the user level without a complex and high cost ground segment and a simple implementation. This analysis will be performed for precision approach applications. Therefore, LPV-200 requirements will be considered. This analysis will then be extended in the last chapter to include also the Galileo system.

3.1 Overview of the analysis

This analysis deals with the simplest method to provide integrity using a GPS system in combination with autonomous user integrity algorithms. In presence of a failure, the RAIM algorithm should be able to raise an alarm in order to warn the user that the computed position is not safe for the specific application. This is done by properly setting the Protection Level and the test statistic. A RAIM is designed to satisfy the required probability of missed detection, therefore a certain number of missed detections are allowed.

Several methods to calculate protection level will be considered. The common base-line as well as the algorithm flow-chart are shown in the next two pictures. It should be noted that only the vertical case will be considered, because for precision approaches the vertical requirement is more stringent than the horizontal one.

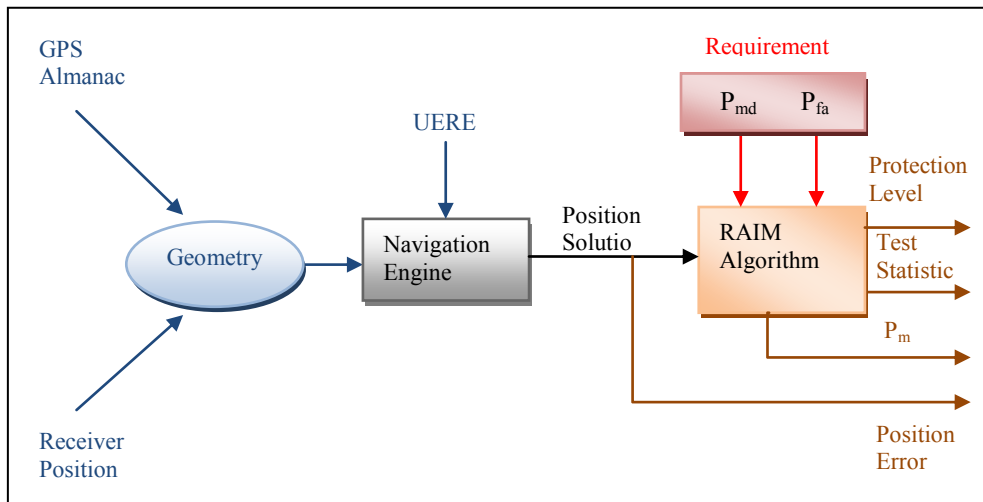


Figure 3-1: GPS+RAIM algorithm base-line

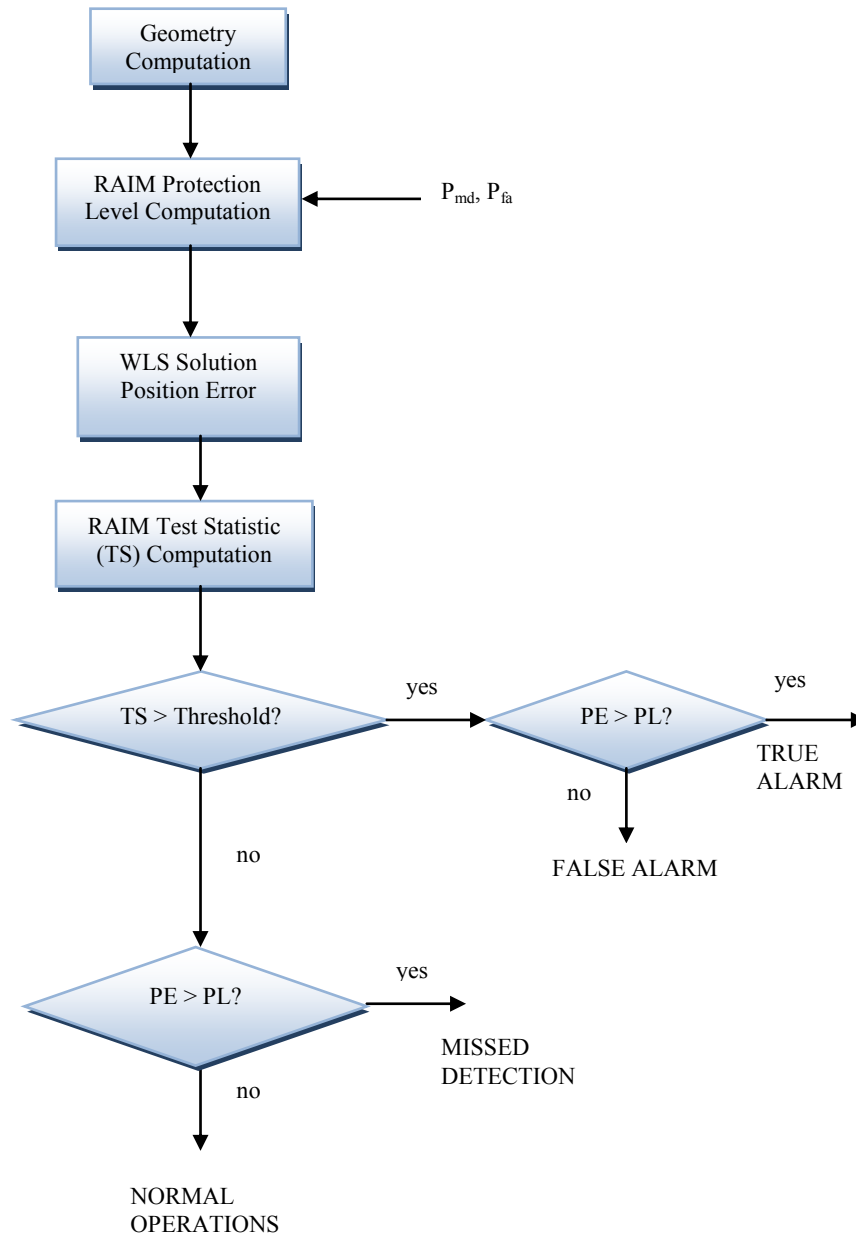


Figure 3-2: GPS+RAIM algorithm flow-chart

In the following tests, several geometries using a fixed receiver and different satellite positions will be considered. Geometries are computed from GPS Almanacs at different epochs and for different positions of the receiver on the Earth. However, in the following sections only results for a single specific geometry will be shown with several RAIM algorithms in different conditions: nominal (no failures), single failure and dual failures. Several software modules have been developed in order to get data from GPS almanacs and to calculate the relevant parameters for testing RAIM algorithms. However, the whole software will be deeply described in chapter 5, since the modules that are used in this section are just a small part of the complete software that has been developed.

In order to have a statistically significant level of confidence, a large number of Monte-Carlo trials should be performed for each geometry. Indeed, the number of trials that are needed to satisfy the required confidence level and margin of error are given by [22]:

$$n = \left(\frac{z}{2e}\right)^2$$

Eq. 3-1

Where n is the number of trials, z is a factor that depends on the confidence level, e is the margin of error. The following table contains values of z for some common confidence levels:

| Confidence Level | z |
|------------------|------|
| 95% | 1.96 |
| 99% | 2.58 |
| 99.9% | 3.29 |

Table 3-1: Values of z factor for some common confidence levels

Therefore, for a confidence level of 99% and a margin of error of 5% on a Probability of Missed Detection equal to 10^{-3} , the total number of trials per geometry should be:

$$\left(\frac{3.29}{2 \times 0.00005}\right)^2 = 1,082,410,000 \text{ trials per geometry}$$

Due to the high computational load, the number of trials has been reduced to 250000. This number comes out from several independent tests that have been successfully performed. Thus, in order to satisfy the probability of missed detection of 10^{-3} /sample, the maximum number of position errors exceeding the protection level should be equal to or less than 250. By counting the number of missed detections over all the random trials it is possible to know the probability of missed detections for the specific geometry and compare it with the required value. The computed P_{md} is then compared with the theoretical value given by the following expression:

$$P_{md} = \Pr(VPL < VPE) \cdot \Pr(TestStat < Threshold) \tag{Eq. 3-2}$$

It is expected that the computed P_{md} is very close to the theoretical value, even if the number of Monte Carlo trials that are performed is less than required for a confidence level of 99% and a margin of error of 5%.

The general test conditions are summarised in the next table.

| General Test Conditions Single Constellation | |
|--|--|
| GPS Almanac | 012.AL3 (SEM format) 2008 |
| GPS week | 1462 |
| GPS seconds of the week | 157456 |
| Probability of Missed Detection | 1×10^{-3} /sample |
| Probability of False Alarm | 4×10^{-6} /sample |
| UERE | Values depend on elevation angles |
| Noise | $\sim N(0, UERE)$ |
| Mask angle | 5 degrees |
| Receiver position (ECEF coordinates) | [1767224.327927657, 5373526.074516900, 2937637.435886630] meters |
| Number of random trials | 250,000 |
| Vertical Alert Limit | 35m (LPV-200) |

Table 3-2: General test conditions for testing RAIM algorithms (single constellation)

On the other hand, GPS UERE values were computed from the following look-up table. These values, which depend on elevation angles, were obtained from independent tests and analyses and could be overly conservative. Indeed, smaller UERE values are expected for modernised GPS.

| GPS UERE budget | | | | | | | | | | |
|-----------------|-----------------------|-----|------|------|------|------|------|------|------|------|
| | Elevation angle (deg) | | | | | | | | | |
| UERE | 0 | 5 | 10 | 15 | 20 | 30 | 40 | 50 | 60 | 90.1 |
| (m) | 1.9 | 1.9 | 1.36 | 1.15 | 1.04 | 0.96 | 0.93 | 0.92 | 0.91 | 0.91 |

Table 3-3: GPS UERE values

3.2 Worst Case Bias

The worst case bias (WCB) is the bias that maximises the missed detection probability (Figure 3-3). In case of dual failure, the worst case couple of biases can be defined in the same manner.

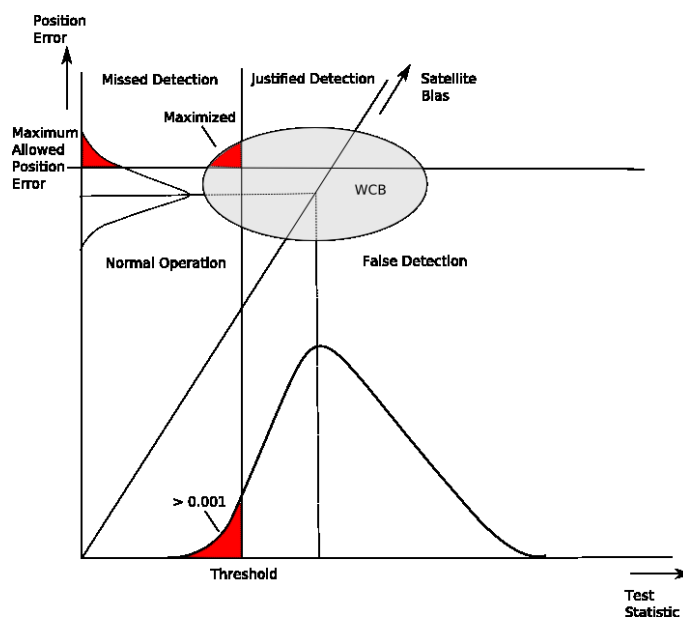


Figure 3-3: Worst Case Bias

In the following tests, for the single failure case, it will be conservatively assumed that the worst case bias is affecting the least detectable satellite. On the other hand, in the dual failure cases it is assumed that the worst pair of bias is affecting the least detectable pair of satellites. In both cases, the worst case biases can be found numerically, by calculating for each bias or pair of biases the resulting P_{md} , with bias values ranging from -20 to 20

metres. However, in the dual failure case this could be computationally involved. Therefore, in the dual failure case the search of the worst pair of biases is restricted to the pairs whose ratio k_{bias} is given by [16]:

$$k = k(i, j) = \frac{b_i}{b_j} = \frac{A_{3i}U_{jj} - A_{3j}U_{ij}}{A_{3j}U_{ii} - A_{3i}U_{ij}}$$

Eq. 3-3

where:

$$\begin{cases} A = (G^T G)^{-1} G^T \\ B = G (G^T G)^{-1} G^T \\ U = I_n - B \end{cases}$$

In this way for each couple of satellites only the pair of biases whose combination maximises the position error is considered.

3.3 Nominal conditions: no failures

When all satellites are behaving nominally, the error ellipse should ideally be in the nominal operations region, even if a certain number of false alarms are allowed, according to the required probability of false alarm. In order to be statistically accurate, this test should consider a number of trials much larger than 250,000. In this way it is possible to accommodate the required probability of false alarm. However, since in this framework it is important to test RAIM capability to detect satellite failures, this analysis is not relevant at the moment and will be neglected.

The next picture shows the RAIM nominal behaviour with 250,000 random trials under the same test conditions that will be adopted for the single failure case (Table 3-2 and Table 3-3), but with no failures and considering only one method to calculate the protection level (i.e., Stanford VPL).

As expected, the error ellipse is in the “Normal Operations” region and the P_{fa} requirement is satisfied. However, as stated before, this result for the false alarm rate is not accurate, since a higher number of random trials would be required to confirm it.

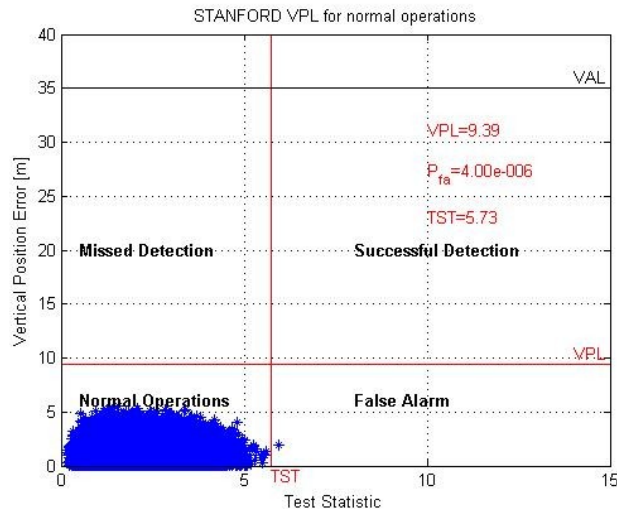


Figure 3-4: RAIM in nominal conditions

3.4 Single failure

A single failure can be detected by a traditional RAIM algorithm by setting properly the protection levels. The required probability of missed detection should be satisfied. This means that the protection level should be computed in order to guarantee that the maximum position error doesn't exceed the protection level more than required by the probability of missed detection.

Two different methods to calculate protection levels have been considered: the first one is the Stanford method (Eq. 2-6), while the second one uses the *pbias* concept (Eq. 2-8, Brown's method). In both cases it is conservatively assumed that the least detectable satellite (i.e., the satellite with the highest slope) is affected by the worst case bias (i.e., the bias that maximises the probability of missed detection). The worst case bias is found numerically running several simulations for different biases: the bias that provides the maximum probability of missed detection is then the worst case bias.

In the next simulations, a step function representing the worst case bias is added to the pseudorange of the least detectable satellite. The bias is not added to the Signal in Space noise, but directly to the final pseudorange at the user level, because it has to represent a failure that has not been detected by the Ground Segment. The general test conditions are given in Table 3-2 and Table 3-3, while specific simulation data are shown in the next table.

| Simulation Data 1 failure single constellation | |
|--|---|
| Bias | Worst case bias on the least detectable satellite |
| Number of satellites in view | 9 |
| Protection Level 1 st case | $VPL = Vslope_{max} T(N, P_{fa}) + k(P_{md})\sigma_V$ |
| Protection Level 2 nd case | $VPL = Vslope_{max} \cdot pbias_B$ |
| P_{md} 1 st case | 5.12×10^{-4} (computed) / 5×10^{-4} (theoretical) |
| P_{md} 2 nd case | 4×10^{-6} (computed) / 1.73×10^{-6} (theoretical) |

Table 3-4: Simulation data (single failure, single constellation)

The results of the performed analysis are shown in the next figures, where the error ellipse is plotted for all the random trials of a selected geometry. As it can be seen, the ellipse is centred on the slope of the biased satellite and it moves along it if the bias magnitude changes.

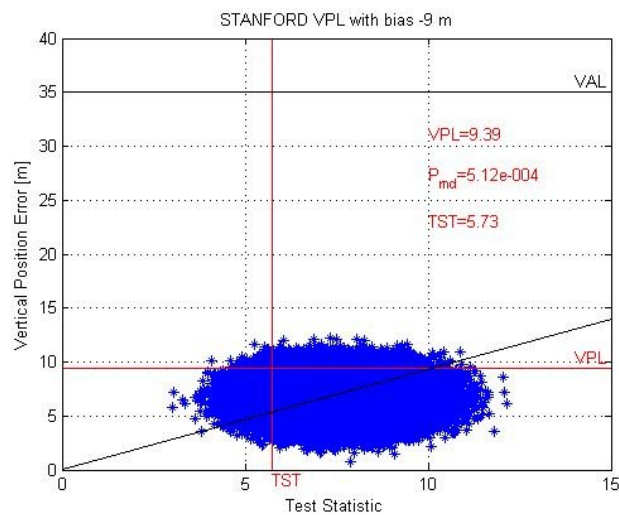


Figure 3-5: RAIM with a bias of -9 meters on the least detectable GPS satellite – Stanford VPL

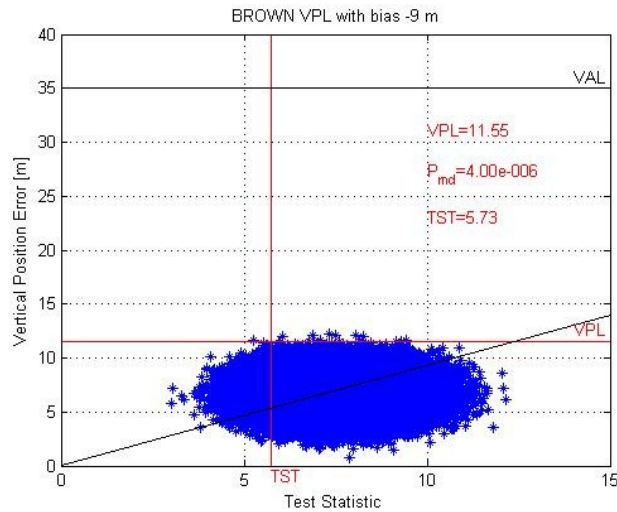


Figure 3-6: RAIM with a bias of -9 meters on the least detectable GPS satellite – Brown's VPL

In both cases, the required probability of missed detection is satisfied, but the second method looks overly conservative in terms of probability of missed detection, providing a larger protection level. This could represent a problem in terms of availability, especially for worse geometries with fewer satellites in view. However, since for LPV-200 and APV-II the required alert limit is far above the computed value of protection level, this, in general, does not represent an issue for these two categories.

Therefore, for LPV-200 and APV-II applications and in case of single failure on the least detectable GPS satellite, both methods are able to properly protect the user. On the other hand, for more demanding categories, such as CAT-I (VAL=10 m), the system is very close to be unavailable in both cases. It should also be noted that in both cases the computed value of the probability of missed detection (calculated by counting the number of missed detections over all the random trials) has the same order of magnitude of the analytical value obtained using Eq. 3-2. This confirms the statistical approach that has been used.

3.5 Dual failure

Traditional RAIM algorithms were not designed to detect two simultaneous failures. This is due to the fact that the probability of having two simultaneous failures on the same system is very small, as seen in the

previous chapters. However, it is basically possible to extend conventional RAIMs to the multiple failures case. This could be done by inflating the Protection Level in order to bound the increased position error. Indeed, in the dual failure cases, as shown in the previous chapter, the maximum slope to be considered is now the one given by the worst pair of satellites. As seen before, there are different techniques to calculate the dual failure slope. However, the problem is that, as shown in [14], this new slope is much larger than the highest slope in the single failure case. This means that the protection level is much larger now and this dramatically affects the system availability.

As an example, the next figures show the results using four different methods: in the first one the protection level is computed using the Stanford method, but with the dual failure slope as given in Angus [15]; in the second and in the third method the dual failure slope is computed according to Brown [14], but in one case the VPL is computed using the Stanford equation and in the other using the *pbiasb* concept. Finally, in the fourth case the dual failure slope is computed following Liu [16] and using again the *pbiasb* concept. As for the single failure case, it is assumed that the worst case biases are on the least detectable pair of satellites. The worst case pair of biases is found again numerically by running several simulations for different couple of biases whose ratio is given by Eq. 3-3. The pair of biases that provides the maximum probability of missed detection is the worst pair. In some cases the methods were slightly modified in order to include the weights also in the slope computation. The general test conditions are the same of the single failure case (Table 3-2 and Table 3-3) and the specific simulation data are summarised in the next table.

| Simulation Data 2 failures single constellation | |
|---|---|
| Bias | Worst case biases on the least detectable pair of satellites |
| Number of satellites in view | 9 |
| Protection Level 1 st case | $VPL = Vslope^1_{maxmax} T(N, P_{fa}) + k(P_{md})\sigma_V$ |
| Protection Level 2 nd case | $VPL = Vslope^2_{maxmax} T(N, P_{fa}) + k(P_{md})\sigma_V$ |
| Protection Level 3 rd case | $VPL = Vslope^2_{maxmax} \cdot pbias_B$ |
| Protection Level 4 th case | $VPL = Vslope^3_{maxmax} \cdot pbias_B$ |
| P _{md} 1 st case | 1.2x10 ⁻² (computed) / 1.2x10 ⁻² (theoretical) |
| P _{md} 2 nd case | 3.49x10 ⁻² (computed) / 3.5x10 ⁻² (theoretical) |
| P _{md} 3 rd case | 0 (computed) / 0 (theoretical) |
| P _{md} 4 th case | 0 (computed) / 0 (theoretical) |

Table 3-5: Simulation data (dual failure, single constellation)

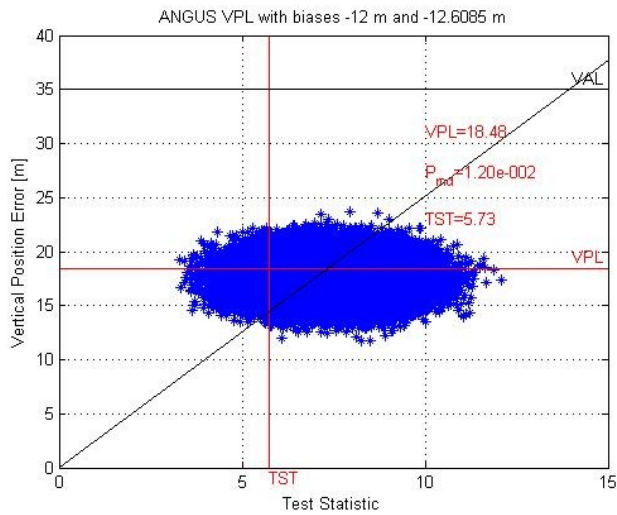


Figure 3-7: RAIM in dual failure case: Angus VPL

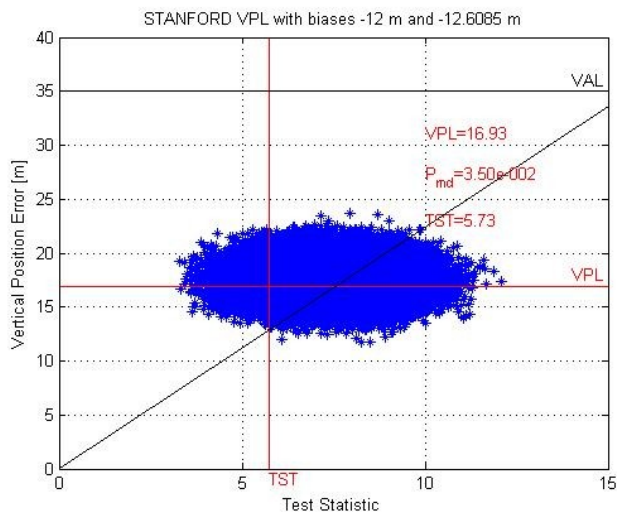


Figure 3-8: RAIM in dual failure case: Stanford VPL

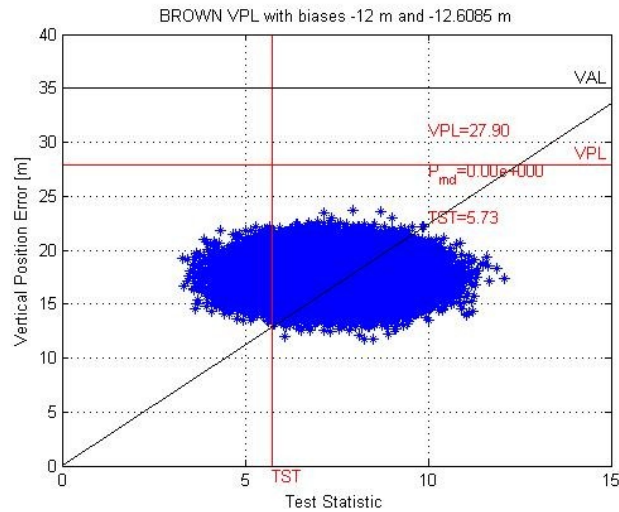


Figure 3-9: RAIM in dual failure case: Brown VPL

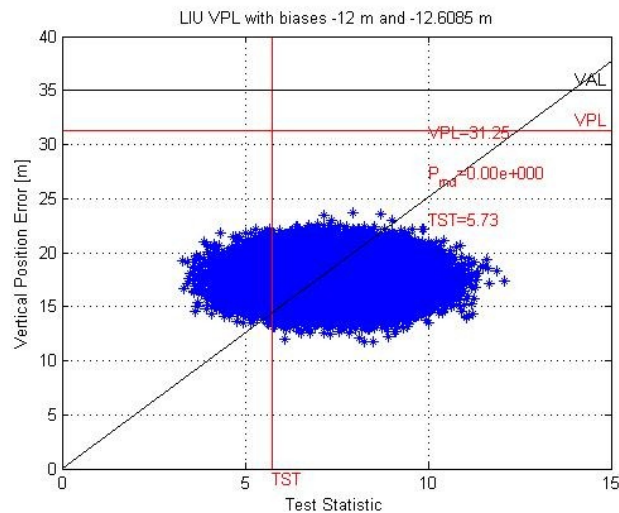


Figure 3-10: RAIM in dual failure case: Liu VPL

As it can be seen, these schemes don't provide integrity. Indeed, in the first two methods the required probability of missed detection is not satisfied. The other two methods satisfy the probability of missed detection, but this is affecting a lot the availability, since the protection level is very close to the alert limit value for LPV-200.

Also in this case, the computed values of the probability of missed detection are very close to the theoretical ones given by Eq. 3-2. It should also be noted that the method using the *pbiasb* concept (Brown and Liu) are again

more conservative than the methods using the Stanford VPL equation (Angus and Stanford).

In conclusion, as expected, a RAIM algorithm with a single constellation is providing limited integrity in the dual failure case.

Chapter 4

GPS Integrity applications: GPS with EGNOS

Satellite Based Augmentation System (SBAS) provides integrity to GPS users. The European Geostationary Navigation Overlay Service (EGNOS) is a satellite based augmentation system (SBAS) recently developed by the European Space Agency, the European Commission and EUROCONTROL. It is intended to supplement the GPS, GLONASS and Galileo (when it becomes operational) systems by reporting on the reliability and accuracy of the signals. According to specifications, horizontal position accuracy should be better than 7 meters. In practice, the horizontal position accuracy is at the meter level. It consists of three geostationary satellites and a network of ground stations. The system started its initial operations in July 2005, being fully operational in late 2006 and showing outstanding performances in terms of accuracy (better than 2 meters) and availability (above 99%); it is intended to be certified for use in safety of life applications in 2008.

Similar service is provided in North America by the Wide Area Augmentation System (WAAS), and in Asia, notably Japan, by the Multi-functional Satellite Augmentation System (MSAS).

The following analysis will explore EGNOS potentiality to protect user from GPS satellites failures. In particular, an original technique will be here introduced in order to analyse the EGNOS reaction in presence of clock anomalies on the GPS satellites.

4.1 Overview of the analysis

In this section a particular scenario has been considered: during years 2006 and 2007, the European Space Agency recorded abnormal behaviours of GPS satellites. Indeed, GPS satellites were affected by several clock anomalies and, without a proper augmentation system, the user could suffer

of an unacceptable position error [19]. Thus, EGNOS was required to protect the user in terms of integrity, keeping the position error low and always bounded by the Protection Levels. In the next sections an original technique to analyse the effect of these anomalies and the EGNOS reaction to them in terms of integrity will be presented, including also the results. This work has been performed in collaboration with the Research Group of Astronomy and Geomatics, Universitat Politècnica de Catalunya (gAGE/UPC), Barcelona, Spain and the European Space Agency. The processing of the GPS and EGNOS signals was performed at Universitat Politècnica de Catalunya (UPC), in Barcelona, using the Basic Research Utilities for SBAS (BRUS [21], gAGE/UPC) and Linux workstations. BRUS is a software package, designed to be in compliant with RTCA/MOPS, and it was developed by gAGE/UPC. One of its main characteristics is the ability to provide wide information about the applied SBAS messages and how the corrections are internally processed.

This analysis aims to show EGNOS potentialities to protect users by applying proper corrections or by eventually excluding a failed satellite from the solution. In this analysis it is also shown how EGNOS Protection Level is properly set in order to bound the position error.

So, the whole analysis was performed in the following steps:

- For all the days in 2006 and 2007, the broadcast clock values for each GPS satellite were compared with a precise reference (<ftp://ftp.unibe.ch>). If the rms value of the difference during the whole day was larger than 10 ns, a clock anomaly was found. In this step, it was also checked the healthy status of the satellites in the GPS navigation message.
- For all the days with clock anomalies, the position error (vertical and horizontal) and the prefit-residuals in GPS Stand-Alone mode and in combination with EGNOS were computed. The prefit-residual is the difference between the measured pseudorange and the modelled pseudorange. In the case of GPS Stand-Alone, the Position Error was computed with and without the “failed” satellite, to verify if without the “failed” satellite the Position Error was significantly lower
- The EGNOS behaviour was assessed by:
 - Checking if the user is protected by either:
 - Correcting the error or

- Warning the user about not using the “failed” satellite to compute the position.
- Checking the Protection Levels.
- Checking the prefit residuals and verifying that EGNOS corrections matched the position error due to the “failed” satellite.
- Finally, to assess the integrity at the user level, the Stanford-ESA Integrity Diagrams were generated.

As it can be seen, this analysis has been performed both at the Signal In Space level and at the user level, in order to give clear and complete results. The last two steps were performed using the fixed receiver in Barcelona, but in many cases the computation was also repeated for other stations in Europe (Toulouse, Delft, Lisbon, Budapest and Sofia), in order to have a more general view of the results.

A flow-chart of the complete analysis is shown in the next figure.

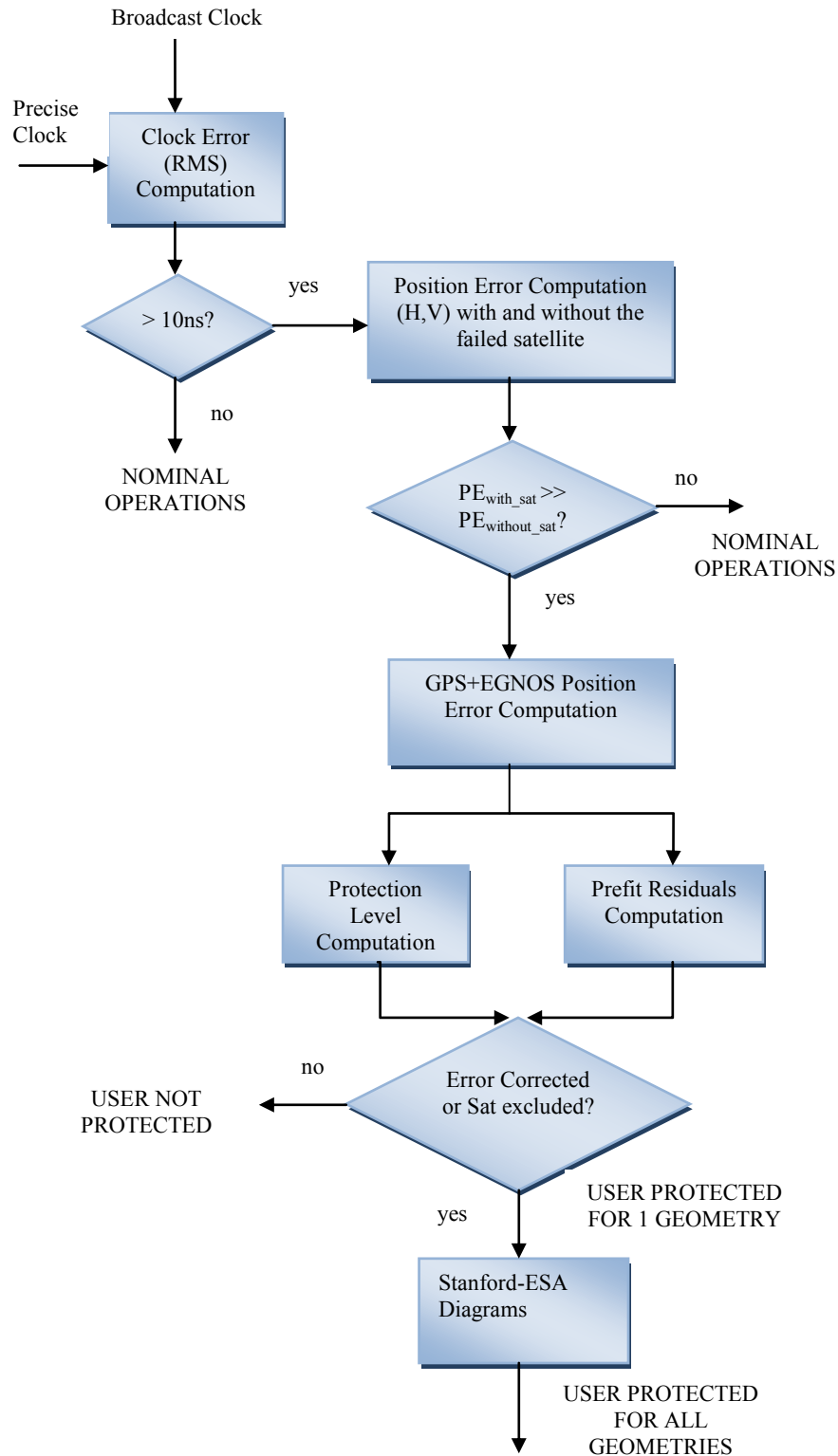


Figure 4-1: EGNOS clock anomalies analysis flow-chart

4.2 Effects of satellite clock anomalies at the Signal In Space level

A GPS clock anomaly is here defined as a divergence between the real and the broadcast satellite clock parameters value, without any warning in the navigation message (i.e., unhealthy status flag not set in the navigation message). Indeed, it can happen that the Ground Segment is not able to correctly estimate and predict the value of the GPS satellite clock parameters. That could be caused either by a physical anomaly in the satellite clock, that suddenly causes large drifts and drifts rates, or by a problem with the Ground Segment, which is unable to follow a “normal” behaviour of the satellite clock. Whatever the reason is, the problem here is that the final user gets wrong information about the value of the GPS clock and consequently a wrong position, without being warned.

In order to have an idea of such divergence, the clock parameters broadcast in the GPS navigation message can be compared *a posteriori* with a precise reference and the corresponding clock rms error for the full day computed. Thus, it can happen that even in presence of a large clock rms error (i.e., broadcast clock parameters much different from the real clock parameters), the corresponding satellite is flagged as “healthy” in the GPS navigation message and used to calculate the position. This represents a potential risk for the user: indeed, an undetected clock anomaly has a direct effect at the Signal In Space level, increasing the pseudorange error. For instance, a clock rms error for the full day of just 10 ns already corresponds to a range error of 3 m. Moreover, there could be also short intervals of epochs in which the divergence between the real and broadcast clock values leads to range errors of hundreds of meters, without the user being warned.

The next figure shows the effect of a clock anomaly at the Signal In Space level: the clock rms error for satellite PRN 30 for the full day is 115,97 ns, which corresponds to a 34.79 meters rms range error, which is very high. The figure also shows a peak of error of more than 150 meters for a short time interval at the end of the day. This situation is truly a potential risk for the user, because this clock anomaly, not detected by the Ground Segment, will mainly contribute to a large position error in a GPS Stand-Alone system, as it will be seen in the next section.

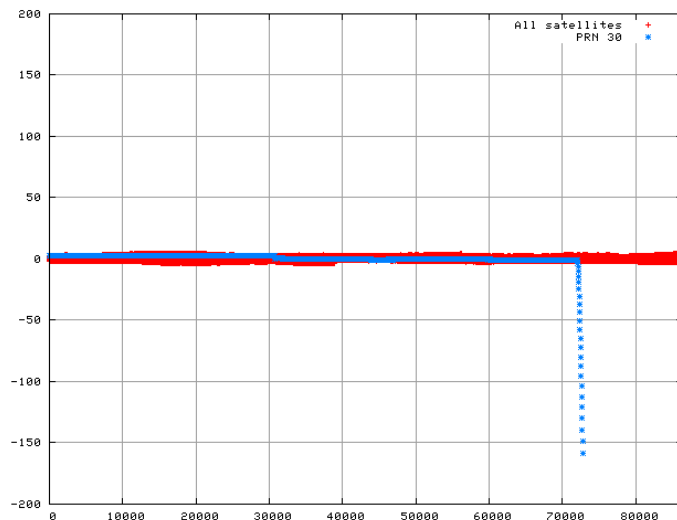


Figure 4-2: Effect of a clock anomaly at the Signal In Space level. On the horizontal axis there are the seconds of the day, on the vertical axis the resulting range error in meters.

The clock anomaly on the satellite PRN 30 generates a very large error in the range domain (blue points), with a peak of more than 150 meters for a short time interval at the end of the day.

4.3 Effects of satellite clock anomalies at the user level

The effect of a clock anomaly at the Signal In Space level corresponds to an effect on the computed position at the user level. The entity of the resulting position error depends on many factors, since the calculated position is affected by different contributions of error, as clock modelling errors, specific receiver geometry, multipath and so on. Thence, the error due to a clock error can be amplified or reduced at the user level, according to the different conditions of the receiver station and to the weight of the satellites in the position computation. This means that it is not easy to identify a clock anomaly only looking at the user domain, but it is also necessary a deep analysis at the Signal In Space level, as done in the previous section. Anyway, a clock anomaly not detected by the Control Segment in a GPS Stand-Alone system can cause position errors of more than 50 meters in at least one of the two planes (horizontal and vertical) and this represents an extremely dangerous situation, especially in critical operations. Indeed, this magnitude of error in the position domain is larger than the alert limits for APV-II and LPV-200 categories in both horizontal and vertical planes.

The effect of the previous clock anomaly at the user level is shown in the next two figures. Since the satellite PRN 30 is flagged as “healthy” in the GPS navigation message, it is used to compute the position in a GPS Stand-Alone system. In the time interval in which the divergence between the real and broadcast clock values reaches a peak of more than 150 m in range, the resulting error in the position domain (red points) becomes very large, around 50 meters in the horizontal plane (Figure 4-3) and 40 meters in the vertical (Figure 4-4). In order to emphasize the effect of the clock anomaly at the user domain, the satellite PRN 30 has been also manually excluded from the solution and the corresponding position error, which is now highly reduced, has been plotted in the same figures (blue points).

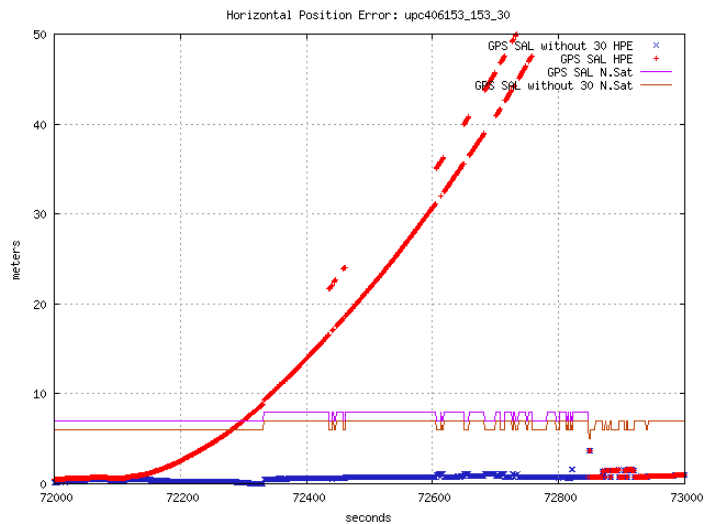


Figure 4-3: Horizontal position error in GPS Stand-Alone mode. On the horizontal axis there are the seconds of the day, on the vertical axis the position error in meters. The header of the file contains the name of the receiver station (in this case UPC4), the date in the format YY DOY (Day Of the Year), the DOY (153 in this example) and the PRN number of the GPS satellite with the abnormal clock behaviour (PRN 30 in this example). It should be noted that the figure is zoomed in the time interval of interest (when the clock jump occurs). The satellite PRN 30 causes a very large error (around 50 meters) in the horizontal plane (red points). Excluding it from the solution, the error highly decreases (blue points). The figure also shows the number of used satellites (violet line), to verify that the satellite PRN 30 is excluded from the solution (brown line).

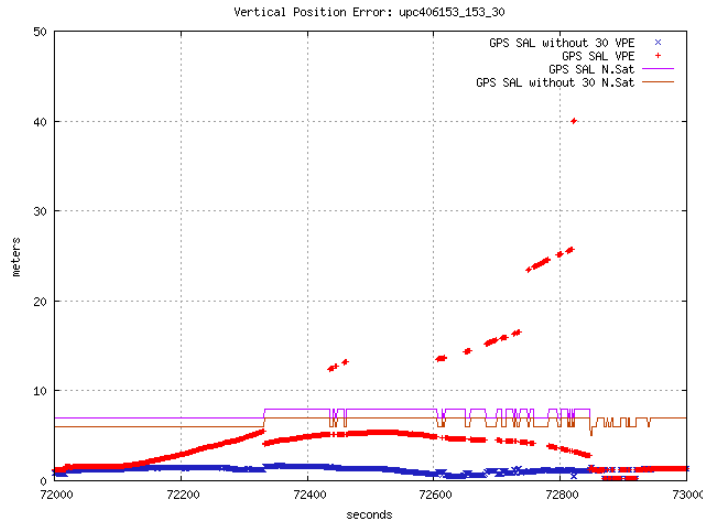


Figure 4-4: Vertical position error in GPS Stand-Alone mode. Also in this plane, the satellite PRN 30 causes a very large error, with a peak of 40 meter (red points). Excluding it from the solution, the error highly decreases (blue points).

It is evident that the high position error is exclusively caused by the clock anomaly: indeed, it appears exactly when the divergence between the real and broadcast clock values becomes very high. Moreover, excluding the satellite with the clock anomaly (PRN 30) from the solution, the position error is highly reduced. This result is also independent from the specific receiver geometry (station in Barcelona, in this case), because the same effects were obtained using different fixed receivers in Europe.

Therefore, in this case the clock anomaly causes a position error larger than the alert limit in the correspondent domain without the user being warned of it.

4.4 EGNOS reaction to GPS clock anomalies

EGNOS capability to protect the user can be verified in few steps:

- At the Signal In Space level, EGNOS prefit-residuals can be compared with prefit-residuals in GPS Stand-Alone mode. The prefit-residual is the difference between the measured pseudorange and the modelled pseudorange. In this way, it is possible to compare the range error in a GPS Stand-Alone system with the final range error obtained after applying fast and long terms corrections that are

broadcast by the EGNOS message. Prefit-residuals also give an idea of the quality of EGNOS behaviour, in terms of being too much conservative or not (i.e., fast and long term corrections overestimating the errors). This analysis is independent from the specific geometry of the receiver station.

- At the user level, the position error using EGNOS message can be compared with the position error in GPS Stand-Alone mode. Moreover, protection levels are expected to bound the resulting position error in both the planes (horizontal and vertical).
- Finally, to assess the integrity at the user level, the Stanford-ESA Integrity Diagrams should be generated. In this way, it is possible to verify that the integrity is assured for all possible geometries for a given receiver station [20].

Since the results at the user level depend on the specific geometry of the receiver, the computation should be repeated for different stations, in order to have a complete control of the situation. This kind of analysis, which considers both the Signal In Space level and the user level, is the best approach to verify EGNOS reaction in presence of clock anomalies.

The prefit-residual y is the difference between the measured pseudorange and the modelled pseudorange. This value is computed for each satellite in view with valid EGNOS corrections available according to the following expression:

$$y = CI - \rho + PRC + dt^{sat} + \Delta t^{sat} + rel - TGD^{sat} + IONO + TROPO$$

Eq. 4-1

where:

- CI is the measured pseudorange for a given satellite.
- ρ is the geometric range, which contains also the EGNOS long term corrections for the satellite coordinates
- PRC are the EGNOS fast corrections
- dt^{sat} and TGD^{sat} are the satellite clock bias and the inter-frequency bias computed from the GPS navigation message
- Δt^{sat} is the EGNOS long term correction for the satellite clock bias
- $IONO$ is the ionospheric delay computed from the EGNOS message
- $TROPO$ is the tropospheric delay computed by the RTCA model [9]
- rel is a (modelled) term to account relativistic effects.

This expression of the prefit-residual clearly shows all the terms of error. It should be noted that the prefit-residuals for the GPS Standalone solution follow the same equation but without the PRC terms, Δt^{sat} and with the IONO delay provided by the Klobuchar model [5]. Moreover, the geometric range is computed using only the GPS navigation message.

EGNOS protection levels are computed according to Eq. 2-1 and Eq. 2-2, but considering EGNOS contributions in Eq. 2-3.

The next two figures show how EGNOS GEO PRN 124 reacted in presence of the clock anomaly seen previously: the position error calculated using EGNOS message is much smaller than the one calculated in GPS Stand-Alone mode and it is now below the required alert limits. This result can be verified for both the components of the error (horizontal and vertical). Furthermore, the protection levels bound the error, giving a safe solution to the user. It should also be noted that, except few isolated points, availability is guaranteed for APV-II and LPV-200 categories, being HPL and VPL smaller than the corresponding HAL and VAL respectively.

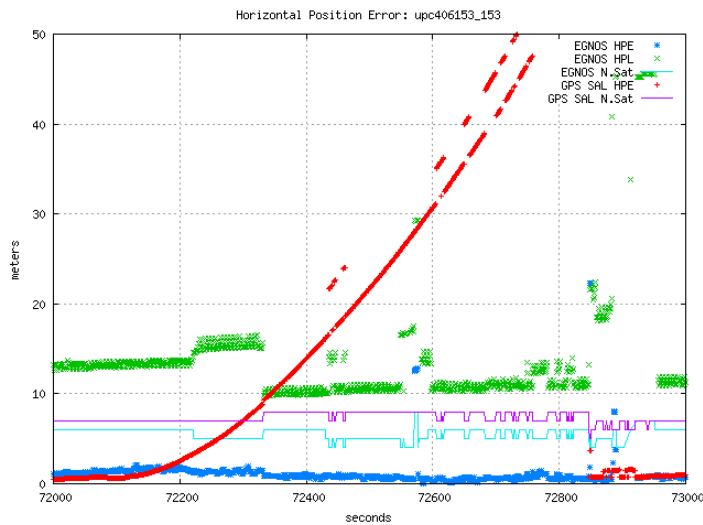


Figure 4-5: – Comparison between the horizontal position error using EGNOS message (blue) and the horizontal position error in GPS Stand-Alone mode (red). On the horizontal axis there are the seconds of the day, on the vertical axis the position error in meters. The position error using EGNOS GEO PRN 124 message is much smaller than the position error in GPS Stand-Alone mode. Moreover, the protection level (green) bounds the error. The figure also highlights the number of used satellite in GPS Stand-Alone mode (violet) and using EGNOS message (light blue): as expected, using EGNOS message some satellites are excluded from the solution.

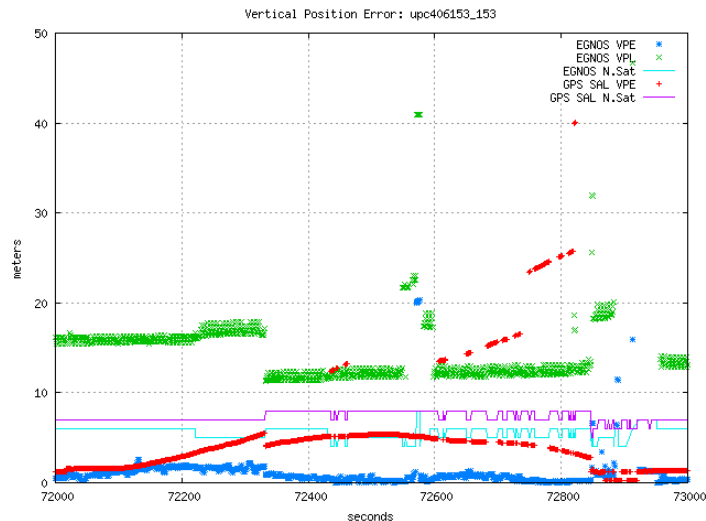


Figure 4-6: Comparison between the vertical position error using EGNOS message (blue) and the vertical position error in GPS Stand-Alone mode (red). Also in this case, when using the EGNOS GEO PRN 124 message, the position error is much smaller and the protection level (green) bounds the error.

To see more in details the EGNOS behaviour in presence of the error, an analysis on the prefit-residuals at the Signal-In-Space level was also performed. Figure 4-7 shows the prefit-residuals in GPS Stand-Alone mode, emphasizing the prefit-residual for satellite PRN 30 (circles), which has a much larger dispersion than the one for all the other satellites (dots). The figure also shows again the same peak of around 150 meters in the range error, which confirms that in GPS Stand-Alone mode no corrections are applied to compensate the error. On the other hand, Figure 4-8 shows how the fast and long terms corrections applied by EGNOS message (filled circles) initially compensate this dispersion and so the resulting prefit-residuals for satellite PRN 30 is close to zero (triangles). Then, since the dispersion is growing too much, from a certain epoch the satellite PRN 30 is excluded from the solution and no fast and long terms corrections are available anymore.

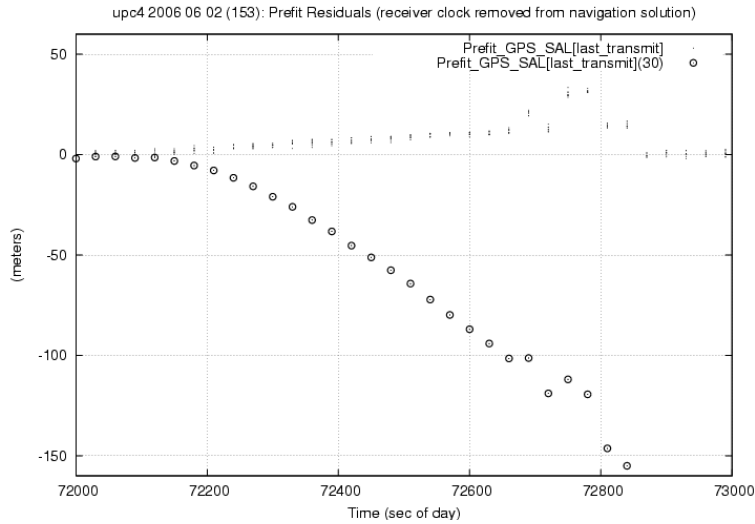


Figure 4-7: Prefit-residual in GPS Stand-Alone mode. On the horizontal axis there are the seconds of the day, on the vertical axis the range error in meters. The prefit-residual of satellite PRN 30 (circles) has a larger dispersion than the prefit-residuals of all the other satellites (dots). Moreover, there is again the peak of around 150 meters in the range error, which shows that no error corrections are applied in GPS Stand-Alone mode.

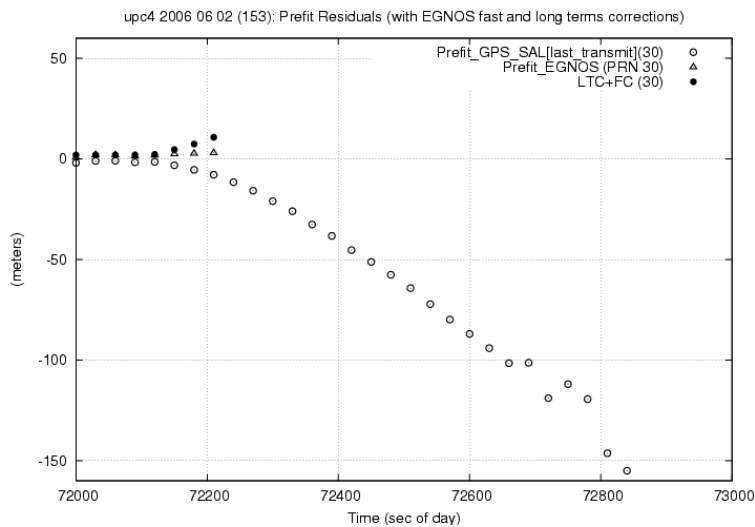


Figure 4-8: The fast and long terms corrections applied by EGNOS GEO PRN 124 (filled circles) compensate the prefit-residual for satellite PRN 30 in GPS Stand-Alone mode (circles). The resulting prefit-residual for satellite PRN 30 (triangles) has a minimum dispersion. Moreover, when the range error has become too large, the satellite PRN 30 is excluded from the solution and no fast and long terms corrections are available anymore.

These results confirm that the used approach – Signal In Space level in combination with user level – is a very clear and complete way to verify the EGNOS behaviour in presence of clock anomalies. Moreover, the results confirmed the expectations: the clock anomaly, which causes a large error in a GPS Stand-Alone system, is detected and corrected by EGNOS.

4.5 Integrity assessment with the Stanford-ESA Integrity Diagrams

In order to assure the integrity for all possible geometries seen by the receiver station, the Stanford-ESA Integrity Diagrams for all the analysed cases have been generated.

The Stanford-ESA Integrity Diagram ([20] and [26]), as the name itself indicates, is a modification of the well known Stanford Plot, where all (xPE, xPL) pairs for all the combinations from 4 to all-in-view satellites are represented at each second instead of representing only the pair (xPE, xPL) for the all-in-view solution.

This diagram has been showing its capabilities as a powerful tool for safety analysis, since the unsafe system performances are amplified by running over all geometries. Indeed, showing that at user level domain there is no situation for any possible geometry in which the error overcomes the protection level, then this would be the best experimental guarantee that at the position domain, for a specific location and epoch, no over-bounding is incurred.

Considering the previous example, where a large clock anomaly was detected and well compensated using the EGNOS message, the Stanford-ESA Integrity Diagrams are generated and plotted in Figure 4-9.

As it can be seen, no violation of integrity occurred for any of the analysed geometry, being all the pairs (xPE,xPL) always above the diagonal: this means that the integrity is always assured for all the possible geometries, because no error overbounding ($xPE > xPL$) happened for any of the analysed geometries.

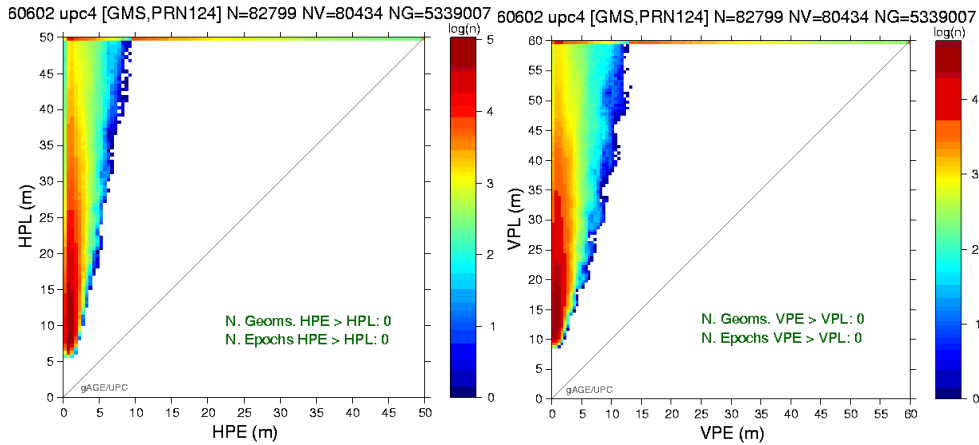


Figure 4-9: Stanford-ESA Integrity Diagrams. The header of these diagrams contains information about the day in the format YYMMDD, the name of the station and server, the PRN of GEO associated to the messages, the number of processed epochs (N), the number of epochs with valid navigation solution in Precision Approach (PA) mode (NV) and the number of computed geometries (NG). The horizontal axis reports the Position Error, while the vertical axis reports the Protection Level. As it can be seen, no error overbounding happened for any of the analysed geometries. Thus, in this case the use of EGNOS message guarantees a safe position to the user.

4.6 Summary of the results and conclusions

The EGNOS reaction to GPS clock anomalies has been assessed for a period of two years. In most of the analysed cases, the Ground Segment correctly detected large divergences between the real and the broadcast satellite clock values and the corresponding GPS satellites were correctly flagged as “unhealthy” in the GPS navigation message. However, there were some cases in which the Ground Segment didn’t detect the clock anomaly and, as a result, the user suffered of an unacceptable position error in GPS Stand-Alone mode. In some cases, there were position errors of almost 50 meters without the user being warned of.

In such critical situations, this analysis showed that EGNOS was able to detect the clock anomalies and highly reduce the position error: in some cases the clock anomaly was compensated with the long and fast terms corrections and this was discovered by computing the prefit residuals; in other cases the user was warned to exclude the satellite with the clock

anomaly from the solution. In all the analysed cases, the position errors were correctly bounded by the protection levels and both integrity and availability were guaranteed.

In addition, the Stanford-ESA Integrity Diagrams confirmed that the user domain error is always bounded by the Protection levels for all combinations of satellites, from 4 to all-in-view, with valid EGNOS differential corrections available.

It should be noted that the results were obtained also comparing different fixed receivers in Europe, in order to have a more general view of the EGNOS behaviour all around Europe and to be independent from the geometry of a specific location.

Chapter 5

Multisystem Integrity

With the advent of Galileo users will be provided with multiple signals coming from different satellite systems. This will improve position accuracy, because the number of satellites in view per user will be almost doubled. Moreover, the higher measurements redundancy will help to guarantee a safer position and the detection of errors. This will result also in an improved availability and in this way the requirements for more demanding flight categories can be satisfied. Therefore, it is necessary to introduce a base-line for a combined system, defining new parameters, new integrity algorithms and possible ways to combine the two independent systems. For example, in a combined system the event of two simultaneous failures is more probable than in a single system. Therefore, the dual failure case has to be taken into account when considering a combined system.

In the next sections, new parameters, concepts and assumptions will be introduced, in order to define the general conditions for a combined system during a precision approach. Then, different techniques to provide multisystem integrity will be described. The first presented method is an extension of the current GPS+RAIM technique. On the other hand, the second method will consider an extension of the Galileo integrity algorithm in order to include also GPS data.

Other possible methods will be briefly described in the last sections, together with future developments.

The aim of this final research is to find a set of techniques to combine the two systems and to offer a base-line for further developments including even more systems and sensors.

5.1 A combined system

Here follows the definition of the parameters to be considered in a dual system in case of single and multiple failures. This study aims to provide a common base-line for different methods that can be used to combine the

GPS and the Galileo systems in order to provide integrity improving availability.

5.1.1 Probability of Failure

5.1.1.1 Satellite failure probability for Galileo satellites

The exponential failure model considered for GPS satellites can't be applied to Galileo satellites. Moreover, for Galileo constellation it can't be assumed that the satellites in orbit have randomly distributed ages. Therefore a different model of the probability of failure for Galileo satellites should be addressed. However, ESA has established a value for the Probability of Failure for Galileo satellites equal to $2.7 \times 10^{-6}/150s$ assuming 10 satellites in view [12]. No information is available about the entity of the pseudorange error to be considered as a failure in Galileo. However, from this value it is possible to derive, as done for GPS, the individual failure probability per satellite and the probability of having multiple simultaneous failures. Nevertheless, it should be noted that in this case a different Ground Segment detection time should be considered when computing the probability of failure during an approach: this time is shorter than 1 hour and, even if no public information is available yet, it could be assumed to be 20 minutes. Therefore, the probability of Galileo satellite failure during an approach is assumed to be:

$$p_{approach} = 2.7 \times 10^{-6}/150 \cdot 1200 = 2.16 \times 10^{-5}/approach$$

Eq. 5-1

Again, it is possible to derive the individual probability of failure and the probability of multiple independent failures. It should be noted that common mode failures are expected to be present also in Galileo and to be more frequent than in GPS, because the ground segment will update several SVs with the same batch of the OSPF (Orbitography and Synchronisation Processing Facility) process. Therefore, a slightly higher value of the probability of common mode failures should be assumed for Galileo. Although a public available value is not given yet, a probability of $2 \times 10^{-8}/approach$ could be considered a good estimation for Galileo common mode failures.

The next table summarises the previous results.

| Parameters | Recommended values |
|--|---------------------------------------|
| Galileo Satellite Failure Probability (10 satellites in view) Precision Approach (LPV-200) | $2.16 \times 10^{-5}/\text{approach}$ |
| Galileo Common Mode Failures Probability Precision Approach (LPV-200) | $2 \times 10^{-8}/\text{approach}$ |

Table 5-1: Galileo Satellite failure probability

5.1.1.2 Satellite failure probability for a dual constellation

In this paragraph values for the probabilities of satellite failure for a dual constellation for precision approach are derived. The computation is based on the previous assumptions.

Let's consider now the following further assumptions:

- For both GPS and Galileo the number of satellites in view is 10, so the total number of satellites for the dual constellation is 20
- Errors in one system are assumed to be uncorrelated with errors in the other system
- The probability of no failures (fault-free case) for GPS and Galileo is almost 1
- The probabilities of two simultaneous failures for a single system are calculated using Eq. 1-13.

Let's use now some notations:

$$p_{GPS} = 1 \times 10^{-5} / \text{approach} / \text{SV}$$

$$p_{GAL} = 2.16 \times 10^{-6} / \text{approach} / \text{SV}$$

$$P_{fail,10,1}^{GPS} = 1 \times 10^{-4} / \text{approach}$$

$$P_{fail,10,1}^{GAL} = 2.16 \times 10^{-5} / \text{approach}$$

$$P_{fail,10,2}^{GPS} = 4.5 \times 10^{-9} / \text{approach}$$

$$P_{fail,10,2}^{GAL} = 2.1 \times 10^{-10} / \text{approach}$$

$$P_{fail,common}^{GPS} = 1.3 \times 10^{-8} / \text{approach}$$

$$P_{fail,common}^{GAL} = 2 \times 10^{-8} / \text{approach}$$

$$P_{fail,common}^{GPS+GAL} = 0$$

$$P_{fault-free}^{GPS} \approx 1$$

$$P_{fault-free}^{GAL} \approx 1$$

Therefore, the probability of having one single failure in the dual constellation is given by:

$$\begin{aligned} P_{fail,20,1}^{GPS+GAL} &= P_{fail,10,1}^{GPS} \cdot P_{fault-free}^{GAL} + P_{fail,10,1}^{GAL} \cdot P_{fault-free}^{GPS} \\ &= 1.22 \times 10^{-4}/\text{approach} \end{aligned}$$

Eq. 5-2

While the probability of having multiple failures, including common mode failures, is given by:

$$\begin{aligned} P_{multiple-failures}^{GPS+GAL} &= P_{fail,10,2}^{GPS} \cdot P_{fault-free}^{GAL} + P_{fail,10,2}^{GAL} \cdot P_{fault-free}^{GPS} \\ &+ P_{fail,10,1}^{GPS} \cdot P_{fail,10,1}^{GAL} + P_{fail,common}^{GPS} \cdot P_{fault-free}^{GAL} \\ &+ P_{fail,common}^{GAL} \cdot P_{fault-free}^{GPS} + P_{fail,common}^{GPS} \cdot P_{fail,common}^{GAL} \\ &+ P_{fail,common}^{GPS+GAL} \\ &\approx 4 \times 10^{-8}/\text{approach} \end{aligned}$$

Eq. 5-3

| Parameters | Recommended values |
|--|---------------------------------|
| GPS+Galileo Satellite Failure Probability (20 satellites in view) Precision Approach (LPV-200) | 1.22x10 ⁻⁴ /approach |
| GPS+Galileo Multiple Failures Probability Precision Approach (LPV-200) | 4x10 ⁻⁸ /approach |

Table 5-2: GPS+Galileo Satellite failure probability

5.1.2 Probability of Missed Detection

5.1.2.1 Probability of Missed Detection for Galileo

The probability of missed detection for Galileo for precision approach can be obtained in the same manner as for GPS:

$$P_{md} = \frac{1 \times 10^{-7}/\text{approach}}{2.16 \times 10^{-5}/\text{approach}} = 4.6 \times 10^{-3}/\text{sample}$$

Eq. 5-4

As before, also in the case of multiple failures, the same requirement for the probability of missed detection will be conservatively considered.

| Parameter | Recommended value |
|--|------------------------------|
| Maximum Allowable Probability of Missed Detection Galileo satellites | 4.6x10 ⁻³ /sample |

Table 5-3: Maximum Allowable Probability of Missed Detection for Galileo

5.1.2.2 Probability of Missed Detection for a dual constellation system

Previous calculations can be easily extended to a dual constellation system, recalling the results that were obtained in section 5.1.1.2:

$$P_{md} = \frac{1 \times 10^{-7}/\text{approach}}{1.22 \times 10^{-4}/\text{approach}} = 8.2 \times 10^{-4}/\text{sample}$$

Eq. 5-5

As before, also in the case of multiple failures, the same requirement for the probability of missed detection will be conservatively considered.

| Parameter | Recommended value |
|--|------------------------------|
| Maximum Allowable Probability of Missed Detection GPS+Galileo satellites | 8.2x10 ⁻⁴ /sample |

Table 5-4: Maximum Allowable Probability of Missed Detection for GPS+Galileo

5.1.3 Probability of False Alarm

5.1.3.1 Probability of False Alarm for Galileo

Also for Galileo, half of the continuity risk requirement for precision approach should be allocated to false alarms. Therefore, also in this case the required probability of false alarm is equal to $4 \times 10^{-6}/\text{sample}$.

| Parameter | Recommended value |
|--|----------------------------------|
| Probability of False Alarm Galileo satellites Precision Approach | $4 \times 10^{-6}/\text{sample}$ |

Table 5-5: Recommended value for Probability of False Alarm for Galileo satellites

5.1.3.2 Probability of False Alarm for a dual system

The same result could be applied to a dual system and therefore it could be considered again half of the continuity risk requirement for the probability of false alarm. However, for a dual system the occurrence of true alerts is more frequent than for a single system. Therefore, a different apportionment should be done now, allocating a larger amount of the continuity risk to true alerts and a smaller amount to false alerts. From several tests and simulations performed during this study and considering the satellite failure probability for a combined system, it was found that a value of $1 \times 10^{-6}/\text{sample}$ represents a safe value for the probability of false alarm.

| Parameter | Recommended value |
|--|----------------------------------|
| Probability of False Alarm GPS+Galileo satellites Precision Approach | $1 \times 10^{-6}/\text{sample}$ |

Table 5-6: Recommended value for Probability of False Alarm for GPS+Galileo satellites

5.2 GPS and Galileo with RAIM algorithms

In this section a first method to combine GPS and Galileo will be discussed. This method is an extension to the technique discussed in chapter 3 and it is the simplest way to combine the two systems. Indeed, measurements, geometry and UERE values from the two systems represent the input for RAIM algorithms that work in a similar manner as seen for a single system.

The next analyses will include again the single and the dual failure cases. It is clearly expected an improved availability, due to a smaller position error and a smaller protection level, because of a better geometry and a higher redundancy of the measurements.

5.2.1 Overview and base-line

The software that has been developed is composed by several modules and the general algorithm base-line is depicted in the next picture, while the algorithm flow-chart is the same as the one for the single constellation case (Figure 3-2).

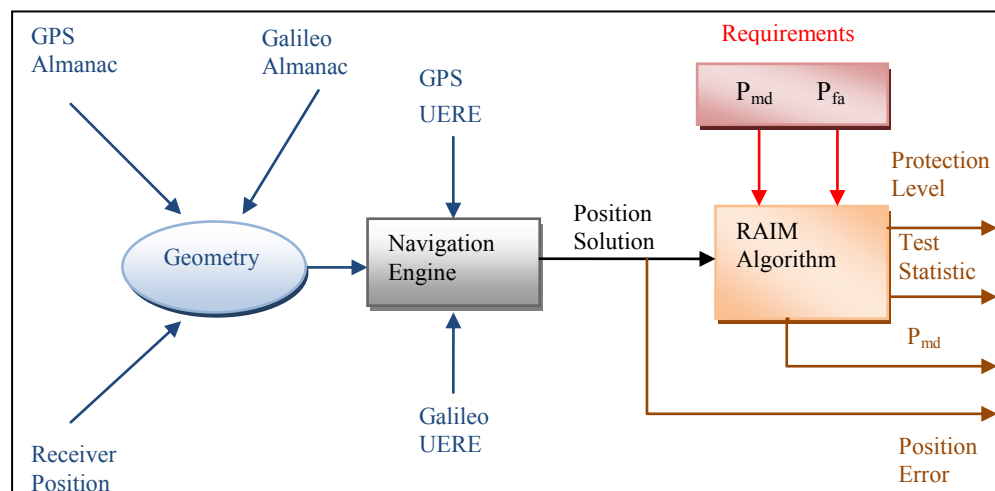


Figure 5-1: GPS+Galileo+RAIM algorithm base-line

As done in chapter 3, several random trials should be performed for any geometry in order to test the RAIM algorithms capability to detect single and multiple failures in a dual constellation scenario. This time the requirement for the probability of missed detection is slightly different, therefore the number of Monte Carlo runs to be considered is 305000 instead of 250000. This number comes out from several independent tests.

Also in this case, the number of missed detections should be less than or equal to 250, in order to satisfy the P_{md} requirement of 8.2×10^{-4} .

The nominal Walker constellation, as defined in [12], has been considered for Galileo and the corresponding Keplerian orbital parameters have been simulated through a specific module of the software that has been developed

and that solves Keplerian equations according to the methods described in [31]. On the other hand, a specific almanac has been used for the GPS constellation and the corresponding orbital parameters have been generated through another module of the software that has been developed, while Keplerian equations are solved in a similar manner as for Galileo. In this way the full 32 satellites GPS constellation was considered, instead of the nominal 24 satellites constellation defined in [4]. The geometries that were tested were generated through additional software considering all the points on the Earth sampled every 3 degrees in latitude from ninety degrees north to ninety degrees south. Each latitude circle has points separated evenly in longitude, defined as:

$$long_{step} = \frac{360}{ROUND\left(\frac{360}{MIN(3deg/\cos(latitude), 360)}\right)}$$

Eq. 5-6

This grid yields to 4603 points in space, which are then sampled every 150 seconds minutes for 72 hours (1728 time points), which is the expected GPS+Galileo geometry repetition. Therefore, the total number of space-time points is:

$$4603 \times 1728 = 7,953,984 \text{ space-time points}$$

This grid analysis is derived from RTCA [9], but it has been extended in order to include also Galileo and, for a global coverage, the Southern Hemisphere and can be applied to precision approaches, whose duration is typically 150 seconds. However, in the following sections only results for some specific geometry will be shown.

Keplerian orbital parameters for each satellite are then converted into a Cartesian reference system (ECEF: Earth Centered Earth Fixed) and into a local reference system (ENU: East, North, Up) in order to calculate the geometry, the position and the corresponding position error and test statistic. This conversion is done by several modules included in the developed software and they consider the rotation matrices and equations described in [32]. Elevation and azimuth angles are computed by a separated module that also checks which satellites are in view and are “healthy” (according to a specific flag in the almanac). Details on how to calculate elevation and azimuth angles can be found in [31] and [32].

It should be noted that for a dual constellation the number of unknowns is now 5 instead of 4, because there are now two clock biases to calculate, one for each system. Thus, design matrices should be inflated in order to include also the additional unknown clock bias of the second system. Therefore, the minimum number of measurements to calculate the user position with a dual constellation system is now 5.

The general test conditions are summarised in the next table.

| General Test Conditions Dual Constellation | |
|---|--|
| GPS Almanac | 012.AL3 (SEM format) 2008 |
| GPS week | 1462 |
| GPS seconds of the week | 157456 |
| Galileo Constellation | Nominal 27 satellites Walker Constellation |
| Galileo week | GPS week 1462 |
| Galileo seconds of the week | GPS seconds of the week 157456 |
| Probability of Missed Detection | 8.2×10^{-4} /sample |
| Probability of False Alarm | 1×10^{-6} /sample |
| UERE | Values depend on elevation angles |
| Noise | $\sim N(0, \text{UERE})$ |
| Mask angle | 5 degrees |
| Receiver position (latitude, longitude, height) | [40°51'N, 14°18'E, 61meters] |
| Number of random trials | 305,000 |
| Vertical Alert Limit | 35m (LPV-200) |

Table 5-7: General test conditions for testing RAIM algorithms (dual constellation)

UERE values for Galileo are defined in [12], while for GPS are the same used in chapter 3. These values depend on elevation angles and therefore during the simulations the following look-up tables are considered.

| GPS UERE budget | | | | | | | | | | |
|------------------------|-----------------------|-----|------|------|------|------|------|------|------|------|
| | Elevation angle (deg) | | | | | | | | | |
| UERE | 0 | 5 | 10 | 15 | 20 | 30 | 40 | 50 | 60 | 90.1 |
| (m) | 1.9 | 1.9 | 1.36 | 1.15 | 1.04 | 0.96 | 0.93 | 0.92 | 0.91 | 0.91 |

Table 5-8: GPS UERE

| Galileo UERE budget | | | | | | | | | | |
|---------------------|-----------------------|------|------|------|------|------|------|------|------|------|
| | Elevation angle (deg) | | | | | | | | | |
| UERE (m) | 0 | 5 | 10 | 15 | 20 | 30 | 40 | 50 | 60 | 90.1 |
| | 1.87 | 1.87 | 1.37 | 1.22 | 1.15 | 1.11 | 1.09 | 1.08 | 1.08 | 1.07 |

Table 5-9: Galileo UERE

5.2.2 Nominal conditions: no failures

When all satellites are behaving nominally, the error ellipse should ideally be in the nominal operations region, even if a certain number of false alarms are allowed, according to the required probability of false. In order to be statistically accurate, this test should consider a number of trials much larger than 305,000. In this way it is possible to accommodate the required probability of false alert. However, since in this framework it is important to test RAIM capability to detect satellite failures, this analysis is not relevant at the moment and will be neglected.

The next picture shows the RAIM nominal behaviour with 305,000 random trials and the general test conditions described in Table 5-7, Table 5-8 and Table 5-9, but with no failures and considering only Stanford Protection level. As expected, the error ellipse is in the “Normal Operations” region, but the P_{fa} requirement is not satisfied. However, as stated before, this result for the false alarm rate is not accurate, since a higher number of random trials would be required to confirm it.

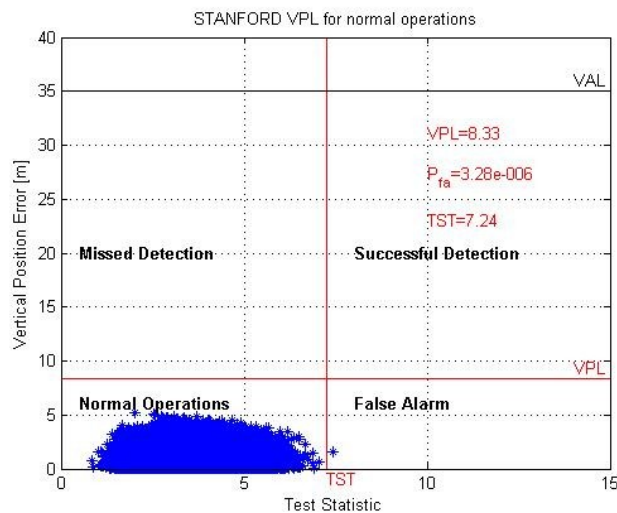


Figure 5-2: RAIM in nominal conditions for a dual constellation

5.2.3 Single failure

In the next tests, it is conservatively assumed that the worst case bias is affecting the least detectable satellite of the dual constellation, which is the satellite with the highest slope, as described in the previous chapters. The worst case bias is again found numerically for any geometry, as done for the single constellation case, by calculating the resulting P_{md} for each bias value ranging from -20 to 20 metres.

The following test considers a realistic scenario: the software simulates a precision approach with the receiver on an aircraft that is flying at 200 feet (61 meters) above the International Airport of Capodichino, Naples, Italy. 200 feet is the decision height to perform a precision approach in category LPV-200.

Two different methods are considered to calculate protection level, as done for the single constellation case: in particular, Stanford method and Brown's method, which uses the *pbiasb* concept, are considered.

The specific simulation data are summarised in the next table.

| Simulation Data Single Failure Dual Constellation | |
|---|--|
| Bias | Worst case bias on the least detectable satellite |
| Number of satellites in view | 18 (9 GPS, 9 Galileo) |
| Protection Level 1 st case | $VPL = Vslope_{max} T(N, P_{fa}) + k(P_{md})\sigma_V$ |
| Protection Level 2 nd case | $VPL = Vslope_{max} \cdot pbias_B$ |
| P_{md} 1 st case | 8.20×10^{-5} (computed) / 8.52×10^{-5} (theoretical) |
| P_{md} 2 nd case | 3.70×10^{-4} (computed) / 3.50×10^{-4} (theoretical) |

Table 5-10: Simulation data (single failure, dual constellation) – International Airport of Capodichino

The next figures show the results of the simulations using the two methods to calculate protection levels.

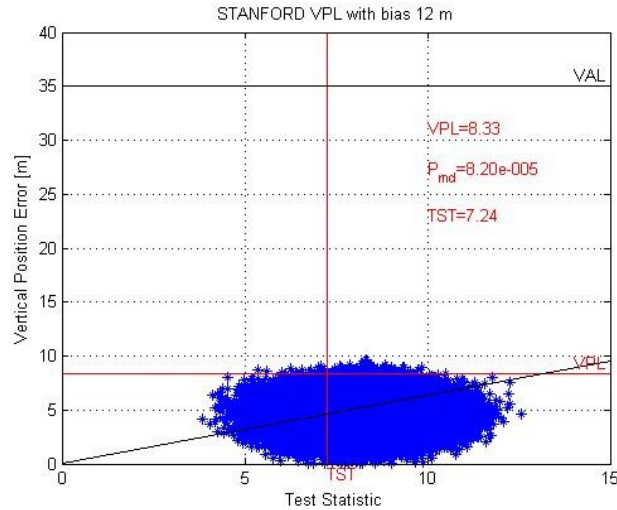


Figure 5-3: RAIM with a bias of 12 meters on the least detectable satellite – Stanford VPL (Capodichino)

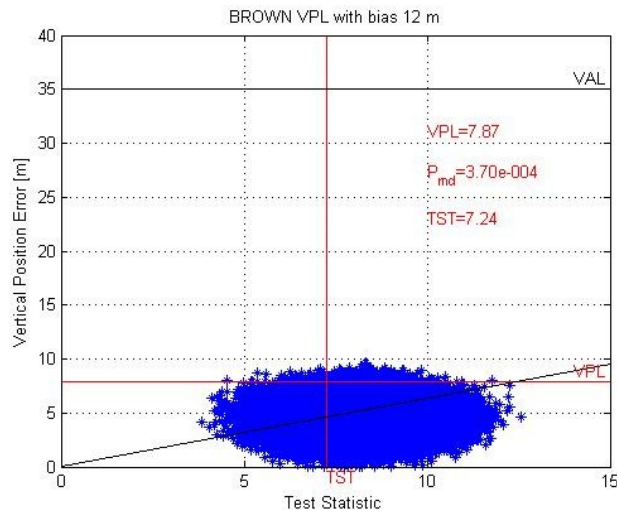


Figure 5-4: RAIM with a bias of 12 meters on the least detectable satellite – Brown VPL (Capodichino)

As expected both methods are working well in terms of probability of missed detection, with the Brown's method being more conservative, since the *pbiasb* concept provides a larger protection level. Also in this case, the computed values of P_{md} are very close to the theoretical ones. Concerning availability, as expected, a dual constellation provides a higher availability than a single constellation. This is due to a better geometry,

because of a greater number of satellites in view. Indeed, a better geometry results in smaller slope values for each satellite and therefore in a lower VPL. Thus, for this specific geometry, availability is guaranteed even for CAT-I (VAL=10 meters).

5.2.4 Multiple failures

For the multiple failures case, five different methods to calculate protection levels and slopes are considered: the Angus' method [15], the Stanford method using the dual failure slope given in [14], the Brown's method [14], the Liu's method [16] and the Stanford method using Liu's slope. As before, it is conservatively assumed that the worst case biases are affecting the worst pair of satellites. The general test conditions are described in Table 5-7, Table 5-8 and Table 5-9.

The next test considers the same scenario used for the single failure test: it is again simulated an approach with the receiver on an aircraft flying at 200 feet over the International Airport of Capodichino. This time the software adds two failures to the worst pair of satellites in view. The specific simulation data are summarised in the next table.

| Simulation Data Dual Failure Dual Constellation | |
|--|--|
| Bias | Worst case biases on the least detectable pair of satellites |
| Number of satellites in view | 18 (9 GPS, 9 Galileo) |
| Protection Level 1 st case | $VPL = Vslope^1_{maxmax} T(N, P_{fa}) + k(P_{md})\sigma_V$ |
| Protection Level 2 nd case | $VPL = Vslope^2_{maxmax} T(N, P_{fa}) + k(P_{md})\sigma_V$ |
| Protection Level 3 rd case | $VPL = Vslope^2_{maxmax} \cdot pbias_B$ |
| Protection Level 4 th case | $VPL = Vslope^3_{maxmax} \cdot pbias_B$ |
| Protection Level 5 th case | $VPL = Vslope^3_{maxmax} T(N, P_{fa}) + k(P_{md})\sigma_V$ |
| P_{md} 1 st case | 5.90×10^{-5} (computed) / 5.61×10^{-5} (theoretical) |
| P_{md} 2 nd case | 3.28×10^{-6} (computed) / 1.01×10^{-5} (theoretical) |
| P_{md} 3 rd case | 0 (computed) / 6.52×10^{-8} (theoretical) |
| P_{md} 4 th case | 3.28×10^{-6} (computed) / 9.64×10^{-7} (theoretical) |
| P_{md} 5 th case | 3.93×10^{-5} (computed) / 3.43×10^{-5} (theoretical) |

Table 5-11: Simulation data (dual failure, dual constellation) – International Airport of Capodichino

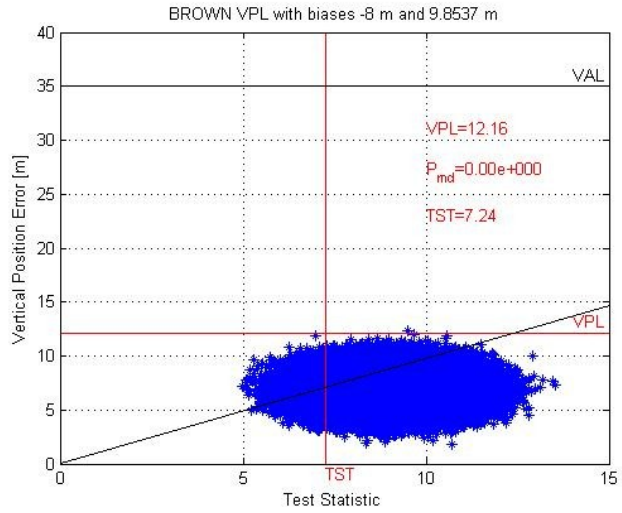


Figure 5-7: RAIM in dual failure case: Brown VPL (Capodichino)

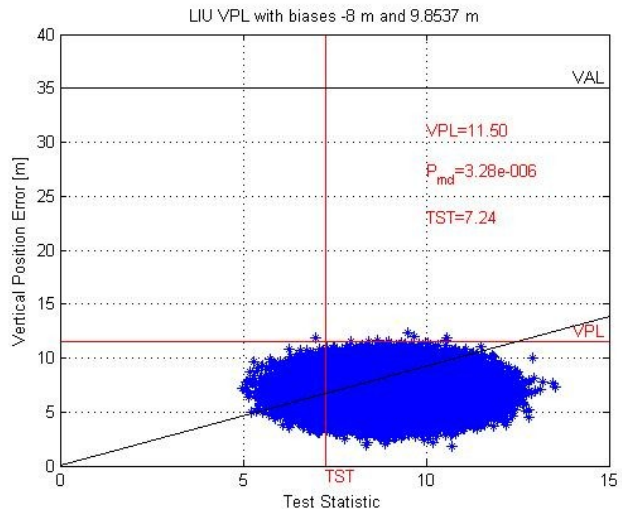


Figure 5-8: RAIM in dual failure case: Liu VPL (Capodichino)

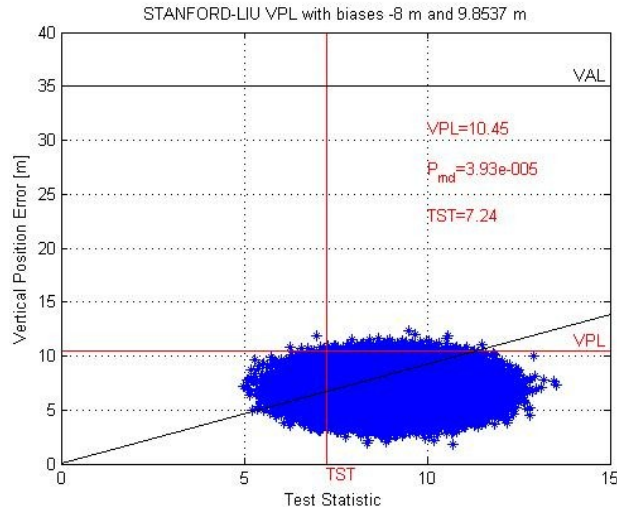


Figure 5-9: RAIM in dual failure case: Stanford-Liu VPL (Capodichino)

As expected, all the methods are consistent in terms of P_{md} , with some slightly differences among them: the methods that use the *pbiasb* concept are more conservative and the Liu's method provides the highest value of the dual failure slope. Therefore, the last method seems to be a good compromise between being conservative and keeping as low as possible the protection level: indeed, in this method the dual failure slope is computed according to the most conservative method, but the protection level is computed using Stanford equation rather than the *pbiasb* concept.

For this specific geometry, all methods satisfy the availability for APV-II and LPV-200, but none of them for CAT-I.

5.2.5 Availability results

All the 7,953,984 space-time points were tested with the developed software as done in the example geometry shown in the previous section. Therefore, complete availability results were obtained: it has been found that RAIM algorithms have capabilities to protect user from dual failure when a dual constellation is considered, at least until APV-II, where the availability, for some methods is more than 99.9%. On the other hand, CAT-I could be guaranteed only for very good geometries and with less conservative methods used to calculate VPL. However, better results are expected considering lower values for UERE budgets.

The following figures summarises the availability results for all the 7,953,984 geometries considering the first method (Angus) to calculate protection level for the dual failure case. In particular, availability for LPV-200 is 100%, while for APV-II is 99.98%. On the other hand, under these assumptions, the availability requirement for CAT-I is not satisfied.

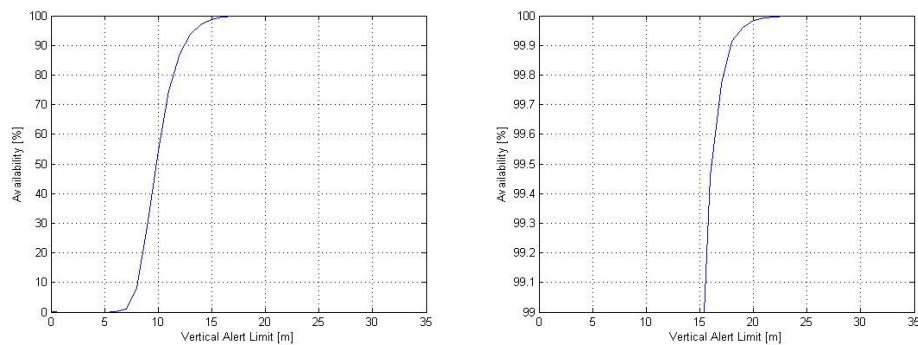


Figure 5-10: RAIM availability for all the 7,953,984 space-time points considering the VPL computed with method #1, using conservative UERE values

Therefore, this technique to combine GPS and Galileo data using a specific RAIM algorithm is very attractive and lead to interesting results both in terms of integrity and availability even for demanding categories of flight without any additional effort in terms of computational load and of system cost.

5.3 GPS and Galileo with the Galileo Integrity algorithm

The following technique considers the Galileo Integrity equation (Eq. 2-16) as the basis for the multisystem integrity algorithm. Indeed, it is possible to collect orbital data and UERE values from both GPS and Galileo and use them as input for the Galileo Integrity equation. The output will be then constituted of the Integrity Risk of the overall combined system.

Given that the algorithm is capable of raising timely warnings to the user whenever the Integrity Risk requirement is violated, the scope of this analysis is to show that with a dual constellation the total integrity risk is always much lower than in single constellation, even in severely degraded scenarios. This means that if a precision approach cannot be performed within a single system, because of a total integrity risk higher than the

requirement, within a combined system the user can safely rely on the computed position, because the total integrity risk is now lower than the requirement. This is the advantage of using a dual constellation and of extending the Galileo integrity equation to the combined system.

5.3.1 Overview and base-line

GPS and Galileo integrity data are the inputs for the Galileo Integrity equation:

$$\begin{aligned}
P_{HMI}(VAL, HAL) &= P_{HMI,V,FF} + P_{HMI,H,FF} + P_{HMI,V,FM} + P_{HMI,H,FM} \\
&= 1 - \text{erf}\left(\frac{VAL}{\sqrt{2} \cdot \sigma_{u,V,FF}}\right) + e^{-\frac{HAL^2}{2\sigma_{u,H,FF}^2}} \\
&+ \sum_{j=1}^N P_{fail,sat_j} \left[\frac{1}{2} \left(1 - \text{erf}\left(\frac{VAL + \mu_{u,V}(j)}{\sqrt{2} \cdot \sigma_{u,V,FM}(j)}\right) \right) + \frac{1}{2} \left(1 - \text{erf}\left(\frac{VAL - \mu_{u,V}(j)}{\sqrt{2} \cdot \sigma_{u,V,FM}(j)}\right) \right) \right] \\
&+ \sum_{j=1}^N P_{fail,sat_j} \left(1 - \chi_{2,\delta_{u,H}}^2 \text{cdf}\left(\frac{HAL^2}{\sigma_{u,H,FM}^2(j)}\right) \right)
\end{aligned}$$

Eq. 5-7

which must be modified in order to include also GPS data. Indeed, the error distribution in the range domain for GPS is given by:

$$\sigma_{URE,i}^2 = \sigma_{URA,i}^2 + \sigma_{UIRE,i}^2 + \sigma_{loc,i}^2 + \sigma_{tropo,i}^2$$

Eq. 5-8

while for Galileo is given by:

$$\sigma_{URE,i}^2 = SISA_i^2 + \sigma_{loc,i}^2$$

Eq. 5-9

Given that the same overbounding technique is used for both the Signal-in-Space error distributions, there is a correspondence between σ_{URA}^2 and $SISA^2$, because they both represent the SIS contribution (clock and ephemeris) to the final error in the range domain. Therefore, GPS σ_{URA}^2 can be used in Eq. 5-7 in the same manner $SISA^2$ is used for Galileo. More details about overbounding techniques can be found in Appendix B.

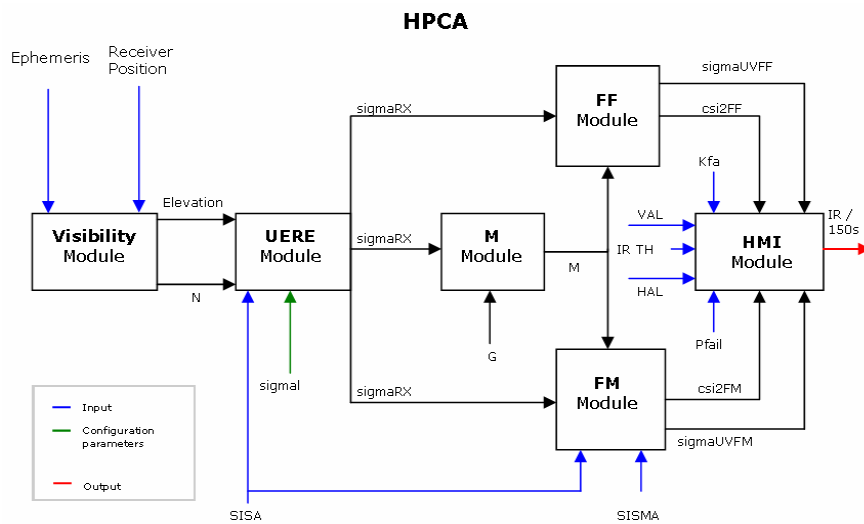


Figure 5-12: Modules of the Galileo Integrity Algorithm

where:

Inputs

- Keplerian orbital data, coming from the GPS and Galileo navigation messages. These elements are collected from real almanacs for GPS, while they are simulated for Galileo through a specific module of the software. Keplerian equations are then solved and the relevant parameters converted into a Cartesian reference system (ECEF) and a local reference system (ENU).
- The estimation of the receiver position, used in the weighted least squares solution. The receiver position is computed in several coordinate frames: ECEF, ENU and also in the spherical system (i.e., latitude, longitude and height). Specific modules of the software have been developed to perform the coordinate conversions.
- The range error contributions for Galileo (SISA and SISMA) and for GPS (URA or UDRE in case of EGNOS) at the Signal-in-Space level. These parameters are generated through a specific module of the software.

Configuration parameters

- VAL and HAL, which depend on the specific application
- P_{md} , P_{fa} , $P_{failure}$, which depend on the system requirements

- IR threshold, which depends on the system requirements and on the specific application

Outputs parameters

- Integrity Risk/150 seconds. Therefore, this is the Integrity Risk computed for the next critical operation, which lasts 150 seconds (i.e., precision approach).

The algorithm is constituted by the following macro-modules:

- The *visibility module* checks the current geometry satellites-receiver. This includes the geometry computation, coordinate conversions and elevation and azimuth angles computation. This module also checks the “healthy” status of each satellite
- The *UERE module* calculates the final UERE at the user level including the Signal-In-Space and the local contributions. The Signal-in-Space contribution is generated through a specific module, while local contributions are computed by a separated module using equations described in the following section.
- The *M module* calculates the typical topocentric weighted design matrix used for least squares position estimation. This matrix is the *K* matrix used in the RAIM algorithm tests. Therefore, a similar module has been used.
- The *FF* and *FM modules* calculate the standard deviation in the vertical and horizontal domain for the fault-free and faulty mode respectively. These modules use the Galileo Integrity equations described in the chapter 2.
- The *HMI module* calculates the final Integrity Risk from the required Vertical and Horizontal Alert Limits. This module uses the Galileo Integrity equations described in chapter 2.

5.3.3 General Test Conditions

The following simulations will show results in nominal and degraded conditions for single and dual constellation. Different levels of degradation of the parameters will be considered. Indeed, the Galileo integrity risk equation doesn't check the consistency of the position solution. Therefore, the Galileo integrity risk equation at the user level is not able to detect bias

on pseudorange, as RAIM algorithms do, because it is assumed that these kinds of failures are already detected by the ground segment. However, the Galileo Integrity algorithm foresees a single undetected failure affecting one satellite. The magnitude of this bias depends on SISA and SISMA, according to the following equation:

$$bias_j = k_{P_{fa}} \cdot \sqrt{SISA_j^2 + SISMA_j^2} \quad Eq. 5-10$$

where j indicates the satellite affected by the bias and $k_{P_{fa}}$ depends on the probability of false alarms and it is usually assumed to be 5.212. In nominal conditions, the previous equation leads to an expected undetected bias with magnitude equal to 5 meters. In this manner, the final integrity risk, including also the single failure contribution, can guarantee a safe position to the user, if it is less than the requirement.

For the next simulations, P_{md} , P_{fa} and $P_{failure}$ values are chosen according to the assumptions made in the previous sections. UERE values for Galileo are given by Eq. 5-9, where SISA is 0.85 m in nominal conditions and 1.0 m in degraded conditions, while local errors are computed according to the following interpolation formula that depends on the elevation angles:

$$\sigma_{loc,i} = a + b \cdot e^{-10 \cdot Elev_i} \quad Eq. 5-11$$

where:

- $Elev_i$ is the current elevation angle for the i^{th} satellite [radians]
- the parameters a and b are computed off-line using as follows

$$\begin{bmatrix} a \\ b \end{bmatrix} = (A^T \cdot A)^{-1} \cdot A \cdot \sigma_i \quad Eq. 5-12$$

being

$$A = \begin{bmatrix} 1 & e^{-10 \cdot E_1} \\ \vdots & \vdots \\ 1 & e^{-10 \cdot E_m} \end{bmatrix} \quad \sigma = \begin{bmatrix} \sigma_1 \\ \vdots \\ \sigma_m \end{bmatrix}$$

where:

- m is the number of reference elevation angles for definition of UERE local component values
- E_i ($i=1$ to m) is the i^{th} reference elevation angle [radians]
- σ_i ($i=1$ to m) is the predicted standard deviation of the UERE local component at the i^{th} reference elevation angle.

The following reference values have been considered for the local UERE as a function of the elevation angles:

| | | | | | | | | |
|---|--------|--------|--------|--------|--------|--------|--------|--------|
| Reference Elevation Angle [radians] i=1 to m | 0.1745 | 0.2618 | 0.3491 | 0.5236 | 0.6981 | 0.8727 | 1.0472 | 1.5708 |
| σ_i i=1 to m [meters] | 1.0300 | 0.7800 | 0.6700 | 0.6000 | 0.5800 | 0.5700 | 0.5600 | 0.5500 |

Table 5-12: Reference values for the predicted standard deviation of the UERE local component as a function of the elevation angles

SISMA values are equal to 0.7 m and 1.0 m in nominal and degraded conditions respectively. URA for GPS satellites is assumed to be equal to 0.7 m and 1.0 for nominal and degraded conditions respectively.

Degraded values of SISA, SISMA and URA represent degradation of the navigation message uploaded by the Ground Segment to the satellites. Indeed, SISA, SISMA and URA are calculated, for each satellite, by the Ground Segment, based on long term observations, and their values are uploaded to the satellites in the same batch. Therefore, a not nominal behaviour of these parameters represents long term errors based on wrong observations. The software that has been developed simulates both nominal and degraded scenarios.

In the following simulations, it has been assumed a similar interpolation formula also for GPS local errors, therefore also for GPS the final UERE is given by:

$$\sigma_{URE,i}^2 = URA_i^2 + \sigma_{loc,i}^2$$

Eq. 5-13

In some tests, a step (bias) is added to the SISA value of 1 or 2 random Galileo satellites and to the URA value of 1 or 2 random GPS satellites.

This represents a severely degraded scenario, because biases on SISA and URA for 1 or 2 satellites represent instantaneous undetected errors affecting only specific satellites. These kinds of errors are short term errors and, if not timely detected by the ground segment, can severely affect the final position error.

The mask angle is conservatively assumed to be equal to 10 degrees for both systems, in order to test geometries with less usable satellites.

1001 epochs are considered for each test, sampled at every 150 seconds, which is the typical length of an approach. Therefore, geometries are assumed to be independent at every 150 seconds, as well as all the other parameters.

It should be noted that for the following simulations a more relaxed value for the integrity risk threshold as been considered, as suggested in [12], instead of the more stringent LPV-200 requirement. However, the final results were not affected by this assumption. On the other hand, for HAL and VAL more demanding values have been chosen [12], instead of the less stringent values of the alert limits for LPV-200. Therefore, if the integrity risk is satisfied for these demanding values, it is also satisfied for LPV-200.

The next tables summarise the general test conditions for single and dual constellation.

| General Test Conditions - Galileo only | |
|---|--|
| Galileo Constellation | Nominal 27 satellites Walker Constellation |
| Galileo week | GPS week 1462 |
| Galileo seconds of the week | GPS seconds of the week 157456 |
| Probability of Missed Detection | 4.6×10^{-3} /sample |
| Probability of False Alarm | 4×10^{-6} /sample |
| UERE | Values depend on elevation angles |
| Noise | $\sim N(0, UERE)$ |
| k_{pfa} | 5.212 |
| Mask angle | 10 degrees |
| Receiver position (latitude, longitude, height) | [40°51'N, 14°18'E, 61meters] |
| Number of tested epochs | 1001 |
| Vertical Alert Limit | 20 m |
| Horizontal Alert Limit | 12 m |
| Integrity Risk Threshold | 1.7×10^{-7} /150s |
| Probability of Failure | 2.16×10^{-6} /150s |

Table 5-13: General test conditions for single constellation (Galileo only)

| General Test Conditions – GPS-Galileo dual constellation | |
|---|--|
| GPS Almanac | 012.AL3 (SEM format) 2008 |
| GPS week | 1462 |
| GPS seconds of the week | 157456 |
| Galileo Constellation | Nominal 27 satellites Walker Constellation |
| Galileo week | GPS week 1462 |
| Galileo seconds of the week | GPS seconds of the week 157456 |
| Probability of Missed Detection | 8.2×10^{-4} /sample |
| Probability of False Alarm | 1.13×10^{-6} /sample |
| UERE | Values depend on elevation angles |
| Noise | $\sim N(0, \text{UERE})$ |
| k_{Pfa} | 5.212 |
| Mask angle | 10 degrees |
| Receiver position (latitude, longitude, height) | [40°51'N, 14°18'E, 61meters] |
| Number of tested epochs | 1001 |
| Vertical Alert Limit | 20 m |
| Horizontal Alert Limit | 12 m |
| Integrity Risk Threshold | 1.7×10^{-7} /150s |
| Probability of Failure | 2.16×10^{-6} /150s |

Table 5-14: General test conditions for dual constellation

5.3.4 Nominal conditions

Here come results in nominal conditions in the following two scenarios: the first case considers only Galileo constellation, the second case considers Galileo in combination with GPS. In both cases, nominal values were considered for SISA and SISMA for Galileo and for URA for GPS. It should be noted that the SISA value provided by the Galileo Integrity Processing Facility (IPF) is multiplied by 1.1 at the user level, in order to take into account further degradations of the signal.

| Scenario #1 – Nominal conditions - Galileo only | |
|--|-----------------------------------|
| SISA-IPF | 0.85 m for each satellite in view |
| SISA at the user level | SISA-IPF·1.1 |
| SISMA | 0.7 m for each satellite in view |

Table 5-15: Simulation data in nominal conditions, Galileo constellation only

The next figure shows results for scenario #1. As expected, for any geometry the total Integrity Risk is lower than the threshold that has been considered. Therefore, no alarm should be raised by the system and the user can safely perform the critical operation (i.e., precision approach).

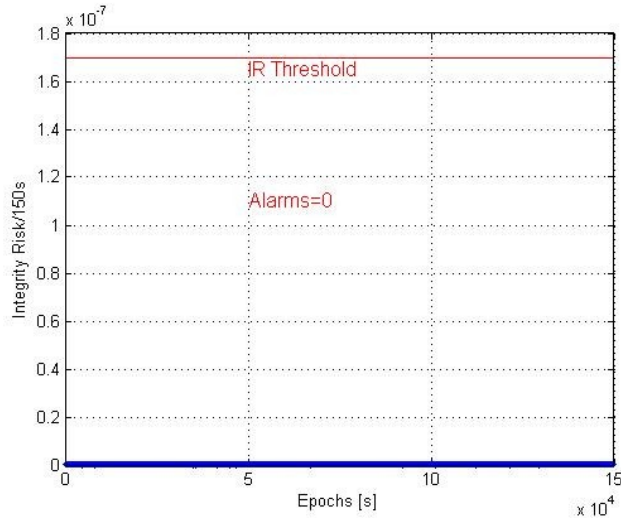


Figure 5-13: Integrity Risk results in nominal conditions (Galileo constellation)

Similar results are achieved with the second scenario, where also GPS constellation is considered.

| Scenario #2– Nominal conditions – GPS-Galileo dual constellation | |
|---|-----------------------------------|
| URA | 0.70 m for each satellite in view |
| SISA-IPF | 0.85 m for each satellite in view |
| SISA at the user level | SISA-IPF·1.1 |
| SISMA | 0.7 m for each satellite in view |

Table 5-16: Simulation data in nominal conditions, GPS-Galileo dual constellation

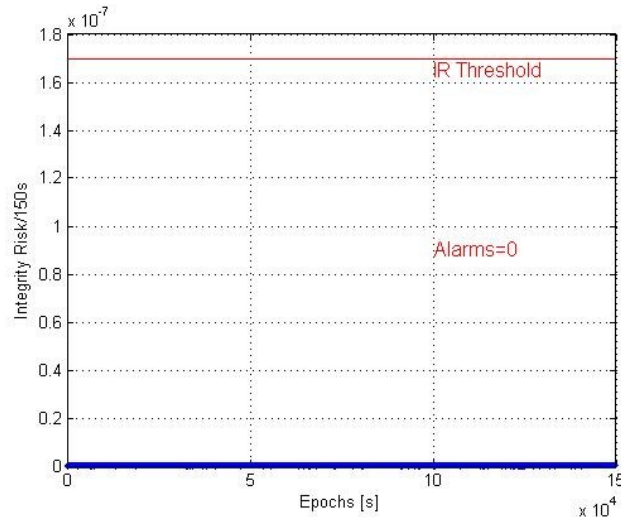


Figure 5-14: Integrity Risk results in nominal conditions (GPS-Galileo dual constellation)

As expected, the final integrity risk is lower than the threshold and no alarms are raised by the combined system.

5.3.5 Degraded conditions

Here follow results in several degraded scenarios, considering a single and a dual constellation.

The first test considers a slightly degraded situation, in which Galileo SISA doesn't have the nominal value of 0.85 m, but 1.0 m for all satellites in view.

| Scenario #1 – Degraded SISA - Galileo only | |
|--|----------------------------------|
| SISA-IPF | 1.0 m for each satellite in view |
| SISA at the user level | SISA-IPF·1.1 |
| SISMA | 0.7 m for each satellite in view |

Table 5-17: Simulation data with degraded SISA, Galileo constellation only

As expected, the total integrity risk is higher than the nominal case, but still below the threshold. Therefore, no alarms are raised in this case and the user can safely perform a critical operation.

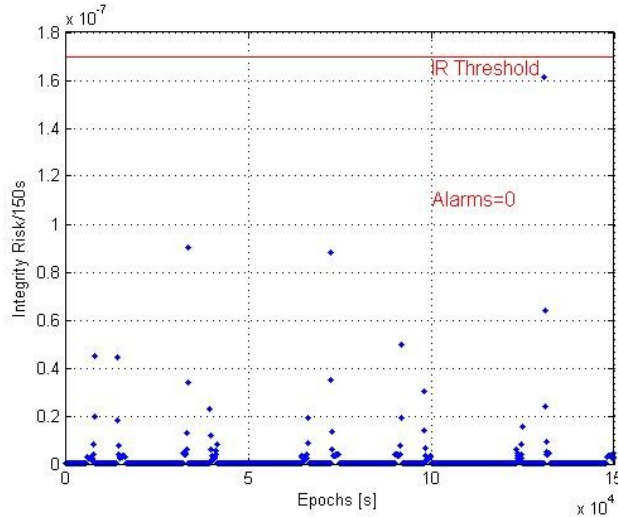


Figure 5-15: Integrity Risk results with degraded SISA (Galileo constellation only)

A similar test has then been performed considering also the GPS system.

| Scenario #2– Degraded SISA - GPS-Galileo dual constellation | |
|--|-----------------------------------|
| URA | 0.70 m for each satellite in view |
| SISA-IPF | 1.0 m for each satellite in view |
| SISA at the user level | SISA-IPF·1.1 |
| SISMA | 0.7 m for each satellite in view |

Table 5-18: Simulation data with degraded SISA, GPS-Galileo dual constellation

As expected, with the combined system the total Integrity Risk is smaller than in the single constellation case, as shown in the next figure.

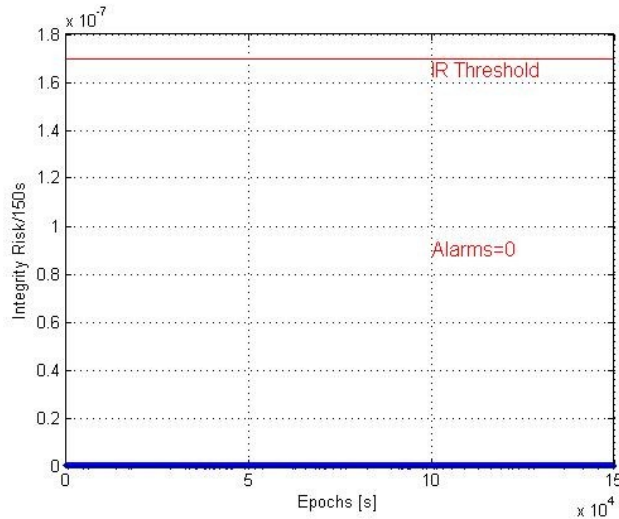


Figure 5-16: Integrity Risk results with degraded SISA (GPS-Galileo dual constellation)

The second test considers a degraded value for Galileo SISMA, being 1.0 m for all satellites instead of 0.7 m.

| Scenario #3 – Degraded SISMA - Galileo only | |
|---|-----------------------------------|
| SISA-IPF | 0.85 m for each satellite in view |
| SISA at the user level | SISA-IPF·1.1 |
| SISMA | 1.0 m for each satellite in view |

Table 5-19: Simulation data with degraded SISMA, Galileo constellation only

In this case, for some geometries, the total integrity risk exceeds the threshold. Therefore, some alarms are raised by the system, to warn the user about an unsafe computed position. This means that for these cases, the precision approach can't be performed relying only on the satellite navigation system. Thus, this situation represents a truly critical event for the user.

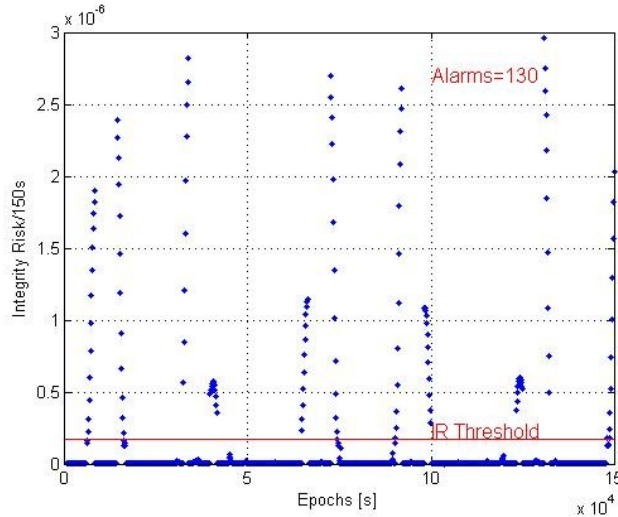


Figure 5-17: Integrity Risk results with degraded SISMA (Galileo constellation only)

This critical situation can be avoided considering a combined system. Indeed, the following results show that in combination with GPS, even in these degraded conditions, the total Integrity Risk can be kept below the threshold and no alarms are raised.

| Scenario #4– Degraded SISMA - GPS-Galileo dual constellation | |
|---|-----------------------------------|
| URA | 0.70 m for each satellite in view |
| SISA-IPF | 0.85 m for each satellite in view |
| SISA at the user level | SISA-IPF·1.1 |
| SISMA | 1.0 m for each satellite in view |

Table 5-20: Simulation data with degraded SISMA, GPS-Galileo dual constellation

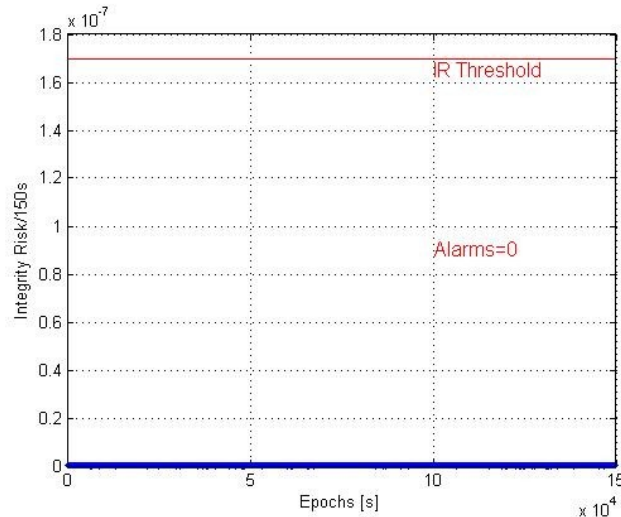


Figure 5-18: Integrity Risk results with degraded SISMA (GPS-Galileo dual constellation)

The next tests consider an even more degraded scenario where both SISA and SISMA are degraded. The first scenario considers only the Galileo constellation, while the second scenario considers the combined system.

| Scenario #5 – Degraded SISA and SISMA - Galileo only | |
|--|----------------------------------|
| SISA-IPF | 1.0 m for each satellite in view |
| SISA at the user level | SISA-IPF·1.1 |
| SISMA | 1.0 m for each satellite in view |

Table 5-21: Simulation data with degraded SISA and SISMA, Galileo constellation only

As expected, in the single constellation case, the total integrity risk is higher than the threshold and there are even more alarms than the previous case.

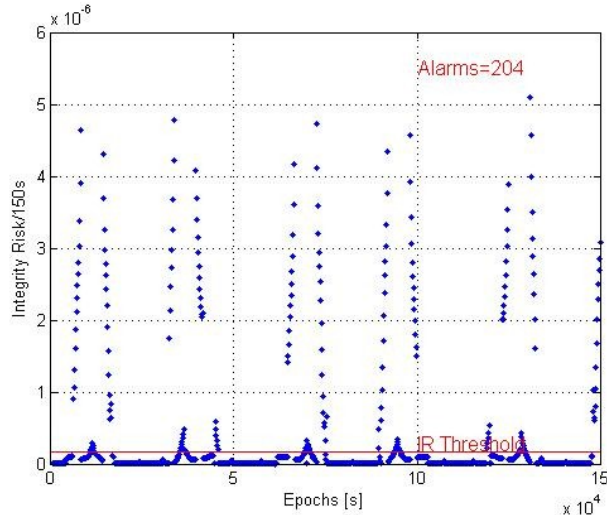


Figure 5-19: Integrity Risk results with degraded SISA and SISMA (Galileo constellation only)

On the other hand, for the dual constellation the total integrity risk is below the threshold and no alarm shall be raised. This means that in a dual constellation, even in this case, the combined system provides a safe position to the user.

| Scenario #6– Degraded SISA and SISMA - GPS-Galileo dual constellation | |
|--|-----------------------------------|
| URA | 0.70 m for each satellite in view |
| SISA-IPF | 1.0 m for each satellite in view |
| SISA at the user level | SISA-IPF·1.1 |
| SISMA | 1.0 m for each satellite in view |

Table 5-22: Simulation data with degraded SISA and SISMA, GPS-Galileo dual constellation

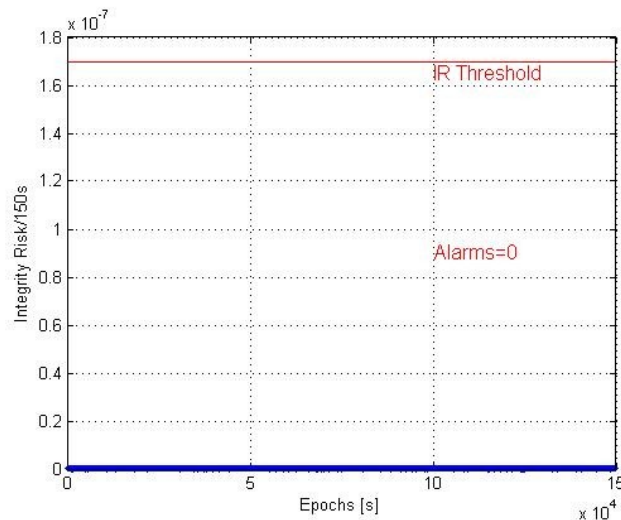


Figure 5-20: Integrity Risk results with degraded SISA and SISMA (GPS-Galileo dual constellation)

The next test will consider also a degrade value for URA, together with degraded values for SISA and SISMA.

| Scenario #7– Degraded SISA, SISMA and URA - GPS-Galileo dual constellation | |
|---|----------------------------------|
| URA | 1.0 m for each satellite in view |
| SISA-IPF | 1.0 m for each satellite in view |
| SISA at the user level | SISA-IPF·1.1 |
| SISMA | 1.0 m for each satellite in view |

Table 5-23: Simulation data with degraded SISA, SISMA and URA, GPS-Galileo dual constellation

Even in this case, for a dual constellation, a precision approach can be safely performed, as shown in the next figure.

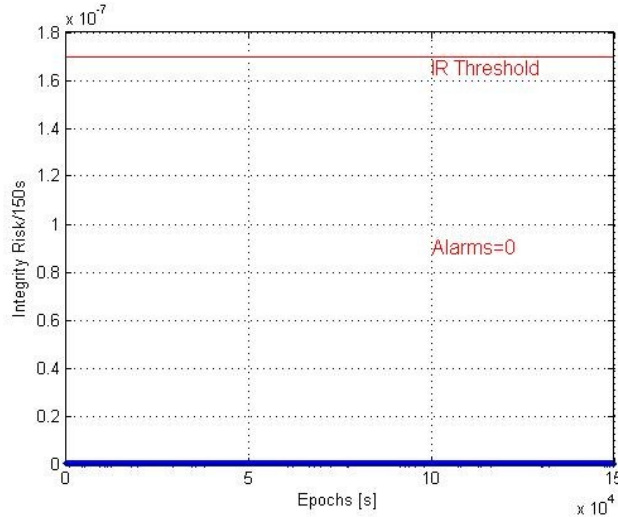


Figure 5-21: Integrity Risk results with degraded SISA, SISMA and URA (GPS-Galileo dual constellation)

5.3.6 Bias on SISA and URA

In these tests a bias (a step) is added to the SISA and URA values for 1 or 2 random Galileo and GPS satellites respectively. These tests were performed in both the nominal and degraded conditions analysed in the previous sections. Therefore, the general test conditions are the same of the previous cases. As stated before, a bias on SISA or on URA can represent an instantaneous undetected failure affecting only a specific satellite.

The next figures will show only the results in the worst case scenario, which is the one with degraded SISA and SISMA values and with biases affecting two Galileo satellites. However, the tests that have been performed have shown agreements to the expected results also in less critical conditions.

| Scenario #1 – Severely Degraded conditions - Galileo only | |
|---|----------------------------------|
| SISA-IPF | 1.0 m for each satellite in view |
| SISA at the user level | SISA-IPF·1.1 |
| Bias on SISA | 5 m |
| Satellites affected by bias | Galileo satellite #1 and #2 |
| SISMA | 1.0 m for each satellite in view |

Table 5-24: Simulation data in severely degraded conditions with SISA bias on two Galileo satellites (Galileo constellation only)

In this case, as shown in the next picture, the total integrity risk is in many cases above the threshold and consequently several alarms have to be raised by the system.

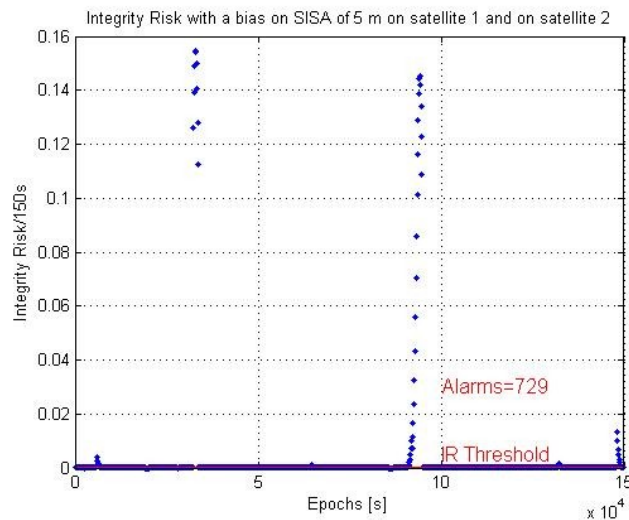


Figure 5-22: Integrity Risk in severely degraded conditions with SISA bias on two Galileo satellites (Galileo constellation only)

However, a combined system still provides a safe solution, being the total integrity risk less than the requirement for all epochs, as shown in the next figures.

| Scenario #2 – Severely Degraded conditions – GPS-Galileo dual constellation | |
|--|----------------------------------|
| URA | 0.7 m for each satellite in view |
| SISA-IPF | 1.0 m for each satellite in view |
| SISA at the user level | SISA-IPF·1.1 |
| Bias on SISA | 5 m |
| Satellites affected by bias | Galileo satellite #1 and #2 |
| SISMA | 1.0 m for each satellite in view |

Table 5-25: Simulation data in severely degraded conditions with SISA bias on two Galileo satellites (GPS-Galileo dual constellation)

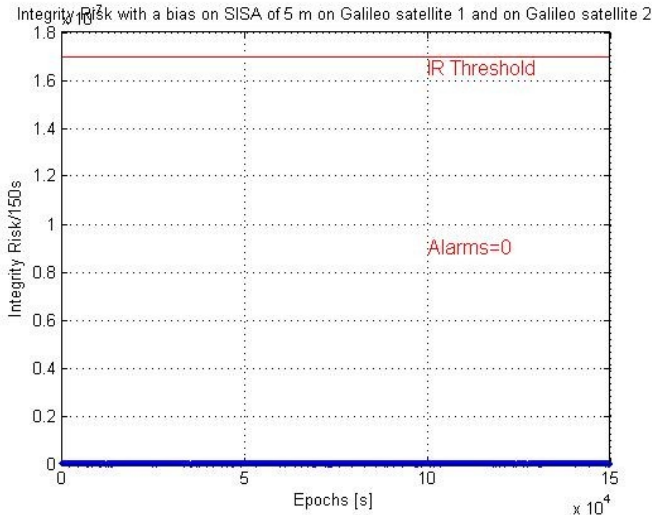


Figure 5-23: Integrity Risk in severely degraded conditions with SISA bias on two Galileo satellites (GPS-Galileo dual constellation)

The last test considers degraded values for URA and also biases affecting two GPS satellites.

| Scenario #3 – Severely Degraded conditions – GPS-Galileo dual constellation | |
|--|--|
| URA | 1.0 m for each satellite in view |
| SISA-IPF | 1.0 m for each satellite in view |
| SISA at the user level | SISA-IPF·1.1 |
| Bias on SISA and URA | 5 m |
| Satellites affected by bias | Galileo satellite #1 and #2, GPS satellite #1 and #2 |
| SISMA | 1.0 m for each satellite in view |

Table 5-26: Simulation data in severely degraded conditions with SISA bias on two Galileo satellites and URA bias on two GPS satellites (GPS-Galileo dual constellation)

Even in this very critical scenario, the Galileo integrity algorithm for the combined system is able to provide an Integrity Risk lower than the specific requirement, as shown in the next figure.

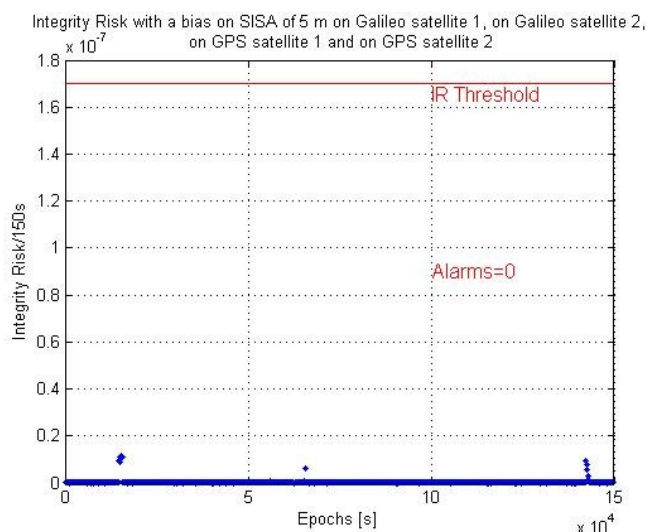


Figure 5-24: Integrity Risk in severely degraded conditions with SISA bias on two Galileo satellites and URA bias on two GPS satellites (GPS-Galileo dual constellation)

Although more critical scenarios can be considered (e.g., more than two biases affecting Galileo or GPS satellites), they are very unlikely to happen and therefore they haven't been considered in this analysis.

In conclusion, this technique even if it is based on a very different concept than protection levels, it has shown the benefits coming out from a combined system using an extended version of the Galileo Integrity equation. In particular, with a dual constellation Integrity Risk requirements can be satisfied even in presence of heavily degraded scenarios.

The Galileo integrity concept is more complete than GPS/SBAS and RAIM integrity concepts and offers more protection to failures. On the other hand, this concept still needs further investigations, in particular regarding assumptions to be used for the error distributions and the parameters to be considered in the integrity equation. Indeed, although more complete, the new integrity concept introduced by Galileo is more complex and less intuitive than SBAS and RAIM protection level concept.

It is important to notice that this technique could be still used in combination with RAIM algorithms, which offer further barriers in case of local errors. As stated before, the Galileo Integrity algorithm at the user level is not able to detect instantaneous local failure as RAIM algorithms do. Therefore, using a combination of the two techniques, as also described in

[24], could lead to a very safe computed position and could guarantee precision approaches even for the most demanding categories of flight.

5.4 Other multisystem integrity techniques

In the next paragraphs other possible multisystem integrity techniques will be briefly described and they represent future possible research topics. Both the techniques here introduced consider the protection level concept as the basis for a multisystem integrity algorithm. In the first case, specific protection levels can be derived directly from the total integrity risk computed with the Galileo integrity algorithm, while in the second case the SBAS protection level concept is used.

5.4.1 Galileo Protection Levels

At the moment aviation receivers use the protection level concept, which is the current standard. Therefore, it could be possible to derive protection levels also for Galileo directly from the computed total integrity risk [12]. This could be done in two ways: the first method is more straightforward, but more conservative, the second method is less conservative, but more computationally involved and results in a degraded availability.

In the first case, whenever the integrity risk at the horizontal and vertical alert limits for the specific phase of flight is below the allocated integrity risk, these alert limits are also output as the protection levels for that specific application. If the computed integrity risk is larger than the allocated one, the system is declared unavailable for this specific user and user geometry and no protection levels have to be provided. Such computation of Protection Level does not affect the Service performance and is equivalent to the Galileo integrity risk computation at Alert Limit. Although no additional workload is requested for the user receiver by this computation, the resulting protection level is very conservative.

In the second case a split between the allocated horizontal and vertical contributions at the user design level has to be done:

$$\begin{aligned} HPL &= f_H^{-1} \left(P_{HMI,H,alloc} (VAL_U, HAL_U) \right) \\ VPL &= f_V^{-1} \left(P_{HMI,V,alloc} (VAL_U, HAL_U) \right) \end{aligned}$$

Eq. 5-14

where:

$$\begin{aligned} P_{HMI,H,alloc} (VAL_U, HAL_U) &= P_{HMI} (VAL_D, HAL_D) \cdot \frac{P_{HMI,H} (HAL_U)}{P_{HMI,H} (HAL_U) + P_{HMI,V} (VAL_U)} \\ P_{HMI,V,alloc} (VAL_U, HAL_U) &= P_{HMI} (VAL_D, HAL_D) \cdot \frac{P_{HMI,V} (VAL_U)}{P_{HMI,H} (HAL_U) + P_{HMI,V} (VAL_U)} \end{aligned}$$

Eq. 5-15

with VAL_D and HAL_D being the vertical and horizontal alert limits of the system design (20 meters and 12 meters respectively), VAL_U and HAL_U the alert limits at the user design level, which depend on the specific application (e.g., for LPV-200 they are 35 meters and 40 meters respectively), $P_{HMI,H}(HAL_U)$ and $P_{HMI,V}(VAL_U)$ the integrity risk calculated at the user design alert limits. Because it is not possible to resolve the inverse functions f_H^{-1} and f_V^{-1} analytically, an iterative method to compute the Protection Levels HPL and VPL must be applied. Therefore, even if this second method produces less conservative values for the protection level, it is more complex and it has the drawback of a fixed split between horizontal and vertical integrity risk, which degrades the availability of the system.

However, the protection level concept in Galileo could then be extended in order to include also GPS in a combined system. Therefore, when the total integrity risk of the combined system is computed, as shown in the previous sections, protection levels could be derived using the methods described here.

5.4.2 SBAS Protection Levels

SBAS Protection Level equations, described in chapter 2, could be extended in order to include also Galileo data for a combined system. In particular, the following two equations should be considered:

$$HPL_{SBAS} = \begin{cases} k_{H,NPA} \cdot d_{major} & \text{(en-route to LNAV)} \\ k_{H,PA} \cdot d_{major} & \text{(LNAV/VNAV, LP, LPV approach)} \end{cases} \quad \text{Eq. 5-16}$$

$$VPL_{SBAS} = k_V \cdot d_U \quad \text{Eq. 5-17}$$

where d_{major} and d_U include now also Galileo's range error contribution (SISA).

This approach has the major drawback of not including any faulty case, as the Galileo Integrity concept does. Therefore, only partial information coming from Galileo is used, because SISMA parameter is not included in the previous two equations, as well as an estimation of the magnitude of the undetected bias. Moreover, as stated in the previous paragraph, a fixed split of the integrity risk due to the protection level concept degrades the total system availability. Nonetheless, this method has the advantage of using the protection level concept, which is the current standard in the civil aviation receiver and it is easier to implement than the complex Galileo integrity algorithm.

Conclusions

So far the integrity concept for modern satellite navigations systems has been presented and some new multisystem integrity techniques have been proposed.

The initial analysis has showed that current GPS needs augmentation systems in order to provide integrity: these augmentation systems improve GPS safety and accuracy, but have some limitations. Indeed, when considering RAIM algorithms in combination with only GPS constellation, a limited integrity is provided and only few categories of flight can be satisfied, because RAIM algorithms have been originally designed to detect only one single failure in one system. Thus, RAIM algorithms in the case of a single constellation are not able to protect user against multiple failures, without paying a high price in terms of availability. Indeed, it has been shown that, while both integrity and availability are satisfied in case of single constellation and single failure, only one of them can be satisfied in case of multiple failures for single constellation: in particular, if integrity is satisfied (in terms of probability of missed detection), availability is not, being the protection level higher than the corresponding alert limit; on the other hand, when protection level is lower than the corresponding alert limit, the P_{md} requirement is no longer satisfied.

Then, it has been shown that SBAS-like systems, such as EGNOS, are able to detect and protect user from multiple failures, but also in this case a high price in terms of system availability could be paid. Indeed, in case of very bad geometries, the system could be declared unavailable when protection levels become higher than the required alert limits. This could happen quite often in case of a single constellation. Moreover, there is an inherent delay that is introduced in the detection of an error, due to the time it takes to uplink information on errors. However, the original technique that has been used to analyse the EGNOS reaction to GPS clock anomalies has shown that EGNOS has excellent capabilities to detect and correct failures due to clock errors in the GPS satellites that were not detected by the GPS Ground Segment. Clock anomalies are usually compensated with the long and fast terms corrections, but in some cases the user can be warned to exclude the failed satellite from the final solution. In all the cases that were analysed, the

position errors were correctly bounded by the protection levels and these results were confirmed using the Stanford-ESA Integrity Diagrams.

The multisystem scenario has then been described and new parameters and definitions have been introduced: in particular, probability of failure, probability of false alarm and probability of missed detection for a dual constellation system have been derived. This scenario represents the test-bed under which the proposed multisystem integrity techniques have been analysed.

The first and most straightforward multisystem integrity method is an extension of the current RAIM algorithms to a dual constellation in presence of multiple failures: this technique has shown very good results both in terms of availability and integrity. Indeed, RAIM algorithms in a combined system are able to protect user even in case of multiple failures without trading integrity with availability. Moreover, this technique adds no additional effort in terms of computational load and system cost.

On the other hand, the second technique is based on the new Galileo integrity concept, which is more complete than current GPS/SBAS and RAIM integrity concepts and offers more protection to failures. The analysis has shown that in case of a combined system, the Integrity Risk requirement can be satisfied even in presence of heavily degraded scenarios. In this way, precision approaches for demanding categories of flight can still be performed. This technique makes use of all the available data coming from GPS and Galileo and combines them in an extended Galileo Integrity equation. However, this concept still needs further investigations, in particular regarding assumptions to be used for the error distributions and the parameters to be considered in the integrity equation. Indeed, although more complete, the new integrity concept introduced by Galileo is more complex and less intuitive than SBAS and RAIM protection level concept and it is still under development.

It is important to notice that the two techniques that have been proposed can be used together, since RAIM algorithms offer further barriers in case of local errors. Indeed, as it has been shown, the Galileo Integrity algorithm at the user level is not able to detect instantaneous local failure as RAIM algorithms do. Therefore, using a combination of these two techniques could lead to a very safe computed position and could guarantee precision approaches even for the most demanding categories of flight.

The other multisystem integrity techniques that have been briefly introduced in the last chapter represent the starting point for new research topics.

Furthermore, additional systems, such as inertial sensors (INS), could be also considered in combination with satellite navigation systems, in order to provide integrity, for example, in railway scenarios, where the satellite signal can be frequently lost in long galleries.

Moreover, the proposed multisystem integrity techniques could be further extended in order to include other navigation systems, such as GLONASS and the upcoming Chinese COMPASS and Indian GAGAN. This also represents a further possible new research topic.

However, it should be noted that the satellite navigation scenario is continuously evolving. Thus, the proposed techniques could be further updated once the upcoming Galileo system will be finally deployed and the current GPS will be completely modernised.

Appendix A

Error sources

All pseudorange measurements are biased, according to the equation [32]:

$$\rho = r + c[\delta t_u - \delta t^s] + I_\rho + T_\rho + \varepsilon_\rho$$

Eq. A-1

being ρ the measured pseudorange, r the geometric range between the user position and the satellite, c the velocity of light in a vacuum, δt_u and δt^s respectively the receiver and satellite clock bias relative to GPST, I_ρ and T_ρ the error contributions due to the ionospheric and tropospheric delays and ε_ρ the contribution of unmodeled effects, modelling errors and measurement errors (e.g., multipath). In the previous equation no explicit reference to the measurement epoch was used for simplicity.

The measurements errors can be grouped in three types:

- errors in the parameter values that are broadcast by a satellite in its navigation message for which the Control Segment is responsible
- errors due to the propagation medium, which affects the travel time of the signal from the satellite to the receiver
- receiver noise, which affects the precision of a measurement and interference from signals reflected from surfaces in the vicinity of the antenna.

A.1. Control Segment errors: satellite clock and ephemeris

The Control Segment errors are due to incorrect values of the satellite clock and ephemeris parameters computed by the Control Segment and broadcast by the satellite in the navigation message. Indeed, the current values of these parameters are obtained using a Kalman filter and then a prediction model is

used to generate the ephemeris and clock parameters to be uploaded to the satellites and broadcast by them in the navigation message. There are errors in both the estimation of the current values of the parameters and the prediction of their future values. The prediction error grows with the age of data (AoD), defined as the time since the last parameter upload. Clearly, these errors are low if an accurate model to estimate and predict the ephemeris and clock parameters is used and if there are frequent data uploads to the satellites.

Satellite clock errors

The GPS satellites clocks are not synchronized with the GPST (GPS Time): indeed there is a bias relative to GPST

$$\delta t^s = t^s - t_{GPS}$$

Eq. A-2

being t^s the time kept by the satellite clock and t_{GPS} the GPS Time, defined by the Control Segment on the basis of a set of atomic standards aboard the satellites and in monitor stations.

The satellite clock bias is modelled as a quadratic function over a time interval. The parameters $\{a_{f0}, a_{f1}, a_{f2}\}$ of this model are computed by the Control Segment on the basis of measurements at GPS monitor stations and they are, respectively, the clock bias (seconds), the clock drift (seconds/seconds) and the frequency drift (seconds/seconds²) and in GPS they are broadcast in subframe 1 of the navigation message.

At time t_{GPS} :

$$\delta t^s = a_{f0} + a_{f1}(t_{GPS} - t_{0c}) + a_{f2}(t_{GPS} - t_{0c})^2 + \Delta t_r$$

Eq. A-3

where t_{0c} is the reference time for the model in GPST and Δt_r is a relativistic correction term, given by:

$$\Delta t_r = Fe\sqrt{A} \sin E_k$$

where (e, \sqrt{A}, E_k) are orbital parameters (subframes 2 and 3 for GPS) and

$$F = \frac{-2\sqrt{\mu}}{c^2} = -4.442807633 \cdot 10^{-10} \frac{\text{sec}}{\sqrt{m}}$$

with:

$$\mu = 3.986005 \cdot 10^{14} \frac{m^3}{s^2} \quad \text{Earth's universal gravitational parameter}$$

$$c = 2.99792458 \cdot 10^8 \frac{m}{s} \quad \text{speed of light}$$

The control segment will utilize the following alternative but equivalent expression for the relativistic effect when estimating the NAV parameters:

$$\Delta t_r = -\frac{2\vec{R} \cdot \vec{V}}{c^2}$$

where \vec{R} is the instantaneous position vector of the SV, \vec{V} is the instantaneous velocity vector of the SV and c is the speed of light.

It is immaterial whether the vectors \vec{R} and \vec{V} are expressed in earth-fixed, rotating coordinates or in earth-centered, inertial coordinates.

These parameters are computed using a curve-fit to predicted estimates of the actual satellite clock errors. Thus, a residual clock error δt remains, which, for GPS, corresponds to a range error of 0.3 - 4 meters. The value of the residual error depends on two factors:

- Type of satellite
- Age of the broadcast data (AOD)

At 0AOD the residual error is 0.8 m, while after 24 hours since the data upload is 1 - 4 m.

Since user tracks satellites with AOD between 0 and 24 hours, in the statistical model for clock errors it is appropriate to average over AOD.

Satellite ephemeris errors

The ephemeris error is usually decomposed into components along three orthogonal directions defined relative to the satellite orbit: radial, along-track and cross-track. In estimation of an orbit based on range measurements, the radial component of the ephemeris error tends to be the smallest. The along-track and cross-track can be several times larger. Anyway, the error in a pseudorange measurement is the projection of the satellite position error vector on the satellite-receiver line of sight, which depends mostly upon the radial component of the ephemeris error. The components of the along-track and cross-track errors along the line of sight are small.

The range error due to the errors in the clock and ephemeris parameters is defined as the root-sum-square value of the clock error and the line-of-sight component of the ephemeris error. The size of this error is estimated and tracked by the Control Segment in real time within 1 m rms. With typical once-a-day data uploads, the current estimates of the rms range errors due to the ephemeris and clock parameters are about 1.5 m each. The Control Segment monitors the growth in parameter errors by comparing the broadcasted values to the best current estimates available. If the estimated range error for a satellite exceeds a threshold, a ‘contingency data upload’ is scheduled (the threshold is 5 m).

The Block IIF satellites are planned to maintain the clock and ephemeris errors below 3 m up to sixty days out of contact with the Control Segment in Autonav mode and up to three hours in normal mode.

A.2. Propagation errors

Ionospheric error

Ionosphere is responsible for signal delay/advance. Since the error due to ionosphere is frequency-dependent, it can be completely eliminated using a dual frequency receiver. In the single frequency case, the ionospheric error can be partially corrected using ionospheric models.

Single frequency model

For a single frequency GPS receiver the ionospheric error can be computed according to the Klobuchar model, as described in [9]. This is an empirical model and it is estimated to reduce the rms range error due to uncompensated ionospheric delay by about 50%. At mid-latitudes the remaining error in zenith delay can be up to 10m during the day and much worse during heightened solar activity.

The model gives the expression for the ionospheric delay for L1, while the delay for L2 can be easily computed using the well known frequency relation.

$$T_{IONO_{L1}} = \begin{cases} F \cdot \left[5.0 \times 10^{-9} + AMP \cdot \left(1 - \frac{x^2}{2} + \frac{x^4}{24} \right) \right] & \text{if } |x| < 1.57 \\ F \cdot (5.0 \times 10^{-9}) & \text{if } |x| \geq 1.57 \end{cases} \quad [s]$$

Eq. A-4

$$T_{IONO_{L2}} = T_{IONO_{L1}} \cdot \gamma \quad [s]$$

Eq. A-5

Where:

$$\gamma = \left(\frac{f_{L1}}{f_{L2}} \right)^2$$

$$AMP = \begin{cases} \sum_{n=0}^3 \alpha_n \phi_m^n & \text{if } AMP \geq 0 \\ \text{if } AMP < 0, & AMP = 0 \end{cases} \quad [s]$$

$$x = \frac{2\pi(t - 50400)}{PER} \quad [rad]$$

$$PER = \begin{cases} \sum_{n=0}^3 \beta_n \phi_m^n & \text{if } PER \geq 72000 \\ \text{if } PER < 72000, & PER = 72000 \end{cases} \quad [s]$$

$$F = 1.0 + 16.0(0.53 - E)^2$$

$$\phi_m = \phi_i + 0.064 \cos(\lambda_i - 1.617) \quad [\text{semi-circles}]$$

$$\lambda_i = \lambda_u + \frac{\psi \sin A}{\cos \phi_i} \quad [\text{semi-circles}]$$

$$\phi_i = \begin{cases} \phi_u + \psi \cos A & \text{if } |\phi_i| \leq 0.416 \\ \text{if } \phi_i > +0.416, & \phi_i = +0.416 \\ \text{if } \phi_i < -0.416, & \phi_i = -0.416 \end{cases} \quad [\text{semi-circles}]$$

$$\psi = \frac{0.0137}{E + 0.11} - 0.022 \quad [\text{semi-circles}]$$

$$t = 4.32 \times 10^4 \cdot \lambda_i + GPStime \quad [s]$$

if $t \geq 86400 \Rightarrow$ subtract 86400

if $t < 0 \Rightarrow$ add 86400

$$0 \leq t < 86400$$

Broadcast parameters

α_n : coefficients of a cubic equation representing the amplitude of the vertical delay (n=0,1,2,3)

β_n : coefficients of a cubic equation representing the period of the model (n=0,1,2,3)

Both the parameters are broadcast by satellites in the navigation message.

Receiver parameters

E : elevation angle [semi-circles]

A : azimuth angle [semi-circles]

ϕ_u : user geodetic latitude (WGS-84) [semi-circles]

λ_u : user geodetic longitude (WGS-84) [semi-circles]

$GPStime$: receiver computed system time

Computed parameters

x : phase [rad]

F : obliquity factor

t : local time [s]

ϕ_m : geomagnetic latitude of the earth projection of the ionospheric intersection point [semi-circles]

λ_i : geodetic longitude of the earth projection of the ionospheric intersection point [semi-circles]

ϕ_i : geodetic latitude of the earth projection of the ionospheric intersection point [semi-circles]

ψ : earth's central angle between the user position and the earth projection of the ionospheric intersection point [semi-circles]

It should be noted that all the angles should be converted to semi-circles:

$$\text{semi-circles} = \text{deg}/180 \text{ and semi-circles} = \text{rad}/\pi$$

however, when using the angles inside the sine and cosine functions they shouldn't be converted to semi-circles.

Dual frequency receiver

A dual frequency receiver is able to accurately calculate the ionospheric error and so to remove it almost completely. Indeed, the ionospheric-free pseudorange is given by:

$$\rho_{iono-free} = \frac{\rho_{L2} - \gamma\rho_{L1}}{1 - \gamma}$$

where ρ_{L1} and ρ_{L2} are the code measurements for L1 and L2.

However this approach has the drawback that measurement errors are significantly magnified through the combination. A preferred approach, as suggested by [6], is to use L1 and L2 pseudorange measurements to estimate the ionospheric error on L1 using:

$$\Delta S_{iono,corrL1} = \left(\frac{f_{L2}^2}{f_{L2}^2 - f_{L1}^2} \right) (\rho_{L1} - \rho_{L2}) \quad [m]$$

$$\Delta S_{iono,corrL2} = \Delta S_{iono,corrL1} \cdot \gamma$$

Eq. A-6

These corrections, eventually smoothed over time, are then subtracted from pseudorange measurements.

When using also phase measurements, it is possible to perform a much more accurate computation of ionospheric delay. Moreover, with phase measurements it is also possible to accurately calculate the Total Electron Content (TEC). TEC is the integral of the electron density on the receiver-to-satellite path. The TEC is measured in electrons/m² or in TEC units (TECU) where 1 TECU = 10¹⁶ electrons/m². 1 TECU corresponds to about 16cm of delay on L1.

Although phase measurements give much more accurate results than code measurements, they have the drawback that integer ambiguity should be resolved. Thus, a combination of phase measurements and code measurements allow a very precise and unambiguous computation for ionospheric delay and TEC.

Tropospheric error

Troposphere induces an error in the range measurement that is frequency-independent. Therefore, there is no way to compensate it using a dual frequency receiver. However, current models well estimate the tropospheric error.

Defining the *refractivity* as [6]:

$$N = 10^6(n-1)$$

two components contributes to the total error due to the troposphere:

$$N_{d,0} \approx a_1 \frac{p_0}{T_0} \quad N_{w,0} \approx a_2 \frac{e_0}{T_0} + a_3 \frac{e_0}{T_0^2}$$

being respectively the dry and the wet component at the sea level, with:

p_0 : partial pressure of the dry component at standard sea level [mbar]

T_0 : absolute temperature at standard sea level [K]

a_1 : empirical constant = 77.624 [K/mbar]

a_2 : empirical constant = -12.92 [K/mbar]

a_3 : empirical constant = 371000 [K²/mbar]

e_0 : partial pressure of the wet component at standard sea level [mbar]

As a function of the height, the two components become:

$$N_d(h) = N_{d,0} \left[\frac{h_d - h}{h_d} \right]^\mu \quad N_w(h) = N_{w,0} \left[\frac{h_w - h}{h_w} \right]^\mu$$

with:

$$h_d = 0.011385 \frac{p_0}{N_{d,0} \cdot 10^{-6}} \quad h_w = 0.0113851 \frac{1}{N_{w,0} \cdot 10^{-6}} \left[\frac{1.255}{T_0} + 0.05 \right] e_0$$

$$\mu = 4 \quad (\text{ideal gas law})$$

At the zenith (elevation angle=90°) the tropospheric error is then:

$$\Delta S_{tropo} = \frac{10^{-6}}{5} [N_{d,0} h_d + N_{w,0} h_w] = d_{dry} + d_{wet}$$

Eq. A-7

The previous formula needs pressure and temperature as inputs, which can be obtained using meteorological sensors.

Another method without using meteorological sensors considers other semi-empirical parameters:

$$d_{dry} = \left(1 - \frac{\beta H}{T}\right)^{\frac{g}{R_d \beta}} \left(\frac{10^6 k_1 R_d p}{g_m}\right)$$

$$d_{wet} = \left(1 - \frac{\beta H}{T}\right)^{\frac{(\lambda+1)g}{R_d \beta}} \left(\frac{10^6 k_2 R_d p}{g_m (\lambda+1) - \beta R_d T} \frac{e}{T}\right)$$

with:

$$k_1 = 77.604 \text{ [K/mbar]}$$

$$k_2 = 382000 \text{ [K}^2\text{/mbar]}$$

$$R_d = 287.054 \text{ [J/kg/K]}$$

$$g_m = 9.784 \text{ [m/s}^2\text{]}$$

$$g = 9.80665 \text{ [m/s}^2\text{]}$$

while the following parameters are given in tables:

β : temperature lapse rate [K/m]

T : temperature [K]

λ : water vapour lapse rate [unitless]

p : pressure [mbar]

e : water vapour pressure [mbar]

and:

H : height [m]

For elevations different than 90°, the tropospheric error is given by:

$$\Delta S_{tropo} = m_d d_{dry} + m_w d_{wet}$$

Eq. A-8

or

$$\Delta S_{tropo} = m(d_{dry} + d_{wet})$$

Eq. A-9

with:

m_d : dry component mapping function

m_w : wet component mapping function

m : general mapping function

An example of mapping function ([6]) is:

$$m(E) = \frac{1.001}{\sqrt{0.002001 + \sin^2(E)}}$$

where E is the elevation angle.

A.3. User level errors

Receiver noise

The code and carrier measurements are affected by random measurement noise, called receiver noise, which includes: noise introduced by the antenna, amplifiers, cables and the receiver; multi-access noise (i.e., interference from other GPS signals and GPS-like broadcasts from system augmentations); signal quantization noise. In the absence of any interfering signals, a receiver sees a waveform which is sum of the GPS signal and randomly fluctuating noise. Therefore, the fine structure of a signal can be masked by noise, especially if the signal-to-noise ratio is low. The measurement error due to receiver noise highly varies with the signal strength, which, in turn, varies with satellite elevation angle and therefore with geometry.

Multipath

Multipath refers to the phenomenon of a signal reaching the antenna via two or more paths. Typically, an antenna receives the direct signal and one or more of its reflections from structures in the vicinity and from the ground. A reflected signal is a delayed and usually weaker version of the direct signal. The subsequent code and carrier phase measurements are the sum of the received signals. The range measurement error due to multipath depends upon the strength of the reflected signal and the delay between the direct and reflected signals. Multipath affects both code and carrier measurements, but the magnitude of the error differs significantly.

Typical multipath error in pseudorange measurements varies from 1 m in a benign environment to more than 5 m in highly reflective environment. The corresponding errors in the carrier phase measurements are typically two orders of magnitude smaller (1-5 cm).

A.4. Error distributions

The final User Equivalent Range Error (UERE) is composed by the three main contributions seen in the previous sections:

- Signal-In-Space (SIS) Range Error, which takes into account ephemeris and clock estimation errors. This parameter, called URE (User Range Error), is not known and therefore it has to be estimated by the ground segment and transmitted to the user. In the case of GPS, the estimation of the URE is the URA (User Range Accuracy).
- Propagation range error, which takes into account the ionospheric and tropospheric delays. However, the tropospheric delay is mostly considered a local phenomenon. The ionospheric contribution in a dual frequency environment is almost negligible.
- Local range errors, which affect the specific user receiver and they include multipath and receiver noise as well as tropospheric delay.

Each of these contributions can be characterised by an error distribution.

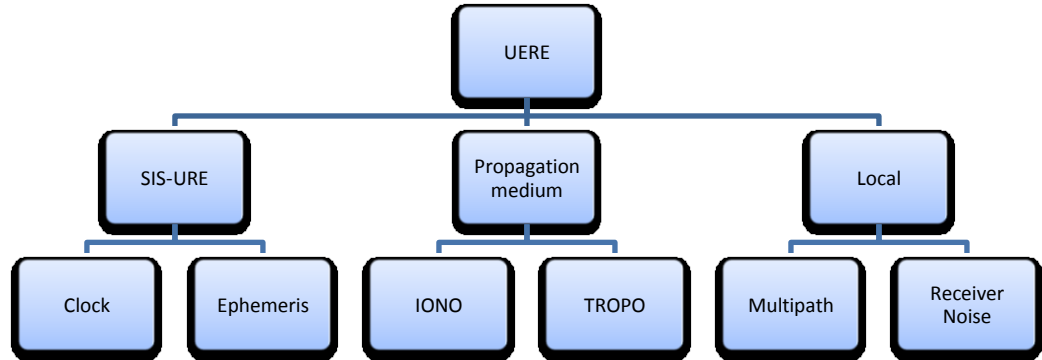


Figure A-1: User Equivalent Range Error

Since the error distributions are assumed to be uncorrelated, we have:

$$\sigma_{URE}^2 = \sigma_{URE}^2 + \sigma_{IONO}^2 + \sigma_{TROPO}^2 + \sigma_{noise}^2 + \sigma_{multi}^2$$

Eq. A-10

The typical error budgets for GPS (both Precise Positioning and Standard Positioning Services) are summarised in the next two tables.

| Segment Source | Error Source | 1 σ Error (m) |
|--------------------|-------------------------------|----------------------|
| Space/Control | Broadcast clock | 1.1 |
| | Broadcast ephemeris | 0.8 |
| User | Residual ionospheric delay | 0.1 |
| | Residual tropospheric delay | 0.2 |
| | Receiver noise and resolution | 0.1 |
| | Multipath | 0.2 |
| System UERE | Total (RSS) | 1.4 |

Table A-1: GPS Precise Positioning Service Typical UERE Budget [6]

| Segment Source | Error Source | 1σ Error (m) |
|-----------------------|-------------------------------|---------------------------------------|
| Space/Control | Broadcast clock | 1.1 |
| | L1 P(Y)-L1 C/A group delay | 0.3 |
| | Broadcast ephemeris | 0.8 |
| User | Ionospheric delay | 7.0 |
| | Tropospheric delay | 0.2 |
| | Receiver noise and resolution | 0.1 |
| | Multipath | 0.2 |
| System UERE | Total (RSS) | 7.1 |

Table A-2: GPS Standard Positioning Service Typical UERE Budget [6]

Appendix B

Overbounding techniques

The Ground Segment monitors the errors in the range domain and provides parameters that characterize the error distribution in the range domain. Since the actual error distribution is not a true Gaussian, broadcast σ values describe a range domain error distribution that is a zero-mean Gaussian and that overbounds the actual range domain error distribution. There are different overbounding techniques:

- Tail overbounding
- Pdf overbounding
- Cdf overbounding

In tail overbounding, the overbounding cumulative distribution (CDF), G_o , obeys the following relationship with respect to the actual CDF, G_a :

$$\begin{cases} G_o(x = -VAL) \geq G_a(x = -VAL) \\ (1 - G_o(x = VAL)) \geq (1 - G_a(x = VAL)) \end{cases}$$

Eq. B-1

Tail overbounding in the range domain does not guarantee tail overbounding in the position domain.

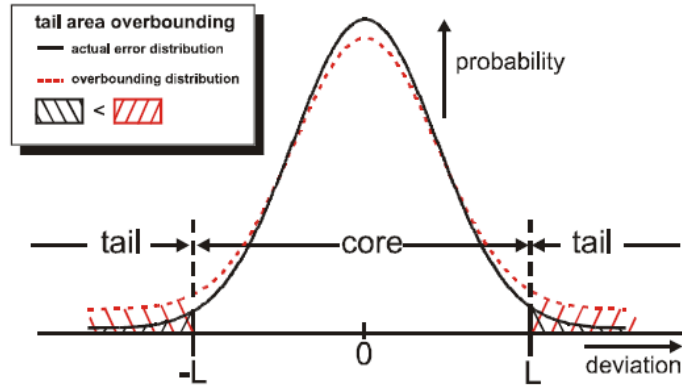


Figure B-1: Tail area overbounding

A Pdf overbound is defined such that the overbounding distribution exceeds the actual distribution for every point outside the VAL:

$$g_o(x) \geq g_a(x), \forall |x| > VAL$$

Eq. B-2

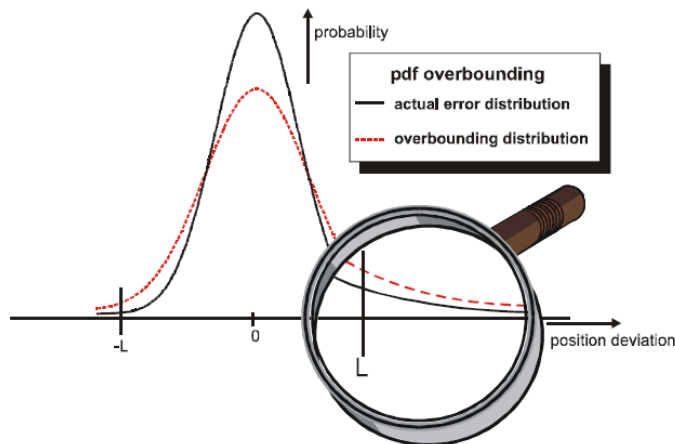


Figure B-2: Pdf overbounding

A Cdf overbound is defined such that the cumulative distribution function of the overbound, G_o , is always shifted towards its tails relative to the actual cumulative distribution function, G_a , according to:

$$\begin{cases} G_o(x) \geq G_a(x), & \forall G_a < \frac{1}{2} \\ G_o(x) \leq G_a(x), & \forall G_a \geq \frac{1}{2} \end{cases}$$

Eq. B-3

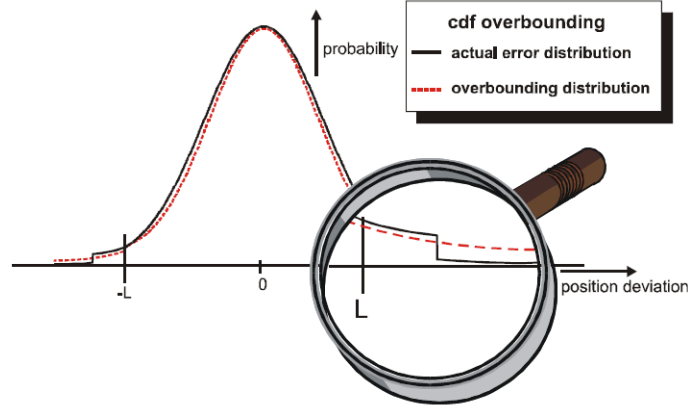


Figure B-3: Cdf overbounding

The Cdf based strategy offers an effective way to link range and position-domain overbounding rather than pdf overbounding, but only for some specific distributions. Indeed, [27] demonstrated that the overbounding in the position domain can be guaranteed only for symmetric, zero-mean, unimodal distributions.

A more general overbounding technique that effectively relates range-domain and position-domain overbounding for an arbitrary distribution is the paired overbounding method described in [28]. This method guarantees overbounding in the position domain even for a shifted median, asymmetric and multimodal error distribution.

The paired overbound consists of a left bound and a right bound, defined relative to the actual CDF:

$$\begin{aligned} G_L(x) &\geq G_a(x), \forall x \\ G_R(x) &\leq G_a(x), \forall x \end{aligned}$$

Eq. B-4

The overbounding Cdf is therefore constructed from the left and right bounds:

$$G_o = \begin{cases} G_L(x), \forall G_L < \frac{1}{2} \\ \frac{1}{2} \text{ otherwise} \\ G_R(x), \forall G_R > \frac{1}{2} \end{cases}$$

Eq. B-5

The paired overbound's additional degrees of freedom enable construction of tighter error bounds, particularly for the case of non-zero mean error distributions. Moreover, the generality of the paired overbound permits bounding arbitrary multipath distributions, including those with more than one mode.

Another overbounding method is suggested by [29] that proposes a pdf overbounding with a finite confidence level. This method provides several advantages, as increasing user availability and relaxing Galileo SISA overbounding requirements still ensuring user integrity risk requirement.

Bibliography

- [1] Galileo Open Service Signal In Space Interface Control Document, Draft 1, February 2008
- [2] “Availability Characteristics of GPS and Augmentation Alternatives”, Phlong, W.S., Elrod. B.D - Journal of the Institute of Navigation, Vol.40, No.4 , 409-428, 1994
- [3] Global Positioning System Standard Positioning Service Signal Specification, 2nd Edition – 2 June 1995
- [4] Global Positioning System Standard Positioning Service Performance Standard - Assistant Secretary of Defense for Command, Control, Communications, and Intelligence, Washington, D.C. – October 2001
- [5] Navstar GPS Space Segment/Navigation User Interfaces - IS-GPS200D - 7 December 2004
- [6] “GPS – Principles and Applications”, E.D. Kaplan, C. J. Hegarty, 2nd Edition, Artech House, Inc. - ISBN 1-58053-894-0 – 2006
- [7] International Standards and Recommended Practices, Aeronautical Telecommunications, Annex 10, Volume 1
- [8] “Wide Area Augmentation System Vertical Accuracy Assessment in Support of LPV200 Requirements”, B. Wanner, B. Declene, D.A. Nelthropp, S. Gordon, ION 63rd Annual Meeting, April 23-25 2007, Cambridge, Massachusetts, USA
- [9] Minimum Operational Performance Standards for Global Positioning System/Wide Area Augmentation System Airborne Equipment – RTCA DO-229D – December 13, 2006
- [10] “The SBAS Integrity Concept Standardised by ICAO. Application to EGNOS”, B. Roturier, E. Chatre, J. Ventura-Traveset, GNSS 2001 May 8-11, 2001; Seville, Spain
- [11] “GPS RAIM: Calculation of Threshold and Protection Radius Using Chi-Square Methods – A Geometric Approach”, R.G. Brown, G.Y. Chin - The Institute of Navigation Redbook, Volume V, Special Issue on GPS Integrity, 1997
- [12] Galileo Integrity Concept - ESA-DEUI-NG-TN/01331, issue 1, 5 July 2005
- [13] “The Galileo Integrity Concept”, V. Oehler, F. Luongo, J.-P. Boyero, R. Stalford, H. L. Trautenberg, J. Hahn, F. Amarillo, M. Crisci, B. Schlarman, J.F. Flamand, ION GNSS 17th International Technical Meeting of the Satellite Division, 21-24 Sept. 2004, Long Beach, CA

- [14] “Solution of the Two-Failure GPS RAIM Problem Under Worst-Case Bias Conditions: Parity Space Approach”, R.G. Brown, Journal of the Institute of Navigation, Vol.44, No.4 , Winter 1997-1998, 425-431
- [15] “RAIM with Multiple Faults”, J.E. Angus, Journal of the Institute of Navigation, Vol.53, No.4 , Winter 2006, 249-257
- [16] “Theoretical analysis of RAIM in the occurrence of simultaneous two-satellite faults”, J. Liu, M. Lu, X. Cui, Z. Feng, IET Radar Sonar Navigation, 2007, 1, (2), pp. 92-97
- [17] “Feasibility Analysis of RAIM to Provide LPV-200 Approaches with Future GPS”, Y.C. Lee, M.P. McLaughlin- ION GNSS 20th International Technical Meeting of the Satellite Division, 25-28 September 2007, Fort Worth, TX
- [18] “Summary of RTCA SC-159 GPS Integrity Working Group Activities”, Y. Lee, K. Van Dyke, B. Decleene, J. Studenny, M. Beckmann - Journal of the Institute of Navigation, Vol.43, No.3 , Fall 1996, 307-338
- [19] List of GPS abnormal events from 2006 for which RMS clock was larger than 10 ns (3 meters error) – T. Springer – European Space Agency, ESA/ESOC – 2007.
- [20] “The User Domain Integrity Assessment Technique (UDIAT). Application to the Analysis of Potential UDRE MIs After EGNOS CPF Switching” – M. Hernández-Pajares, J.M Juan, J. Sanz, A. Aragón, P. Ramos-Bosch – 30 March 2007
- [21] “Basic Research Utilities for SBAS (BRUS)” – M. Hernández-Pajares, J.M. Juan, J. Sanz, X. Prats, J. Baeta. – V Geomatics Week, Barcelona, Spain, 2003.
- [22] S-Q Course Book, D. Ellard, P. Ellard, 17 November 2003
- [23] “The World After SA: Benefits to GPS Integrity”, Karen L. Van Dyke, DOT/Volpe Center, 2000
- [24] “Combined Galileo and EGNOS Integrity Signal: a multisystem integrity algorithm”, C. Pecchioni, M. Ciollaro, M. Calamia, 2nd Workshop on GNSS Signals & Signal Processing - GNSS SIGNALS’2007, ESTEC, 24-25 April 2007
- [25] “Weighted RAIM for Precision Approach”, T. Walter, P. Enge, Proc. ION GPS 1995, September 12-15, 1995, Palm Springs, CA, pp. 1995-2004
- [26] “The User Domain Integrity Assessment Technique (UDIAT)”, Sanz, J.; Ramos-Bosch, P.; Aragon-Angel, A.; Ciollaro, M.; Ventura-Travesset, J.; Toran, F.; Lopez, C., 4th ESA Workshop on Satellite

- Navigation User Equipment Technologies, 1-10 December 2008, ESTEC
- [27] “Defining Pseudorange Integrity – Overbounding”, B. DeCleene, ION GPS 2000, pp. 1916-1924
- [28] “Paired Overbounding and Application to GPS Augmentation”, J. Rife, S. Pullen, B. Pervan, P. Enge, IEEE Position, Location and Navigation Symposium, pp. 439-446, 26-29 April 2004
- [29] “Making GNSS Integrity Simple and Efficient – A New Concept Based on Signal-in-Space Error Bounds”, J. Mach, I. Deuster, R. Wolf, W. Werner, ION GNSS 2006, September 26 - 29 2006, Fort Worth Convention Center, Fort Worth, Texas
- [30] “Assessment of GALILEO performance based on the GALILEO System Test Bed experimentation results”, M. Falcone, F. Amarillo, E. Van Der Wenden, Proceedings of the 17th International Technical Meeting of the Satellite Division of the Institute of Navigation ION GNSS 2004, September 21 - 24, 2004, Long Beach Convention Center, Long Beach, California
- [31] “Satellite Orbits – Models, Methods, Applications”, O. Montenbruck, E. Gill – Springer 2005 – ISBN 3-540-67280-X
- [32] “Global Positioning System – Signals, Measurements and Performance”, P. Misra, P. Enge – Ganga-Jamuna Press 2006 – ISBN 0-9709544-1-7
- [33] “Global Positioning System: Theory and Applications – Volume II”, B.W. Parkinson, J.J. Spilker Jr., P. Axelrad, P. Enge – Progress in Astronautics and Aeronautics, Paul Zarchan Editor-in-Chief, AIAA (American Institute of Aeronautics & Astronautics), 1st edition (January 15, 1996), ISBN 156347249X